Effect of Sonication Time and Clay Loading on Nanoclay Dispersion, Tensile and Hardness Properties of Epoxy-Clay Nanocomposite

BY

Adinoyi Muhammed Jamiu

A Thesis Presented to the

DEANSHIP OF GRADUATE STUDIES

KING FAHD UNIVERSITY OF PETROLEUM & MINERALS

DHAHRAN, SAUDI ARABIA

In Partial Fulfillment of the
Requirements for the Degree of

MASTER OF SCIENCE

In

MECHANICAL ENGINEERING

June 2010

KING FAHD UNIVERSITY OF PETROLEUM AND MINERALS

DHAHRAN 31261, KINGDOM OF SAUDI ARABIA

DEANSHIP OF GRADUATE STUDIES

This thesis, written by

MUHAMMED JAMIU ADINOYI

under the direction of his Thesis advisor and approved by his Thesis committee, has been presented to and accepted by the Dean of Graduate Studies, in partial fulfillment of the requirements for the degree of

MASTER OF SCIENCE IN MECHANICAL ENGINEERING.

Thesis Committee

Dr. Nesar Merah (Chairman)

Dr. Zuhair M. Gasem (Member)

Dr. Nasser Al-Aqeeli (Member)

Dr. Amro Al-Qutub
Department Chairman

Dr. Salam A. Zumo
Dean of Graduate Studies

Date: 16/10/10

DEDICATION.

THIS WORK IS DEDICATED TO MY LATE

BELOVED PARENTS

MALLAM ADINOYI SULEIMAN BALA

&

MALLAMA FATIMAH ANASE.

(MAY ALLAH BE PLEASED WITH THEM)

ACKNOWLEDGMENTS

In the name of Allah, the most Compassionate, the most Merciful. I am most grateful to Allah for He bequeaths me the favour to live in sound health and to undertake this task successfully. O Allah! Accept my gratitude for I know it is worthless, and deny me not your favour for I know I am full of faults. May your Blessings and Peace continue to shower on the best of mankind, Muhammad (P.B.U.H), his household and the righteous believers.

I wish to appreciate the kindness and encouragement of my thesis committee, comprising of Prof. Nesar Merah, Dr. Zuhair Gasem and Dr. Nasser Al- Aqeeli. Without their high-quality advice, encouragement and good human relationship, this work may not have come to fruition. Their desire to see that I made a good thesis was clear from the outset. I am proud to have you as my committee members. I am particularly thankful to my Advisor, Prof. Merah for his patience in spite of all my shortcomings. I must confess that this work attained the status of a master thesis due to his untiring attitude to encouraging, advising and supporting me in the work. His relentless revision of the many drafts brought it to this standard.

I am thankful to the authority of the King Fahd University of Petroleum and Minerals, especially the Mechanical Engineering Department, and the Government of Saudi Arabia for providing me the environment to pursue this level of study. I am also grateful to Dr. Khaled Mezghani who advised on curing procedures and mold design. My thanks go to Mr. Ali Kamal of the ME workshop who machined the mold and the tensile specimens. I appreciate the assistance of Engr. Mohammed Al-Saeed of the Physics Department for conducting the

X-ray scanning on time even though the samples were much. I am grateful to Mr. Al-Abbas Saleh for his help in carrying out the Scanning Electron Microscopy imaging. I must not fail to recognize Mr. Muneer Al-Qadhi, a PHD student in the Mechanical Engineering Department working in the same area of epoxy-clay nanocomposite, for his practical assistance and support throughout the work. My gratitude goes to all Mechanical Engineering graduate students, faculties and staff. I am as well grateful to Engr. Ammar M. Ghadri of Bondstrand, Dammam, from whom we acquired the materials for this work.

I am highly indebted in thanks to my entire family members. Your kind physical, moral and spiritual supports have been my source of propulsion to achieving any worthy endeavours. I am especially grateful to Dr. Adinoyi AbdulKareem Bala who not only opened my eyes to this level of academic pursuit but also provided, and continues to provide, the necessary support to me in all aspect of my life. The valuable supports of Brethren Adinoyi Yusuf, Adinoyi Yakubu, Adinoyi Momohjimoh and all the Adinoyis are not ignored. My wife, Hajiya Sidikat, and daughters, Na'eematullah Oyiza and Tasneem Onize, have been wonderful partners. I appreciate your various supports, patience and understandings. I am proud of you all.

To all my friends and colleagues back at home and here in KFUPM, I am ever grateful to you all. I can not imagine what this experience would have been without your supports.

As it is not possible to mention here every individual who made this programme a fulfilling experience, yet I have taken into acknowledgment every one of you. Thank you all.

TABLE OF CONTENTS

Contents **Page**

LIST OF TABLES

Table **Page**

LIST OF FIGURES

Figure **Page**

NOMENCLATURE

Abbreviations

cps	Count per second
d	d-spacing
DSC	Differential scanning calorimeter
EDS	Energy dispersive spectroscopy
GPa	gigapascal
hr	hour(s)
min	minutes
mm	millimeter
MPa	megapascal
SEM	Scanning electron microscope
t	sonication time
TEM	Transmission electron microscope
W/g	Watt per unit gram
XRD	X-ray diffraction

Symbols

θ	Angular position of X-ray diffraction peak
Å	Angstrom
ºC	Degree celcius
E	Modulus of elasticity
º	Degree
Sut	Fracture strain
T_g	Glass transition temperature
ε_f	Fracture strain
x	Clay loading

Thesis Abstract.

Name: **Adinoyi Muhammed Jamiu.**

Thesis Title: **Effect of sonication time and clay loading on nanoclay dispersion, tensile and hardness properties of epoxy-clay nanocomposite.**

Major Field: **Mechanical Engineering.**

Date: **8th June, 2010.**

In the present work, epoxy-nanoclay composites have been prepared using *in situ* polymerization under sonication times of 5, 10, 30 and 60 minutes for clay loadings of 2, 4 and 5%. Characterizations of the nanocomposites were carried out using DSC, XRD, EDS and SEM. The effects of sonication time and clay loading on nanoclay dispersion in epoxy were investigated. Tensile and hardness properties were also evaluated in relation to sonication time and clay amount.

The XRD results revealed that nanocomposites were largely intercalated with few exfoliation or disorderly intercalated sites. The change in sonication time did not produce significant variation in the intergallery spacings of the nanocomposites. Tensile properties measurement showed that tensile strengths of nanocomposites were lower than that of the neat epoxy. The elastic moduli were enhanced relative to the neat epoxy as the clay loading increased but decreased with increasing sonication time. Nanocomposites with higher d-spacing generally showed the potential of better tensile strength. Measured nanocomposites hardness remained practically the same at all clay loadings and sonication times. The glass transition temperature, T_g, of the neat epoxy decreased from 161ºC to 155ºC when 2% clay was added. Change in the sonication time did not produce any significant variation in the T_g. SEM imaging showed that nanocomposite micro structures are rough and highly brittle due to the presence of clay. EDS result confirmed the blending of epoxy with nanoclay.

Master of Science Degree

King Fahd University of Petroleum and Minerals,

Dhahran, Saudi Arabia.

خلاصة الرسالة.

الاسم : أدينوي محمد جاميو.

عنوان الرسالة : تأثير زمن الصوتنة وتحميل الطين على تشتت النانو طين ،

وخصائص الشد و الصلابة لمركب الطين الايبوكسي المتناهي في الصغر.

مجال التخصص : الهندسة الميكانيكية.

التاريخ : ٨ يونيو ٢٠١٠م.

في هذا العمل ، تم تحضير مركبات النانو طين – الايبوكسي باستخدام البلمرة الموضعية تحت التعرض لأزمنة صوتنة من ٥ ، ١٠ ، ٣٠ و ٦٠ دقيقة لتحميل طيني ٢ و ٤ و ٥ ٪. ونفذت توصيفات المركبات المتناهية في الصغر باستخدام DSC ، XRD ، EDS و SEM . وقد تم التحقق من تأثير زمن الصوتنة وتحميل الطين على تشتت النانو طين في الايبوكسي. كما تم أيضا تقييم خصائص الشد والصلابة في ما يتعلق بزمن الصوتنة وكمية الطين. وكشفت نتائج XRD أن المركبات المتناهية في الصغر بصورة عامة إقحام بتقشير قليل أو مواقع إقحام مضطربة. هذا التغيير في زمن الصوتنة لا ينتج عنه تفاوت كبير في المباعدة البينية لأروقة المركبات المتناهية في الصغر. وأظهرت قياسات خصائص قوة الشد للمركبات المتناهية في الصغر كانت أقل من الايبوكسي النقي . ولكن تم تعزيز وحدات معاملات الرجوعية المرنة بالنسبة للايبوكسي النقي ، بزيادة تحميل الطين وتقيل زمن الصوتنة. المركبات المتناهية في الصغر ذات التباعد الدالي الأعلى أظهرت عموما إمكانات قوة شد أفضل. الصلابة المقاسة للمركبات المتناهية في الصغر ظلت عمليا نفسها لجميع تحميلات الطين وأزمنة الصوتنة. درجة حرارة التحول الزجاجي ، ح ز ، من الايبوكسي النقي انخفضت من ١٦١ إلى ١٥٥ درجة مئوية عندما تمت إضافة ٢ ٪ من الطين. التغيير في زمن الصوتنة لم يسفر عن أي تفاوت كبير في ح ز. وأظهر التصوير SEM أن الهياكل الدقيقة بمركب متناهي في الصغر هي هشة للغاية و خشنه بسبب وجود الطين. أكدت نتيجة EDS المزج بين الايبوكسي مع النانو طين.

شهادة ماجستير علوم

جامعة الملك فهد للبترول والمعادن ،

الظهران ، المملكة العربية السعودية.

CHAPTER 1

1.0. INTRODUCTION

The quest for better material performance has consistently put materials engineers and scientists in the search for superior and highly efficient materials. The emergence of nanotechnology in the last few decades has made huge impact in the research for superior material performance. The success of this novel technology has led to the development and utilization of nano-size materials. Nanosize materials are materials with at least one dimension less than 100 nm. This relatively novel material has shown very attractive mechanical, thermal, electrical and physical properties. Among the numerous nanocomposite materials which emerged in the last decades, polymer-nanoclay system has attracted considerable research and academic attention because of its usually attractive material properties. This organic-inorganic hybrid of polymer matrix and nano-size clay reinforcement has usually shown superior mechanical and physical properties above their micro and macro counterparts. Major differences in behaviour between conventional and nanostructured materials result from the fact that the latter have much larger surface area per unit volume [1]. Owing to the high aspect ratio of the reinforcement, they show several advantages over typical composites in terms of mechanical, thermal, physical and barrier properties [2]. The reinforcing inorganic silicates contain individual particles having surface area greater than 750 m^2/g and aspect ratio in the range of 100-1500 nanometers [1, 3]. The large surface area and aspect ratio dominates the interaction of these materials with polymers. In addition, small amount of modified clay material, usually 0.5-10%, is needed to bring a dramatic change in polymer properties, which contrasts with the 40-70% needed for

micro-fillers to make impact on polymeric matrix. This also makes the materials even lighter than most conventional composites. Even so, available research data pertinent to polymer nanocomposites somewhat leads to contradictory conclusions. For instance, the ingression of clay in polymer materials was to reported to have led to: reduction in the moisture absorption of the polymer [4, 5, 6], increased corrosion resistance [6], increased tensile strength [7, 8, 9], flexural strength and modulus [10, 11, 12], compressive strength [11, 13], heat distortion temperature [3], hardness [7, 14,], toughness [15, 16], flame retardancy and thermal stability [17]. In many other cases, only marginal increase or absolute reduction in tensile strength [2, 18, 19, 20], flexural and compressive strength [21], glass transition temperature, T_g [20, 21, 22, 23, 24] were observed.

One aspect where researchers seem to have agreed is that polymer nanocomposites properties are highly dependent on their morphology, which is the extent of clay exfoliation/intercalation inside the polymer. Exfoliation is the complete separation of the clay particles within the polymer matrix, while intercalation qualifies the finite increase in clay intergallery space yet retaining its stacking form. Generally, exfoliated structures are reported to possess better properties than the intercalated ones of the same particles concentration [1, 4]. Exfoliated polymer-nanoclay composite yields the maximum improvement in properties because maximum reinforcement is achieved [3]. However, the level of exfoliation/intercalation achievable is influenced by the type of polymer matrix [4, 25], the clay type [9], the clay concentration [1], the type of clay functionalizing agent [17], and, more significantly, the mixing techniques [16, 19, 28] adopted. Details of both types of internal structure can be revealed by x-ray diffraction (XRD) and transmission electron

microscopy (TEM). TEM is the best usual method to obtain a direct visualization of the dispersion state. But it is highly localized, as it only probes a very small volume which may or may not be the true representation of the entire material [28]. However, x-ray techniques, though probing a small area when compare to the bulk material, can analyze a volume about 1 mm^3 with standard equipment. The use of x-ray in analyzing the structure of polymer-clay nanocomposite has become an integral part of nanocomposite research. The ease and availability of x-ray often makes it a choice in nanocomposite structural analysis [29]. The scanning electron microscopy (SEM) or high resolution scanning electron microscopy (HRSEM) is another important tool in nanocomposite structural analysis. They provide micro-structural details of the nanocomposite usually from fractured surfaces and are very useful tools for comparable purpose.

One important step in polymer-nanocomposite preparation is mixing together the polymer and clay powder. Appropriate mixing tools have to be used to ensure that the clay layers are well dispersed in the polymer matrix for optimum microstructure which in return yields the desired material properties. Mechanical stirrer, shear mixer and ultrasonic equipment are the widely used mixing tools for the process of blending. They are either used individually or the latter supplementing the formal in the mixing process. Ultrasonication has been used extensively in polymer-clay blending. The various researchers utilize different mixing times in their mixing process. Part of the focus of the present research is to find the effect of mixing time on the structure and some other important mechanical properties of epoxy-clay nanocomposite.

Polymer-clay nanocomposite has potential application in food and drug packaging against moisture [26] and in pipes for liquid transportation. It has been used in the body panel of automobiles such as doors, hoods and bumpers [29]. The pioneer group at the Toyota research laboratory used the nanoclay modified Nylon6 in the timing belt of the Toyota engine [29].

1.1. Methods of synthesizing polymer-clay nanocomposite.

Different processing routes have been adopted in the synthesis of polymer-clay nanocomposites. The choice of a method depends on the type of polymer, the suitability and practicability of the process to the polymer type and the process parameters needed to be studied. The economy of process is also an important consideration. The major types of processing methodology for polymer nanocomposites are discussed in the following sections.

1.1.1. Solution intercalation

In this method, both the polymer and clay are dissolved in suitable solvent for intercalation or exfoliation to take place. The technique is based on the known fact that the silicate stacks are held together by weak interlayer forces which can be overcome in appropriate aqueous solution. After the silicate layers have been swollen by polymer, the solvent is vaporized, usually under vacuum, or precipitated to recover the polymer-clay hybrid. During evaporation of the solvent, the layer silicates reassemble, sandwiching the polymer to form polymer nanocomposite. Intercalated nanocomposite is to be highly possible under this method [26]. The disadvantage of this process is the low chance of finding a solvent in

which both polymer and silicate are soluble. It is also not feasible for large scale production considering the amount of solvent that would be needed.

1.1.2. Template synthesis

This is a recently developed processing method for polymer-clay nanocomposite. Synthetic clay is prepared within the polymer matrix through in situ hydrothermal crystallization of gels from a mixture of silica sol, magnesium hydroxide, lithium fluoride and selected water-soluble polymers in solution. As the polymer aids the nucleation and growth of the inorganic host crystal, it gets trapped within the layers as they grow. This method allows the task of modifying clay with onium ions to be skipped, and has the potential of promoting well dispersed system. Yet, it is rarely workable with many polymers. Also, the clays under this condition are described as poorly ordered fluorohectorite and have the ability to aggregate presenting a disadvantage [26]. The description of this method suggests that high temperature is involved in processing. Hence, it can lead to polymer degradation.

1.1.3. Melt intercalation

The technique is a solvent free method. It consists of blending the layered silicate with the polymer matrix in the molten state. If conditions are favourable, i.e., the polymer and nanoclay are compatible, molten polymer chain can migrate into the intergallery space of the clay. The effectiveness of melt intercalation can be improved by using microwave (MW) irradiation. The energy is mainly absorbed by the water molecule associated to the interlayer cations. As a result, the polymer and eventually the clay minerals are heated, prompting rapid entry of the polymer into the interlayer space of the clay. The MW-assisted melt

intercalation saves energy and time compared to the conventional heating oven [26]. The technique of melt intercalation of polymer into phyllosilicates is considered as one of the major practical steps forward in the field of nanocomposite preparation. Melt intercalation is already in use at commercial level to prepare polymer-clay nanocomposite.

1.1.4. *In situ* polymerization

This is a widely used technique for nanocomposite preparation and the only practical method for preparing epoxy-clay nanocomposite. It was the method used by the pioneer of the application of polymer nanocomposite [30]. This process employed the monomer of the intended polymer for intercalation or exfoliation. It consists of swelling the layered silicates with the monomers or monomer solution of the polymer, and then followed by polymerization inside the intergallery space of the clay. Crosslinking (polymerization) reaction is then initiated by mixing the monomer-clay blend with suitable organic initiator called curing agent which causes crosslinking to proceed at ambient or elevated temperature. Self-polymerization polymer can start to crosslink by the application of heat or radiation. *In situ* method has proved to be most successful for epoxy-clay nanocomposite preparation both at laboratory and industrial scale. This is because epoxy is a thermosetting plastic that is scarcely soluble in many solvent and once crosslinked can not be remolded by reheating. Like melt intercalation, *in situ* polymerization has been used at commercial scale to prepare polymer nanocomposite.

1.2. Structural models of polymer-clay composite

As mentioned in the previous section, the performance of polymer-clay nanocomposite is

very dependent on its morphology. This morphology implies to the manner of clay residence within the polymer. A mere blend of polymer and clay does not necessarily produce a nanocomposite [29]. The structure of the clay-polymer mixture as revealed in x-ray diffraction (XRD) spectrum or transmission electron microscopy (TEM) determines whether a nanocomposite is formed or not. There are three forms of polymer-clay composite on the basis of structural characteristic.

1.2.1. Polymer-clay composite

Polymer-clay composite can be described as a mere physical mixture of polymer and clay in which no polymer chain enters the gallery of the clay. Its features are analogous to the traditional micro composite material (figure 1.1a). Because there is no miscibility between the clay and the polymer, the mechanical property is usually poor and there is the tendency for phase separation [29].

1.2.2. Intercalated nanocomposite

In this type of nanocomposites, one or few polymer chain(s) enters into the gallery layer of the clay particle causing a finite increase in intergallery separation (figure 1.1b). The stacking arrangement of the clay layer is still maintained. The result is a well ordered multilayer structure of alternating polymeric and inorganic layers, with a repeat distance between them. Intercalation causes less than 20–30Å separation between the platelets [29].

1.2.3. Exfoliated or Delaminated nanocomposite

An exfoliated nanocomposite is formed when the individual clay layer is separated from the clay stack and dispersed randomly and independently within the polymer matrix (figure 1.1c). Under this condition, the clay gallery structure is completely destroyed, hence the name delaminated nanocomposite. It has been established by researchers [1, 27] that exfoliated nanocomposite shows better material properties than its intercalated counterpart. Therefore, the interest of the majority of research is an exfoliated morphology, because its structure makes available maximum surface area for interaction and load bearing. It is observed that completely exfoliated structure is hard to achieve [1, 14,]. The major possibility is a mix of partially exfoliated and partly intercalated structure [1, 20, 27].

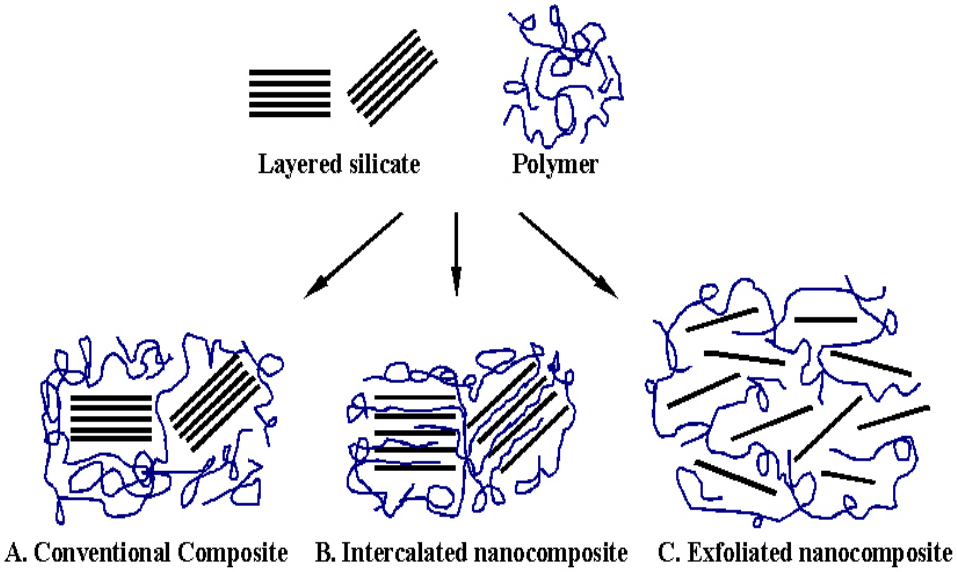

Figure 0.1. Schematic of different type of nanocomposite arising from interaction of layered silicates and polymer [31].

1.3. Mixing methods

To obtain nanocomposite from a blend of polymer and clay, clay aggregates and particles should be broken into their nanoscale building blocks or, at least, some polymer chains ingress the space between clay layers with the help of some dispersion processes [28]. So, the swelling of nanoclay in polymer for in situ polymerization technique requires suitable blending means. Mixing nanoclay into polymer, especially epoxy, has been through mechanical and ultrasonication techniques. Prior to swelling clay in polymer by either means, manual mixing, through the use of stirring rod or any other suitable mixing tool, is usually done for initial swelling and for breaking down clay aggregates. This pre-mixing also prevents clay powder from 'flying away', especially under sonication. Whatever processing method chosen, the primary goal is to separate or swell the clay particles and uniformly disperse them in the polymer.

1.3.1. Mechanical mixing

Mechanical mixing or shear mixing is a very broad term that can be applied to mechanical blades, rollers or manual hand mixing used for mixing clays with the resin [32]. Shear mixing method, high pressure mixing method, direct mixing, centrifugal mixing and three-roll milling can be classified under mechanical means. All these involve the action of high speed rotating blade or ball mills with a shearing action that disrupt the gallery pattern of the clay. During mixing, the shear action of these tools also breaks the clay platelet reducing its aspect ratio.

1.3.2. Ultrasonication

Ultrasonication is a technique that uses ultra-high frequency vibration via a phenomenon called cavitations to disperse clay in polymer. The sonication action creates pressure waves in the processed media. This action forms millions of microscopic bubbles (cavities), which expand during the negative pressure phase and burst violently during the positive excursion. This phenomenon, referred to as cavitation, creates millions of shock waves in the liquid, as well as elevated pressures and temperatures at the implosion sites. Although the cavitational collapse lasts but a few microseconds, and the amount of energy released by each individual bubble is minute, the cumulative effect causes extremely high levels of energy to be released into the processed media.

1.4. Epoxy resins and nanoclay materials

In this section, the two materials; epoxy and nanoclay, which combine to form epoxy-clay nanocomposite are discussed. This will include the major characteristics and applications of both materials.

1.4.1. Epoxy resins

Both thermosetting and thermoplastics have long been used extensively in the processing of polymeric nanocomposite. Among thermosetting polymers, epoxy resins stand out because of their wide range of properties that suit varieties of engineering applications. It also has that unique feature of being compatible with a variety of curing agents. The amount of epoxy resins manufactured and consumed are insignificant in comparison with polyethylene, polypropylene and polystyrene, yet in terms of complexity of technology, variety and

breadth of application, epoxy resins are surely superior to all other plastics and resins [33]. The main portion of epoxy resin is derived from bisphenol-acetone and epichlorohydrin (Figure1.2).

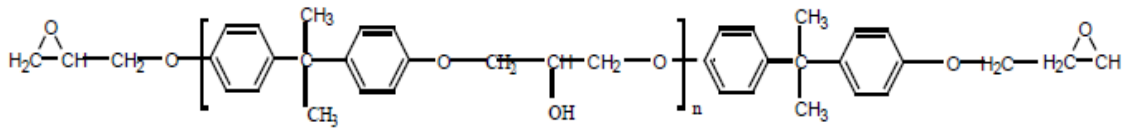

Figure 1.2 Chemical structure of an epoxy resin [31].

The resin is characterized by reactive oxirane ring which can be reacted with curing agents or catalytically homopolymerized to form a hard infusible three-dimensional network in which the resin molecules are crosslinked together by means of strong covalent bonds. This reaction is termed polymerization, but is more commonly called curing or hardening. Cured epoxy resins have good mechanical properties, superior dimensional stability and good resistance to heat and chemical attack [34]. Because no small molecules, such as water, or volatile liquid is liberated during the curing of epoxy resin, they unusually exhibit low shrinkage, and they can be formed and cured under contact or low pressure [34]. Epoxy is used in flooring, pipe coating and adhesives. Also, huge amount of epoxy resins are used in glass fiber reinforced polymers (GFRP) pipes for water and crude oil production, transportation and storage, and as well as in automobile and aircraft structures. The simple resin-curing agent combination alone seldom provides a material with all the properties required for use in particular application, and other materials must be added so as to modify the properties of the cured resin [33].

1.4.2. Clays

(Nano)clays are naturally occurring material composed primarily of fine-grained minerals which are plastic with certain amount of water contents and harden when dried or fired. Synthetic clays have also been formulated from clay element through chemical processes. Clays have layer structure with one dimension in the nanometer range; the thickness of which is about 0.7-1 nm, hence the name nanoclay (Figure 1.3).

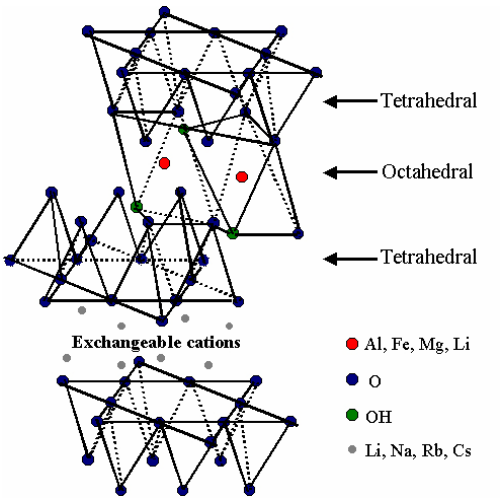

Figure1.3: Idealized structure for montmorillonite [31].

The clay layered structure is either in 1:1 or 2:1 proportion. The commonly used nanoclay for polymer-nanocomposite processing is the montmorillonite. Montmorillonite belongs to the 2:1 proportion clay. These types of clays have each platelet (layer) in the clay particle made up of an octahedral sheet sandwiched between two opposing tetrahedral sheets. The layer is usually negatively charged, and the space between two adjacent layers is occupied by anhydrous cations whose position depends on the layer charge location. Common tetrahedral site ions are Si^{4+}, Al^{3+} and Fe^{3+}. Ions such as Al^{3+}, Fe^{3+}, Fe^{2+}, Mg^{2+}, Zn^{2+} and Li^{+} are found in the octahedral sites. The ions in both the octahedral and tetrahedral sheets are

coordinated to oxygen ions which gives the layer its net negative charge. The interlayer spaces are generally occupied by Na^+, K^+, Ca^+, and Mg^+ ions, which balance the negative 2:1 layer charge. Interlayer ions are commonly hydrated and readily exchangeable. It is reported that most of the technological application of clay, nanocomposite inclusive, is related to the reaction that takes place in the interlayer space [26]. The clay particle is usually about 1 nm thick with other dimensions being above 100 nm, giving the clay an aspect ratio in the range of 100-1000.

The composition of the clay particles (ionic and polar in nature) normally makes it hydrophilic, which mean its interaction with organic substance is quite difficult. However, the presence of the replaceable cations in the interlayer space makes possible the modification of the clay chemistry. For the preparation of polymer-clay nanocomposites, the exchangeable inorganic cations are replaced by cationic organic molecules (e.g., aliphatic and aromatic amines) which change the clay from being hydrophilic, or organophobic, to organophilic. Commonly used organic cations are alkylammonium ions. These organic molecules increase the miscibility of the clay with polymers. Nanoclay particles are of colloidal size with high specific area. It has large cation exchange capacity and variable interlayer separation. It also has the ability to show interlayer swelling in water, and under optimum condition, the layer can completely delaminate (exfoliate). The ability of clay particle to increase in layer spacing (intercalation) or completely delaminate (exfoliation) is the driving force behind nanocomposite mechanical, electrical and physical properties [26].

1.5. Thesis outline

The introductory chapter has been devoted to polymer nanocomposites in general even though the focus of this work is epoxy-clay nanocomposite. Polymer nanocomposite is a generic name for a material group with similar characteristics both in preparation, characterization and properties. Therefore, a general discussion for the group aptly applies to any of its members. The rest of this thesis will focus on epoxy-clay nanocomposite. Chapter two will be the literature review with emphasis on the topics pertinent to the thesis objectives. At the end of chapter two, the objectives and scope of the work are stated. In chapter three, detailed experimental procedures will be presented. These include mixing methods, curing cycle, characterizations using wide angle x-ray diffraction (WAXD), differential scanning calorimetry (DSC), scanning electron microscopy (SEM), energy dispersive spectroscopy (EDS) and mechanical testing. This will be followed by experimental results and discussions in chapter four. Conclusions and recommendations for future work directions are given in chapter five.

CHAPTER 2

2.0 LITERATURE REVIEW

2.1 Introduction

Ever since a research group at Toyota incorporation, Tokyo, Japan, reported improvement in the properties of Nylon 6 by incorporating nanoclay into it [30], the interest in polymer-clay nanocomposite has grown. Consequently, numerous researches have been conducted in this area over the years to further explore the behaviours and potentials of polymer-clay systems. Reports of change in the tensile strength, elastic modulus, impact strength, hardness, fracture toughness, flame retardancy, thermal stability and reduction in moisture absorption of polymers in general abound in the open literatures. Many factors are identified as being responsible for the final morphology and behaviours of this class of materials. More importantly, there is the convergence opinion in the open literature that the degree of clay exfoliation/intercalation is the major controlling factor for the improvements observed in the properties of polymer-clay nanocomposites [12, 15, 16]. Exfoliation and intercalation (figure 1.1) are the technical terms to describe the state of dispersion of the clay in the polymer (Refer chapter one and figure 1.1). Thus, the modifications in the properties of polymers in general and epoxy in particular, are almost always a function of the manner and level of dispersion of the clay phase in the epoxy matrix. The processing route chosen, on the other hand, influences the level of exfoliation/interaction that can be achieved. The need to investigate the effect of processing parameters on the final morphology and the properties of epoxy/nanoclay system is therefore important. With the understanding of parameters involved in a particular processing method and the way they control the morphology and

property of the nanocomposite, nanocomposites of predetermined structure and feature can be prepared. The review that follows sieves through some of the research activities in the area of polymer/clay nanocomposites with emphasis on the work done on the subject of epoxy/clay nanocomposites.

2.2. General literature survey on epoxy-clay nanocomposite

Isik et al [2] have reported the synthesis and characterization of impact modified epoxy/montmorillonite nanocomposites from Araldite M and Cloisite 30B. Blending was done by mechanical stirrer for 2 hours and ultrasonic bath for 30 minute. X-ray analysis showed increase in the d-spacing from 1.83 nm to 3.82 nm for 3% montmorillonite. The glass transition temperature (T_g) rose from 72^{o}C for neat epoxy to 85^{o}C for nanocomposites at same nanoclay content of 3%. However, the enhancement in the T_g could also be due to the presence of an impact modifier, polyether polyol, as there was decrease in T_g when no polyether polyol was present in the nanocomposites. Tensile strength was decreasing with increasing amount of clay. This was attributed to higher concentration effect of clay agglomerates at high clay contents which decreased polymer-clay surface interaction. The tensile modulus, however, increased as clay content increased. They inferred that since the clay has a higher modulus than the polymer, and composite being dependant on the ratio of the filler modulus to matrix modulus, hence the improved tensile modulus of nanocomposite.

Mechanical properties of nanocomposites prepared from the epoxy resin Araldite 251 and Garamite 1958 clay were investigated by Ho et al. [8]. While the ultimate tensile strength and Vickers' hardness of the nanocomposite were rising with increasing nanoclay volumes,

its ductility initially dropped gradually, then decreased drastically to 70% of the ductility of the pure epoxy at 8wt% of clay. Five percent weight samples of nanocomposite showed the highest level of improvement. Above 5wt% of clay, both the ultimate tensile strength and Vickers' hardness began to drop. The maximum increases were 5% for ultimate tensile strength and 15% for Vickers' hardness. It was concluded by the authors that for good mechanical properties, the nanoclay level be kept below 5wt%.

An experimental investigation on the mechanical properties of clay/epoxy nanocomposites produced in a centrifuge was carried out by Samandari et al. [9]. Four different types of nanocomposites from four Cloisite based montmorillonite, designated as A, B, C and D, of varied cation exchange capacity (CEC); 125, 95, 90, and 90 millieqivalent (meq)/100 g, respectively were prepared. The polymer used in their work was epoxy Araldite K3600 kit, described as consisting of low viscosity epoxy resin and hardener. Clays A, B and C were modified with quaternary ammonium salt, while D had ternary ammonium as the compatibilizer. They observed that the elastic moduli of the nanocomposites increased with increasing clay loading. The highest being 1.6 GPA at 6% clay content, shown by the nanocomposite whose clay was modified with ternary ammonium salt. They claimed that the decrease in the modulus after 6% clay content was because of the ductility of the clay becoming dominant at increasing clay volume, because clay has lower ductility relative to epoxy. The tensile strength increased with increase in clay volume except the clay D of 90 meq/100 exchange capacity modified with quaternary ammonium. The fluctuations in measured tensile strengths were linked to the presence of air bubbles and different surface modifiers. They found that for the type of epoxy used, curing temperature of about100ºC

gave the optimum enhancement of mechanical properties. This implies that curing cycle temperature depends on the type of epoxy-hardener mixture.

Zhou et al. [10] used an ultrasonicator to disperse K-10 montmorillonite in SC-15 epoxy resin. The sonication time was 90 minutes for all samples prepared with 1, 2, 3 and 4wt% nanoclay loadings. Improvement in flexural properties was recorded in all the nanocomposites over the neat epoxy. The maximum increase in both the flexural strength and flexural modulus was from the 2wt% nanocomposite. A 27.1% increase in flexural strength and 31.6% rise in flexural modulus were reported for the 2wt% nanocomposites above the pure epoxy.

A comparative study of nanocomposites synthesized by sonications and shear mixing was conducted by Dean et al. [11]. They used Bath sonicator, Cell disruptor horn sonicator and shear mixing method to process 1, 2.5 and 5wt% nanocomposites from SI-ZG-15 epoxy resin and Nanomer I.28E. Each sample prepared by the sonication bath lasted a total duration of 4 hours- 3 hours for dissolving the clay in acetone while 1 h was used to blend the epoxy with dissolved clay. A mixing time of 60 minutes was used for the samples processed by cell disruptor horn sonicator. Results of flexural and compressive tests from their work revealed improvement in the nanocomposites over the virgin epoxy. In addition, they have shown that the samples synthesized by sonications showed better improvement in mechanical property over the ones prepared using shear mixing device. The authors also reported that SEM images of fractured samples showed that clay particles were more uniformly dispersed and separated in the sonicated samples than those of the shear mixer.

Their results from dynamic mechanical thermal analysis (DMTA) indicated that the glass transition temperatures, T_g's, of the nanocomposites were not better than that of the neat epoxy. Only three out of the nine samples prepared had their T_g's 5ºC above that of the neat epoxy. The rest of the samples had T_g's, below or same as the neat epoxy.

The effect of processing parameters and clay volume fraction on the mechanical properties of epoxy-clay nanocomposites were studied by Zunjarro et al. [12]. Two different processing routes were adopted by the authors, namely, shear dispersion and ultrasonic disruption. The nanocomposite starting materials were Nanomer I.30E clay and Epon 862 epoxy resin. The clay amount was varied from 0.5 to 6 wt%. They compared the trend of mechanical properties in relation to the clay concentrations and processing methods. The investigation by x-ray diffraction showed exfoliated clay structure in some of the nanocomposites they fabricated. They reported that low clay-content nanocomposites of 0.5-2wt% clay loading showed complete exfoliation, while the 4% clay nanocomposites structure was unaltered in its intergallery spacing. Flexural modulus increased monotonously with increasing clay volume. From SEM micrographs, they concluded that the high speed shear mixing method rather than ultrasonication resulted in better exfoliation and mechanical properties. This is in contrast with the results obtained by Dean et al [11] who summed up that ultrasonication was better than shear mixer for clay dispersion.

Epoxy-clay nanocomposite as matrix for glass fibre-reinforced composites was developed by Kornmann et al. [13]. Clay nanocomposite made from synthetic clay fluorohectorite and DGEBA CY 225 resin was used as laminates over glass fiber. Results of mechanical testing

showed that 10wt% of the layered silicates added to the epoxy increased its Young's modulus by 54%; from 3 GPa to 4.7 GPa. A 36% decrease in tensile strength was also reported. The nanocomposites as matrix in glass fibre laminates marginally increased its Young's modulus by 6%, while the flexural strength increased by 27%. The increase was linked to the presence of layered silicate at the surface of the glass fibre which might have improved the interfacial properties between the epoxy-clay matrix and the reinforcing fibres.

Lam et al. [14] assessed the micro-hardness of nanocomposites prepared under different sonication time from Araldite GY251 and Nanolin DK1 clay. SEM images of nanocomposites at varied sonication times initially indicated a decrease in the cluster size of clay at increasing sonication duration. They observed from SEM micrographs and by the use of Bragg's equation on data from their X-ray diffraction that exfoliation was not enhanced by prolonged sonication. Only the sizes of nanoclay clusters were reportedly changed from nearly 100 nm in diameter at 5min to 10 nm at 10 min. A maximum micro-hardness value of 12.05 Hv was reported at 10 min sonication time. Above 10 minutes, the micro-hardness value went down to 7.09 Hv at 60 min (figure 2.1). An increase in cluster size and distance was reported from SEM micrograph for nanocomposites sonicated above 10 minutes, which they claimed explains the reduction in the micro-hardness. They, thus, concluded that the best sonication was 10 minutes since the maximum enhancement in hardness was obtained.

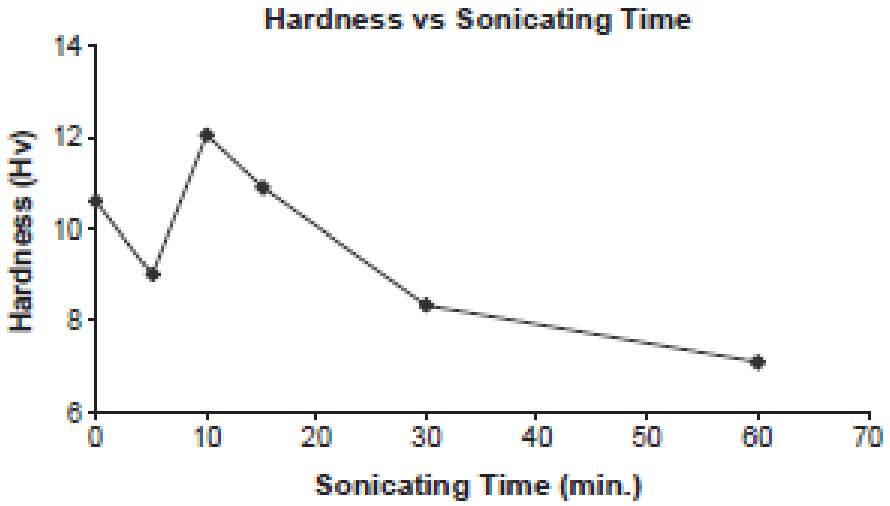

Figure 2.1 variation of microhardness with sonication time for 4% nanocomsite [14].

Liu et al. [15, 16] reported the processing of high performance epoxy nanocomposites by mixing N, N, N′ N′-tetraglycidyl-4, 4-diaminodiphenylmethane (TGDDM) and an octadeyl amine modified montmorillonite, Nanomer I.30E, through direct mixing method (DMM) and high pressure mixing method (HPMM). They also processed composites from unmodified clay, Cloisite Na^+. Their aim was to study the correlation between morphology and mechanical/physical properties of the nano/filler composites. They observed that there were agglomerates present in both the Cloisite Na^+ (filler) composite and nanocomposites. The size (about 25 μm in diameter) and quantity of agglomerates in the nanocomposites, especially the DMM samples, were reportedly larger than those in the filler composites. The HPMM samples have fewer agglomerates with maximum diameter of 1-2 μm compared to those of DMM at the same clay loading. The diameters of agglomerates increased with increasing clay loading in the sample made by DMM. The less agglomerates present in the HPMM specimens were attributed to high level of exfoliation. SEM image showed the presence of voids in the sample from DMM. Also, fracture surface images showed a smooth,

featureless surface for the pure epoxy as opposed to the rough surface of the nanocomposite. They noticed that the HPMM approach decreased the solubility of the hardener (DDS) in the epoxy (TGDDM), produced high void content and violent exothermic polymerization at higher clay content. Thus, the HPMM, in spite of the high level of exfoliation achievable, may not be realistic for high clay content. Both enhancement and compromise in mechanical properties were reported. They reported an increase in the modulus of the epoxy mixed with modified clay by 20%, but only 10% increase in that embedded with untreated clay. However, the nanocomposite has slightly lower yield strength than the composite filled with unmodified clay. While the results of this work showed the influence of modified clay on epoxy's physical and mechanical properties, the role which processing method plays in the morphology of nanocomposites and, by extension, their properties is obvious.

Dai et al. [17] made comparative studies of the effect of intercalating agent on the physical properties of epoxy-clay nanocomposite materials. In the study, dodecyltriphenyl-phosphonium bromide (Φ_3P^+-C_{12}) and hexadecyltirmethyl-ammonium bromide (Me_3N^+-C_{16}) were used as the modifying agents for MMT-Na^+. Wide angle powder XRD showed that both modified clay have higher d-spacing than the pristine clay. The Φ_3P^+-C_{12}- modified clay was reported to have superior dispersion capability. TEM morphological images of nanocomposites from the Φ_3P^+-C_{12}- modified clay were reported to have better dispersion of clay on their surfaces. An enhancement in the storage modulus of the neat epoxy from 2311 MPa to 3597 MPa was reported. Glass transition temperature, T_g, was also enhanced by 44% and this was attributed to the clay modifying agent.

Velmurugan and Mohan [18] synthesized nanoclay-epoxy composite at room temperature using electric shear mixer with an approximate speed of 1000 rpm. The processing materials were Araldite LY566 resin and garamite-1958 nanoclay with triethyl tetra amine (TETA) as the curing agent. X-ray diffraction patterns indicated an increase in the intergallery distance of the modified clay in the epoxy representing either an intercalated or exfoliated structure. They observed an improvement in the elastic modulus, which they linked to the exfoliation/intercalation of nanoclay particles in the matrix. The nanocomposites were however lower in tensile strength than the neat epoxy. This was attributed to the presence of voids in the nanocomposites which caused material failure early enough during tensile testing. The Shore hardness of both the neat epoxy and 1-5 wt% nanocomposites were almost the same. The hardness of the nanocomposite began to rise above the neat epoxy after more than 5wt% of clay was added. A maximum D Shore hardness of 86 was achieved, shown by nanocomposite 10wt% clay content.

Yasmin et al. [19] assessed the morphology and mechanical behaviours of clay-epoxy nanocomposites produced by three-roll mill method. The epoxy resin, Araldite GY6010, and tallow modified clay, Cloisite 30 B, were used as the synthesizing materials. Using transmission electron microscopy images (TEM), a homogeneous dispersion of clay particles in polymer cross section was reported for all clay volumes, even at high viscosity. With the level of exfoliation/intercalation achieved, they suggested that the extra shear force and residence time applied in the study was beneficial. A 25% improvement in elastic modulus at 1wt% clay loading was reported, and it rose to 80% when the clay loading was increased to 10wt%. Unlike the elastic modulus, the tensile strength of nanocomposite was lower than

that of pure epoxy (figure 2.2a). They assumed that the low strength of the nanocomposite relative to virgin epoxy was due to the processing technique. They noted that the compounding of nanoclay in an epoxy matrix with a three-roll mill produced a highly viscous and foamy material, and the higher the clay content the higher the viscosity. Thus the highly viscous mixture hinders complete degassing of the nanocomposite before casting. This produced voids in the cast nanocomposite which thereby became crack initiation sites at low strain. With prolonged degassing and casting done in open mold, an improvement in the tensile strength of about 45% was observed (figure 2.2b). However, this value was still lower than the neat epoxy by 5MPa, accounting for 8% decrease in tensile strength. Consequently, they concluded that with better degassing, nano-to-microsize void would be reduced resulting in improved tensile strength.

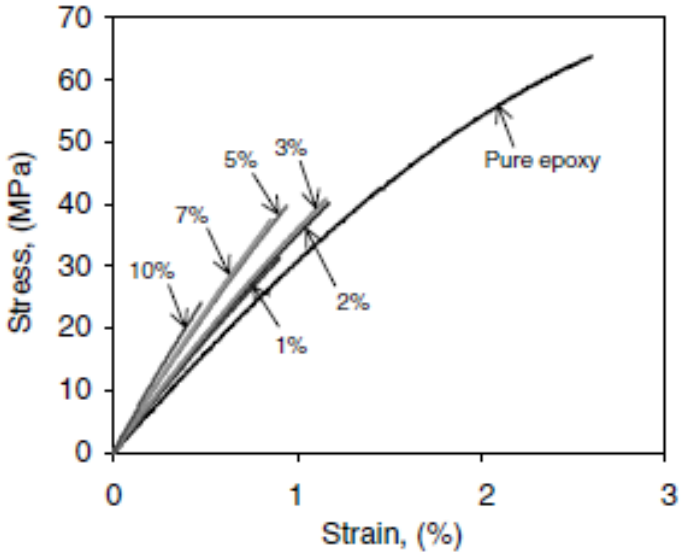

Figure 2.2a: Stress-strain behaviour of clay nanocomposites [19].

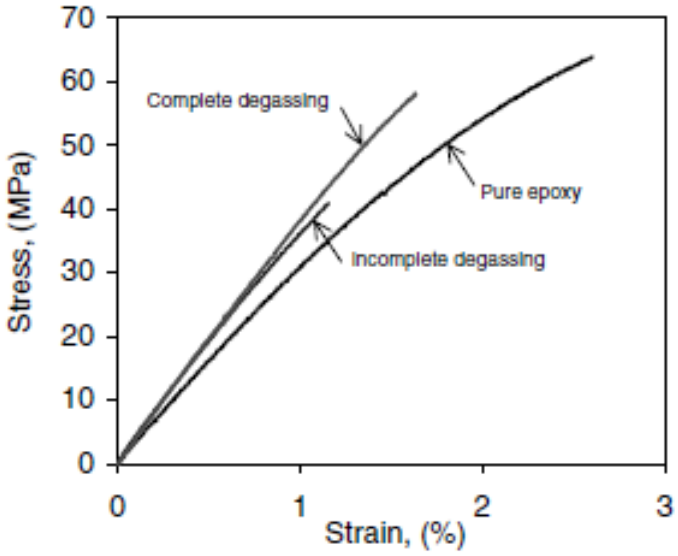

Figure 2.2b: Effect of degassing on the tensile strength of 3 wt% nanocomposite [19].

Hussein et al [20] prepared epoxy clay nanocomposites from Epikote system, a bisphenol based epoxy, and I.30E clay to study the effect of nanoclay concentration on the cured behaviour of the system using on-line cured system. Epoxy-clay blends of 1%, 2%, 3%, 5% and 8% clay were mixed by a combination of mechanical stirrer and ultrasonication. They found that the addition of clay reduced both the gelation time and the total reaction time of the epoxy system. They have reported from wide angle x-ray diffraction analysis that intercalation resulted for all the compositions. Besides intercalation, platelets of delaminated layers were observed in Transmission electron microcopy (TEM). From Differential Scanning Calorimeter (DSC), the glass transition temperature, $T_{g,}$ was found initially to be marginally lower than or showed no difference from the neat epoxy for clay contents up to 3% clay fraction. Beyond 3%, the decrease in T_g became noticeable. Tensile properties of nanocomposite were found to be lower than that of the neat epoxy, except at 1% clay fraction when its tensile strength was above the neat epoxy by a marginal 2 MPa (figure 2.3).

However, modulus of elasticity of nanocomposite was higher than that of the neat epoxy and it was attributed to the higher modulus of the clay. The authors claimed that the gradual decrease in tensile strength with higher clay contents was due to the stress concentration effect of stacked layer structure particle, which ultimately reduce the adhesion strength at nanoclay matrix interface.

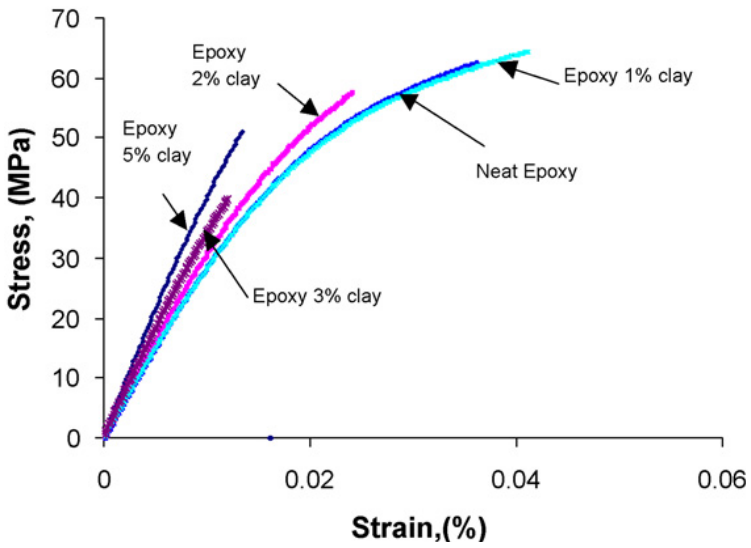

Figure 2.3: Stress-strain behaviour of epoxy-clay nanocomposites [20].

Wang and Qin [22] studied the effect of ultrasonic stirring time on the thermal and mechanical properties of epoxy-nanoclay composites made from the DOW epoxy, D.E.R.332, and Nanomer I.30E nanoclay. The curing agent used was 4, 4′-diaminodiphenylsulphone (DDS). Observation made from X-ray diffraction in the Bragg's angle range of 2-5º showed no peak for the nanocomposites. They suggested that the absence of any peak may be due to the fact that the inter-lammellar distances are too wide to be detected by the X-rays. With the extent of clay separation the authors observed, they

concluded that increasing duration of ultrasonic stirring time caused both the swelling time and the rate of diffusion of the epoxy monomers into the clay to also increase. This allowed homopolymerization to occur to a greater extent, as a result, separating the clay layers further apart. However, a decrease in glass transition temperature, T_g was noticed when the ultrasonic stirring time was increased.

Wang et al. [23] studied the influence of clay concentration on the morphology and properties of clay-epoxy nanocomposites prepared by in-situ polymerization under ultrasonication. Diglycidyl ether of bisphenol A (D.E.R 332) and the hardener 4, 4'-diaminodiphenylsulphone were mixed using mechanical mixer at 400 rpm for 30 minutes. The clay, Nanomer I.30E modified with alkyammonium ions, was added and stirred mechanically for 1 hr, and then the whole mixture was stirred ultrasonically for 2 hours. Samples of 2.5, 5 and 7.5 wt% were prepared during the study. From x-ray diffraction data, they confirmed the separation of clay layers in the epoxy. The layer spacing decreased with increased clay concentration which was attributed to homopolymerization of epoxy monomers between clay layers. The glass transition temperature (T_g) was also reported to be decreasing with increasing clay amount because of the presence of more alkylamonium ions. They claimed alkyammonium ions took part in the chemical reaction with epoxy groups prior to the addition of hardener resulting in the formation of more branched polymer which has lower T_g instead of crosslinked polymer. They concluded that ultrasonication is effective in dispersing clay in polymer, yet it depends on the amount of clay, and that complete exfoliation is difficult.

Benfarhi et al. [24] reported the synthesis of epoxy-clay nanocomposites by light-induced

crosslinking at room temperature. The nanocomposite starting materials were montmorillonite K10 nanoclay modified with hexadecyltrimethylammonium chloride and Araldite CY-179 epoxy resin. Triarylsulfonium SbF6 salt (Cyracure UVI-6976) was used as cationic-type photoinitiator. The authors claimed that the use of photo-initiated polymerization provides solvent-free route for processing polymer-nanoclay composite. They reported drops in both the glass transition temperature from 93ºC to 30ºC and the Young's modulus from 1320 to 910 MPa. The glossiness of the nanocomposite was less than the neat epoxy which they attributed to uniform distribution of the nanoparticles.

Qi et al. [27] investigated the effect of nanoclay additives on the mechanical properties of DGEBA-based epoxy. Unmodified montmorillonite (MMT-Na^+) and three modified clay types, namely Cloisite 30B, Nanomer I.30E and MMT-CPC, were used to produce different nanocomposites. The general trend of their results showed there was increase in tensile moduli. Unusually, the untreated clay showed the highest level of improvements; 26.9% rise in tensile modulus for 10wt% clay. The increase in tensile modulus was attributed to the stiffness effect of the clay. Both the tensile strength and failure strains were lower than the neat epoxy. The MMT-CPC nanocomposite showed a 30.4% decrease in strength, while the cloisite 30B nanocomposite had a 43% decrease in failure strain. The findings of this work seem contradicting with most other works in which modified clay, rather than unmodified one, is shown to give a higher value of tensile modulus. However, morphological data from the work indicates inhomogeneous, low degree of exfoliation and the presence of voids and agglomerates, which underscore the reason for the decreases that were observed in the properties of the nanocomposites. Under such condition, the authors reported that the clay

volume becomes the controlling factor rather than the dispersion or the surface modifiers.

Part of the work of Harnandez et al. [28] was to compare dispersion of clay in nanocomposites prepared by both melt process and ultrasonication. After mixing Cloisite 30B clay in a THF solution for 30 minute sonication time, DGEBA LY556 resin was added, mixed mechanically, and cured with MDA. They concluded from the small angle x-ray scattering (SAXS) analysis of their samples that ultrasonication produced more homogeneously distributed clay particles than the melt process which contain large size agglomerates.

2.3. Thesis objectives

The foregoing literature survey reveals that the extent of clay dispersion in polymer matrix is the most significant factor controlling the physical, thermal and mechanical properties of epoxy-clay nanocomposite. However, the quality of exfoliation/intercalation that is achievable is influenced by the type of polymer matrix, clay type and concentration, type of clay functionalizing agent, curing agent, curing temperature and the mixing techniques adopted. Also, there is no convergent agreement on the change observed in the properties resulting from the nanocomposites. From the works of authors who used sonication techniques, the conclusion can be reached that the method is an effective means of dispersing clay in epoxy. However, the number of researchers who investigated the effect of sonication time, an important processing parameter, on the mechanical properties is scarcely enough to come to the firm conclusion on the effect of sonication time on nanocomposite properties. Thus, the aim of the present work is to synthesize epoxy-clay nanocomposite via *in situ*

polymerization using ultrasonication technique for blending. Different sonication times of 5, 10, 30 and 60 minutes will be used. The clay dispersion in relation to sonication time will be studied. The tensile properties and Vickers hardness of each nanocomposite will be investigated in relation to sonication time. Clay amounts of 2, 4 and 5 per hundred grams of epoxy resins will be considered. The main objectives of the thesis are:

i. To synthesize epoxy-clay nanocomposite using different sonication duration under *in situ* polymerization

ii. To study the effect of sonication time and clay loadings on clay dispersion in epoxy resin.

iii. To study the effect of sonication time and clay loading on the tensile properties and Vickers' hardness of epoxy-nanoclay composites.

iv. To investigate the relationship between nanoclay dispersion and nanocomposite properties.

2.4. Work justification and motivation

Fibre-glass reinforced epoxy (FGRE) pipes are replacing metal pipes for water and oil transportation in the Kingdom of Saudi Arabia. However, the moisture absorption of epoxy and its composite are still major problems that are not yet solved. Absorption of moisture degrades epoxy base pipes. Recent works at reducing the water absorption of epoxy by incorporating nanoclay has led to the reduction in the mechanical strength, especially tensile properties of epoxy. The present study hopes to find out the effect of different clay amounts on epoxy-nanoclay composite whose broad application will be to reducing the moisture

absorption rate of epoxy used for fibre glass reinforced epoxy (FGRE) pipes. The outcome of which would be of importance to industries within the Kingdom producing fibre glass reinforced epoxy (FGRE) pipes. Moreover, the sonication technique adopted in this work for blending epoxy with clay is simple and economical.

CHAPTER 3

3.0. EXPERIMENTAL PROCEDURE

In this section, the materials used for processing the epoxy-clay nanocomposite are described with respect to their sources and key properties. The step-by-step experimental procedures adopted in the present work are detailed out and the equipments used in conducting experiments and analyzing samples are explained.

3.1. Materials

The epoxy used in the present work is Araldite GY6010 CRS, manufactured locally by Jubail Chemical Industries Company (JANA). It is a general purpose unmodified liquid epoxy resin based on bisphenol A and epichlorohydrin and is widely used in cold or heat cured systems [35]. It finds application in coatings, adhesives, matrix, filament winding and is the major raw material for pipe industries in the Kingdom. The curing agent is Aradur^{TM} 42 manufactured by Huntsman Advanced Materials Americas, USA [36]. It is a low viscosity, cycloaliphatic polyamine. This hardener will not give a 100% cure for the epoxy, but for the targeted application of the composite, an optimum cure level suitable for it can be achieved. The key properties of both materials as supplied by the manufacturers are presented in table 3.1. The nanoclay is an onium-ion modified montmorillonite which comes by the commercial name I.30E. It was acquired from Nanocor Inc, USA. It is widely used in nanocomposite processing because of its ability to swell with relative ease. Important physical properties as supplied in reference [37] are given in table 3.2.

Table 3.1: Properties of Epoxy and Hardener.

Properties	**Epoxy**	**Aradur^{TM} 42**
Colour	clear	clear
Odour	slight	ammoniacal
Physical state	liquid	liquid
Viscosity @ 25^{o}C (mPa.s)	10,000-12000	10-20
Density @ 25^{o}C (g/cm^{3})	1.15-1.18	0.92
Flash point (^{O}C)	≥200	≥110
Solubility in H_2O	insoluble	NA
Epoxy value (eq/g)	0.532-0.5495/100	
Weight per epoxide (g/eq)	182-188	

Table 3.2. Specific key data for the nanoclay.

Properties	**Nanoclay**
Colour	white to gray
Odour	negligible
Physical state	powder
Solubility in H_20	negligible
Specific gravity	1.7
Boiling point	not available

3.2. Synthesis of epoxy-clay nanocomposites

3.2.1. Mixing of epoxy and nanoclay (Sonication process)

Sonic vc-33 high intensity ultrasonicator (figure 3.1) from Sonics equipment was used for blending the liquid epoxy and the required clay fraction. It operates at a frequency of 20 KHz and a power rating of 750 watt. With a standard probe of 13 mm tip diameter, the equipment can process material volume in the range 10-250 ml. The ultrasonicator is simple and easy to operate.

Figure 3.1: Set-up for sonicating epoxy and clay.

The clay proportion was measured following the method of Liu et al [15, 16]. In the authors approach clay fractions were determined as a percentage of 100g of epoxy resin. The percentage clay is then evaluated as the fraction of the weight of the epoxy, hardener and clay combined. In the current work, the required amount of epoxy and clay were measured into a beaker placed on Mettler Toledo pb303-s weighing balance (figure 3.2). This weighing instrument has a precision of 0.1 milligram. The weighing capability is from 0.2 to 320 grams.

Figure 3.2: Mettler Toledo weighing balance

The measured clay and epoxy were then gently mixed together using a stirring rod. This initial mixing is important for partial swelling of epoxy, better clay distribution, breaking down clay aggregates and preventing the clay powder from 'flying away' when taken for sonication. The beaker with the hand-mixed epoxy-clay blend was placed under the sonicator probe and clamped to a retort stand to prevent movement during sonication. Sonication was done for 5, 10, 30 or 60 minutes over a water bath (figure 3.1). A thermocouple was attached to the beaker containing the mixture to monitor the temperature of the composite during processing. The temperature was maintained around 60-70^{o}C during sonication by constantly adjusting the volume of water in the bath as the temperature tended to shoot above the set

value. This prevented excessive temperature from being induced into the material which could have led to material degradation or outright burning. The sonicator preset amplitude of 40% was used for all sonication operation. This amplitude was arrived at after several trials for the weight (60 gram) of epoxy used. With this amplitude, the equipment can be used without the need to provide external cooling source for it. Sonication was followed by degassing for 45 minutes under complete vacuum at room temperature in a Shellab vacuum oven connected to a vacuum pump (figure 3.3).

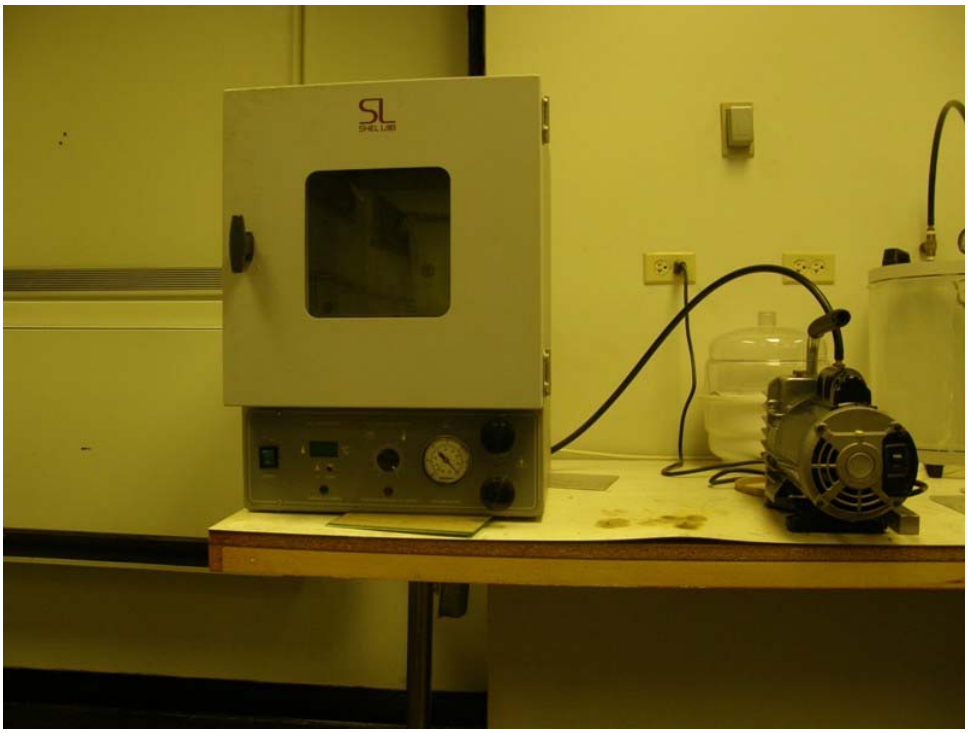

Figure 3.3: Vacuum oven and pump for degassing and curing.

The curing agent, Aradur^{TM} 42, also called isophorodiamine (IPD), was then added to the epoxy-clay blend at room temperature in the ratio of epoxy to hardener 100g: 24g and stirred for about 7 minutes with a stirring rod until a homogeneous mixture was achieved.

The epoxy-nanoclay-hardener was degassed for 40 minutes: initially at 72 cmHg for 20 minutes (by leaving slightly open the air valve vent of the oven to prevent material surging to the top of beaker and pouring away) and after which the air vent was closed for complete degassing at 76 cmHg for 15 to 20 minutes. At the end of degassing process, the epoxy-clay blend was poured into an aluminium mold (figure 3.4). Refer section 3.3 for details of mold design and assembling)

Figure 3.4: Aluminium mold for casting

3.2.2. Curing

Curing is the chemical process which converts the epoxy-clay/ curing agent mixture from liquid to a hard infusible three-dimensional network in which the resin molecules are crosslinked together by means of strong covalent bonds. After pouring the blend into the mold, it was quickly transferred to the vacuum oven (Refer figure 3.3) already preheated to 120°C and cured initially for 2 hours at 120°C. Post curing followed at 150°C for 2 hours

and 170^{o}C for 1.5 hours for optimal crosslinking. The curing cycle was arrived at following a differential scanning calorimetery (DSC) analysis of samples cured at different temperatures and times. At the end of curing, sample was allowed to cool to room temperature before removing from the mold. At least three plates of the mold dimension were prepared each for the neat epoxy and nanocomposites. The synthesis of unfilled epoxy followed the same procedure but with only one degassing step of 2 hours for it only involved one mixing process and contained no clay. The composition for the nanocomposite and duration of sonication is summarized in table 3.3.

Table 3.3: Composition and sonication duration for the epoxy-clay nanocomposite

	Nanocomposite compositions (gram)			
nanocomposite	**epoxy**	**clay**	**hardener**	**sonication time (min)**
2%-5min	60	1.5	14.4	5
2%-10min	60	1.5	14.4	10
2%-30min	60	1.5	14.4	30
2%-60min	60	1.5	14.4	60
4%-5min	60	3.1	14.4	5
4%-10min	60	3.1	14.4	10
4%-30min	60	3.1	14.4	30
4%-60min	60	3.1	14.4	60
5%-5min	60	3.9	14.4	5
5%-10min	60	3.9	14.4	10
5%-30min	60	3.9	14.4	30
5%-60min	60	3.9	14.4	60

3.3. Mold design and Assembling

The mold was made from aluminium plates because it is a good heat conductor and cheaper when compared to either steel or copper. It is in two parts: a base solid plate of dimension 200 x 100 x 10 mm and an upper hollow section of outer dimension 200 x 100 x 5 mm and 170 x 90 x 5 mm inner dimension (figure 3.5). The length dimension satisfies a minimum length for type M1 tensile specimen of ASTM D683-93 standard [38]. At least two tensile specimens can be machined from each polymer plate cast from this mold. The base plate provides the platform for the upper section which defines the dimension of the intended polymer to be cast. The two-part mold is assembled by bolting together the sections via 5 mm-diameter holes drilled through the upper surfaces of the mold parts. During assembling, a replica of the hollow part was made from a thin polymer film (image projector slide sheet) of 0.12mm thickness and placed between the parts to prevent leakage of material from the mold after pouring. To prevent sticking of the cured component to the mold, the latter was polished with abrasive paper and the surface thoroughly cleansed with WD40 cleansing chemical before pouring the epoxy-clay-curing agent mixture.

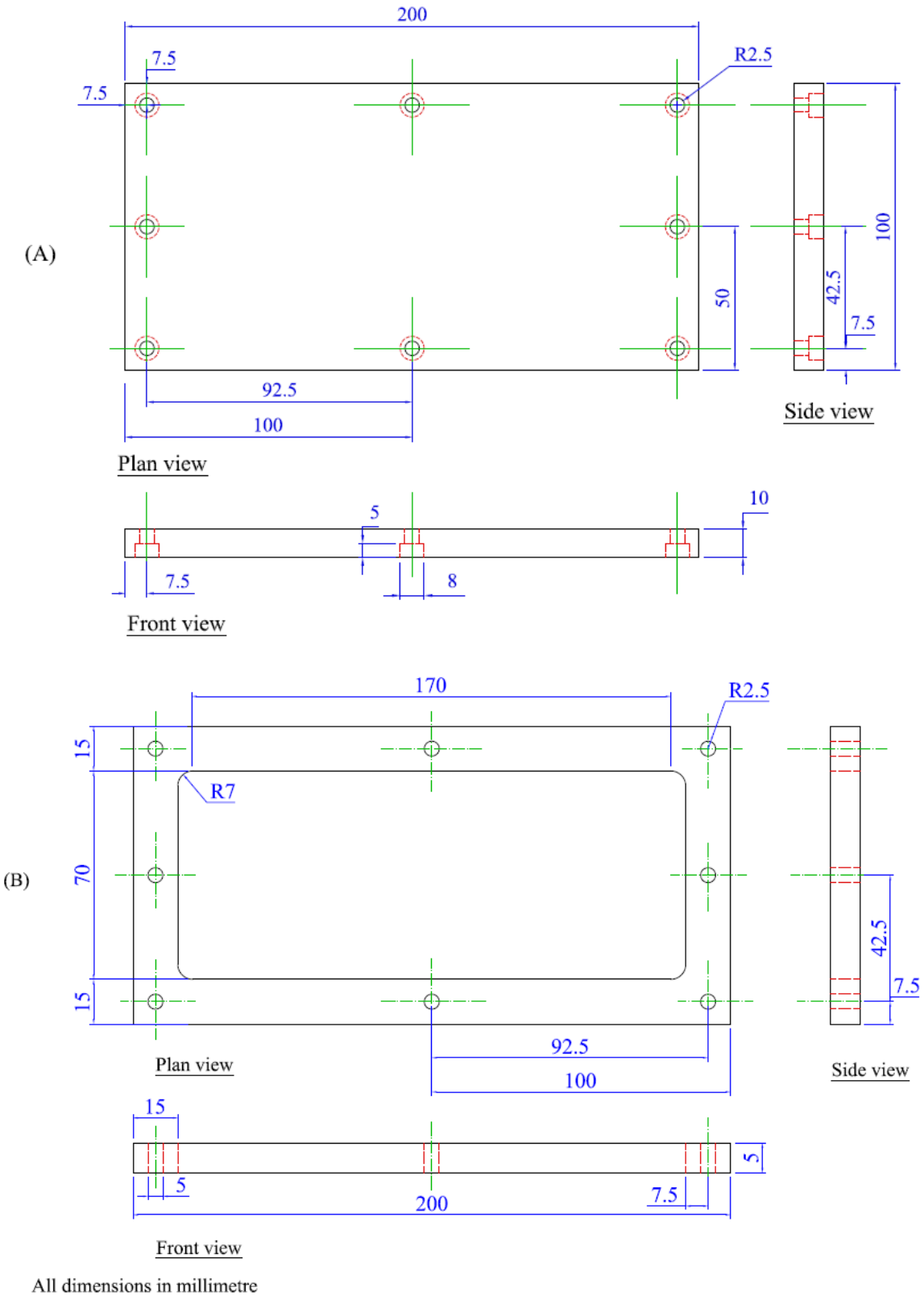

Figure 3.5: Orthographic views of mold parts: (A) base part, (B) upper part.

3.4. Characterization

3.4.1. Differential Scanning Calorimetry (DSC)

Differential scanning calorimeter was used to determine the optimum curing state and glass transition temperature of the neat epoxy. It is stated for Aradur 42 that full curing could not be achieved with it when used for most araldite resins [36]. To achieve optimum curing which will be suitable for the application of the present study, the epoxy was cured at different temperature and time cycles and the glass transition temperature determined. The curing cycle that gave a glass transition temperature close to the full curing state without any noticeable change in the physical appearance of the epoxy was then used as the optimum curing cycle for the neat epoxy and the nanocomposites. Samples cured at different temperatures and times as shown in table 3.4 were used to study the optimum curing cycle.

Table 3.4: Temperature and time cycles used to study the cure of epoxy

No	**Initial curing**	**Post curing**	
1	120ºC for 2 hrs	150ºC for 2 hrs	-
2	120ºC for 2 hrs	150ºC for 3 hrs	-
3	120ºC for 2 hrs	150ºC for 2 hrs	170ºC for 2 hrs
4	120ºC for 2 hrs	150ºC for 2 hrs	170ºC for 1.5 hrs
5	120ºC for 2 hrs	150ºC for 2 hrs	180ºC for 1 hr
6	120ºC for 2 hrs	150ºC for 2 hrs	200ºC for 2 hrs

To determine the level of curing and glass transition temperature,T_g, for the epoxy and nanocomposites, thin samples were chipped from a specimen and weighed on a Mettler Toledo AG 285 weighing balance. Weights between 6-10 mg were measured. The sample was then placed in an aluminium crucible of 40 µl and covered with its lid. A hole was punched on the crucible lid to expel any trapped gas that might affect the result of the experiment. The crucible containing the sample was then placed beside an empty reference aluminium pan in the heating chamber of DSC-822^e oven (figure 3.6) and heated from 25ºC to 200ºC at a heating rate of 10 ºC/min in an argon gas inert environment flowing at 100 ml/min flow rate. Cooling was provided with liquefied nitrogen gas. Once optimum curing was achieved for the pure epoxy, the same curing cycle was applied for all the nanocomposites. Three tests each were conducted for the neat epoxy and 2% nanocomposites samples to evaluate the glass transition temperatures, T_g. The effect of sonication time on the glass transition temperature for 2% nanocomposites was also investigated.

Figure 3.6: Differential Scanning Calorimetry (DSC) Equipment

3.4.2. Wide Angle X-ray Diffraction (WAXD)

X-ray diffraction has become a powerful tool for the analysis of nanocomposite structure especially in polymer-clay nanocomposites research. It is a non-destructive analytical tool capable of presenting the dispersion state of clay in polymers. Its availability and flexibility of use relative to other structural analytical tools makes it handy in nanocomposite structural representation.

Wide angle X-ray diffraction was conducted on the nanoclay powder, cured unmodified epoxy and all prepared samples of nanocomposites from a Shimadzu wide angle X-ray diffraction equipment (Figure 3.7). This was to view the structural features of the materials and as well measure the level of clay separation in the nanocomposites. Test pieces for the cured epoxy and nanocomposites were flat sections in the form of blocks of dimensions 10 x 10 x 2.5 mm which were cut out of the bulk samples. They were placed in sample holders and mounted in the sample chamber of the X-ray diffraction equipment. The equipment was under a voltage 40kV and a current of 30mA. Cu Kα radiation of wavelength 1.5406Å was used to perform continuous scans on powder nanoclay, unfilled epoxy and epoxy-clay nanocomposites at a scan rate and size of 0.5^{o}/min and 0.02^{o}, respectively. The Bragg's angle (2θ) range was 2-10°. In order to view the distribution of swollen sites in the nanocomposite, at least six tests were conducted on each nanocomposite sample with test specimens cut out from different sections of the bulk materials.

Figure 3.7: Shimadzu Wide Angle X-Ray Equipment

3.4.3. Fractographic Analysis and Energy Dispersive Spectroscopy

Microstructural examinations of the fractured surfaces of the tensile specimens were performed using a Scanning Electron Microscopy (SEM) (figure 3.8). SEM can produce very high-resolution images of a sample surface, revealing details about less than 1 to 5 nm in size [39]. Due to the very narrow electron beam, SEM micrographs have a large depth of field yielding a characteristic three-dimensional appearance useful for understanding the surface structure of a sample. The SEM used is a high resolution scanning electron microscope with

a magnification range of x10 to x300, 000. Before mounting the specimen on the stub for scanning in the SEM chamber, the fractured surfaces for analysis were coated with gold on a JEOL Fine Coat Ion Sputter JFC-1100 sputtering equipment to make the surface of the sample electrically conductive and preventing it from being charged.

Images from SEM were transferred for Energy Dispersive Spectroscopy (EDS) analysis. The EDS analysis was done to determine the elemental composition of epoxy, nanocomposites and powder clay. It was also used to identify the various sites in the nanocomposite structure.

Figure 3.8: Scanning Electron Microscopy

3.5. Mechanical properties testing

3.5.1. Tensile test

Tensile properties are fundamental properties for polymers and polymer-phased nanocomposites. They are very important in engineering material design and specification. Other perhaps than hardness, measurement of tensile stress-strain properties is the most common mechanical measurement on most polymer material. Even where a material is to be used in bending, shear or compression, tensile property is commonly measured as a general guide to quality [40]. The tensile strength, elongation at break and elastic modulus are the basic parameters used to quantify the tensile properties of materials.

Tensile tests were conducted on neat epoxy and nanocomposites specimens to measure the tensile stress, the modulus of elasticity and the strain at fracture. Instron 5569 (figure 3.9) from Instron Incorporation, USA, was used to carry out the tensile tests. The machine is computer controlled with Bluehill data acquisition software. A load cell of 50 KN is attached to the moveable crosshead. Type MI tensile test specimens (figure 3.10) were prepared according to ASTM standard D638M-93 [38] from unmodified epoxy and epoxy-clay nanocomposites of all cases of sonication times and clay amounts considered in this work. Silicon carbide abrasive paper of the grade 200 CW and 600 CW were used to smooth the edges of the specimens to remove any obvious flaws. Constant crosshead movement of 5±25% mm/min [38] was then applied until the specimen fractured. At least 6 specimens each were tested for each condition and repeatability.

Figure 3.9: Instron 5569 tensile testing machine.

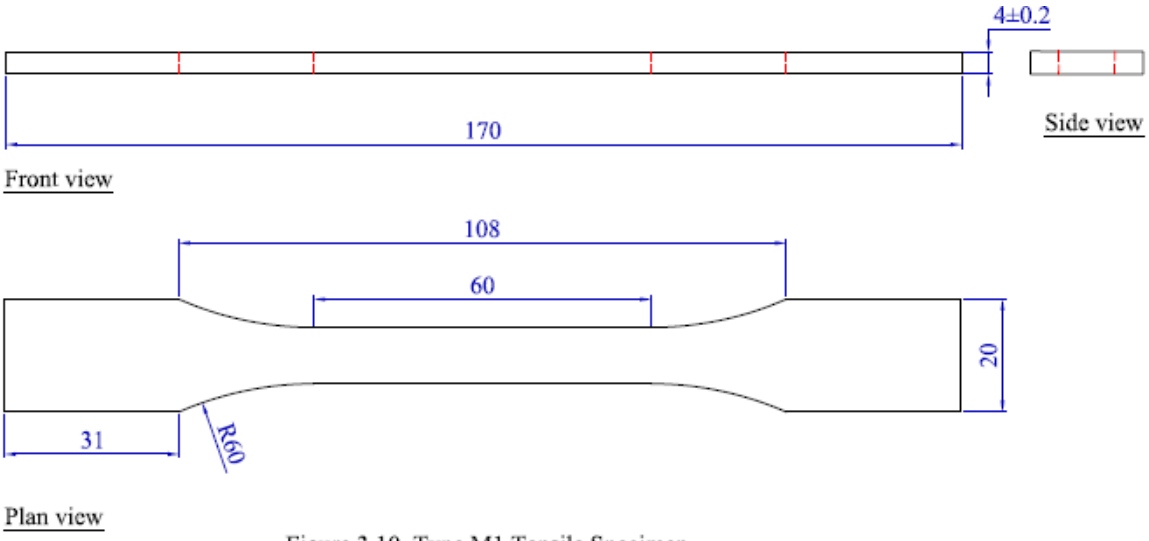

Figure 3.10. Type M1 Tensile Specimen

3.5.2. Vickers hardness test

The hardness of a material is its ability to resist plastic deformation or scratch. The Vickers test is often easier to use than other hardness tests since the required calculations are independent of the size of the indenter, and the indenter can be used for all materials irrespective of hardness [41]. It is not a true material property, but an empirical value that should be seen in conjunction with the experimental methods and hardness scale used [41].

Hardness tests were conducted using a BUEHLER micro hardness tester (figure 3.11) equipped with a diamond shape indenter. Four flat pieces each in the shape of blocks of dimensions 20 x 20 x 4.5mm were cut from different sections of both the unfilled epoxy and the nanocomposite plates. To determine the hardness of a piece, it was placed on the specimen mount of the tester and the objective lens of the microscope attached to the equipment was adjusted until the sharpest image of the piece was obtained. The indenter was then moved directly above the piece and indented for 10 seconds. A load of 200 gf was used. Vickers hardness was auto-calculated from the tester. At least 10 indentations per specimen were taken for averaging.

Figure 3.11: Buehler micro-hardness tester

CHAPTER 4

4.0. RESULTS AND DISCUSSION.

4.1 Synthesis of epoxy nanocomposite.

It was observed in the current work that blending of clay with epoxy changed the chemical kinetics of the epoxy. Both the pot life and gel time of the epoxy was decreased. The polymerization of nanocomposites started earlier than the pure epoxy. This is probably due to the presence of onium ions in the organoclay. Chen et al [4] observed that crosslinking of nanocomposites set out earlier than neat epoxy. They attributed it to the possibility of the catalytic effects of the ammonium acidity in the gallery of clay. Other researchers [16, 20] have also reported the catalytic action of clay due to onium ion presence. It was also seen in the current study that sonication introduced a lot of air bubbles and caused the blend to foam. This made degassing difficult especially with increase in the clay amount, as it made the mixture more viscous. Mixing epoxy with clay also changed the physical appearance of epoxy. The colour changed from a colourless transparent material to light yellow colour which change in intensity with increasing sonication time.

4.2. Glass transition temperature, T_g.

The glass transition temperature, T_g was found using the midpoint construction method with the aid of the STARe thermo-mechanical analysis software provided with the DSC-822^e equipment by Mettler Toledo. To find the glass transition temperature, the software was used to construct tangent lines at the points where change occurred in the heat-temperature

curve due to change in the heat capacity of the sample. The mid point of intersection of the tangents represents the glass transition temperature T_g of the material as shown in figure 4.1.

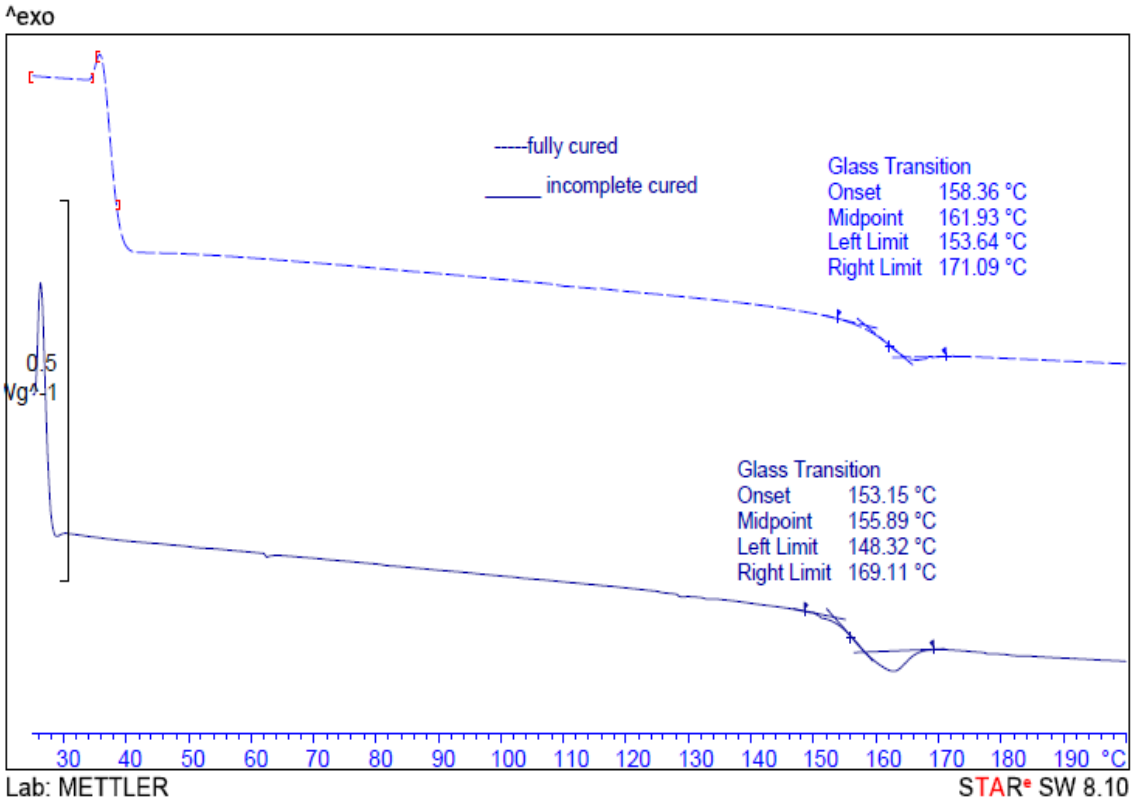

Figure 4.1: Mid-point construction method for finding glass transition temperature of polymeric material.

As stated in section 3.4.1, the curing agent used can not produce full crosslinking for the type of epoxy used in the present work. The results presented here are those for optimum curing conditions which satisfy the requirement for the application of the present study. Moreover, in order to gain an insight into the T_g if the epoxy were fully cured, a completely cured state was obtained by taking a repeated DSC scan on an earlier scanned sample. The heating effect of the repeated scan caused the sample to crosslink completely and also removed any effect

that may have been introduced by processing. From the repeated scan, the T_g for a completely cured system was found to be 161.54±0.38ºC. The curing cycles investigated and the corresponding glass transition temperatures, T_g's, are given in table 4.1.

Table 4.1: Results of glass transition temperature (T_g) for the curing cycles investigated

	Initial curing	**Post curing**		**T_g**
1	120ºC for 2 hrs	150ºC for 2 hrs	-	146.47ºC
2	120ºC for 2 hrs	150ºC for 3 hrs	-	149.18±1.34ºC
3	120ºC for 2 hrs	150ºC for 2 hrs	170ºC for 2 hrs	158.95±0.54ºC
4	120ºC for 2 hrs	150ºC for 2 hrs	170ºC for 1.5 hrs	159.26±0.07 ºC
5	120ºC for 2 hrs	150ºC for 2 hrs	180ºC for 1 hr	-
6	120ºC for 2 hrs	150ºC for 2 hrs	200ºC for 2 hrs	-

The T_g's for the last two conditions in table 4.1 were not investigated because post curing the sample at temperature above 170ºC began to introduce brownish colour on the material. This was suspected to be the start of degradation. At 200ºC, the nanocomposite sample degraded completely which led to the conclusion that degradation starts at 180ºC. Since the T_g obtained for the 120ºC for 2 hours, 150ºC for 2 hours and 170ºC for 1.5 hours cycle was close to the T_g at full cured state, this cycle was chosen as the optimum curing cycle for the epoxy and nanocomposites.

The heat-temperature curves and results of the glass transition temperature, T_g for neat epoxy and the 2% nanocomposites cured at 120ºC for 2 hours, 150ºC for 2 hours and 170ºC for 1.5 hours are shown in figures 4.2a-b and table 4.2, respectively. Both the T_g's for the first (single) and second (repeated) DSC scan are reported.

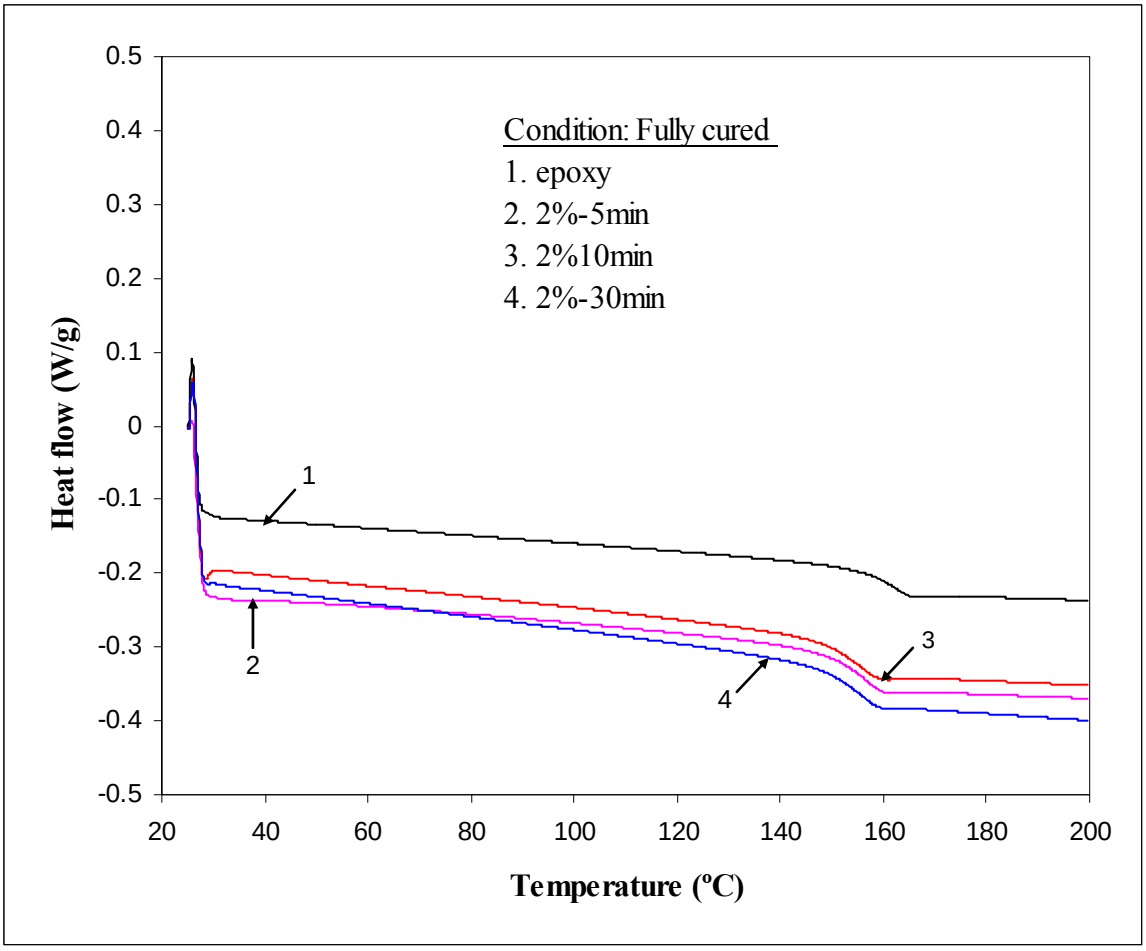

Figure 4.2a: Heat flow-temperature curve to determine glass transition temperature for completely cured epoxy and 2% nanocomposites (obtained from a repeated DSC scan).

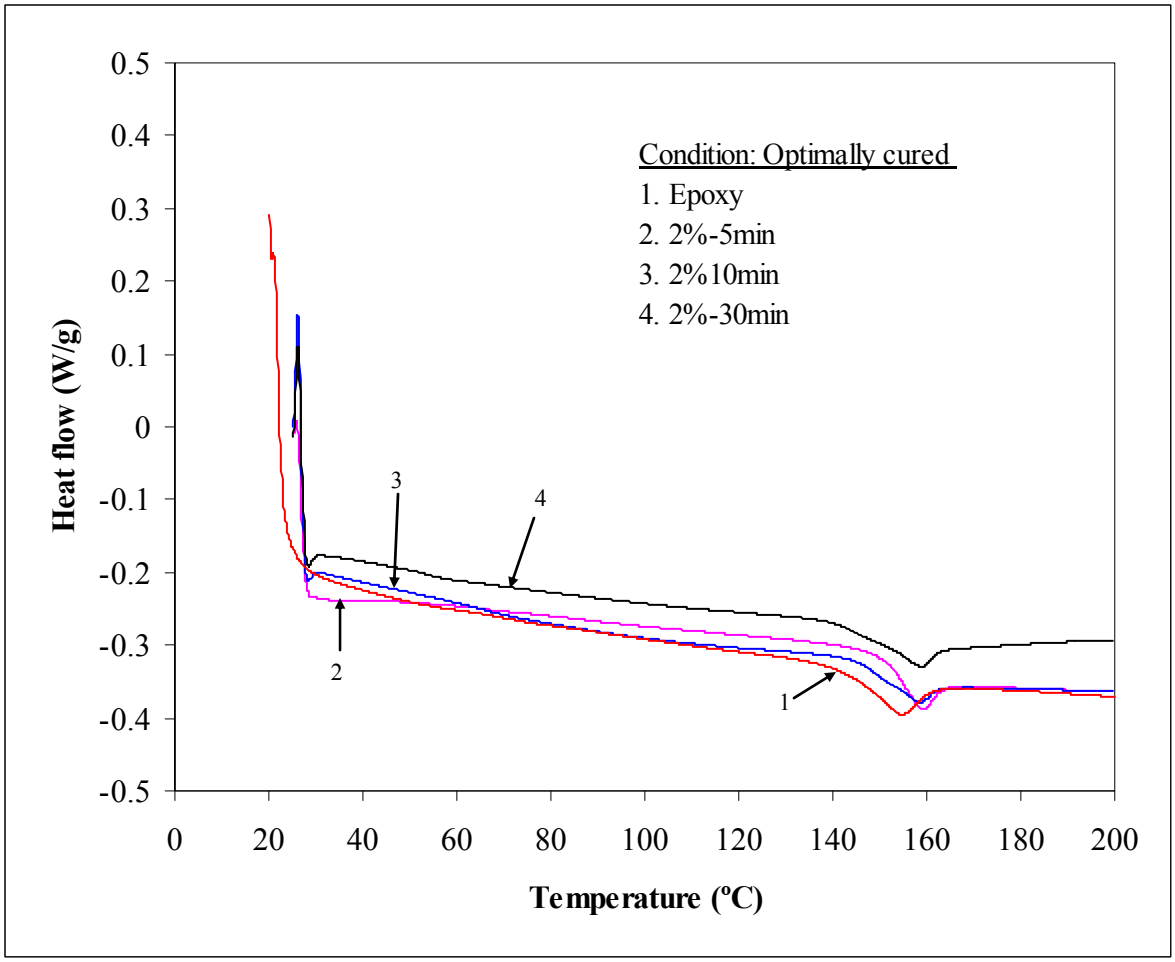

Figure 4.2b: Heat flow-temperature curve to determine glass transition temperature for optimally cured epoxy and 2% nanocomposites (obtained from single DSC scan).

Table 4.2: Mean glass transition temperature, T_g, for neat epoxy and 2% nanocomposites

		2% nanocomposites		
	Neat epoxy	**2%-5min**	**2%-10min**	**2%-30min**
T_g (ºC) 1st DSC scan	159.26±0.07	155.66±0.23	150.42±0.4	148.45±0.36
T_g (ºC) 2nd DSC scan	161.54±0.38	155.25±0.02	154.87±1.07	154.39±0.07

It is obvious from table 4.2 that T_g for the completely cured epoxy and nanocomposites as obtained from a second (repeated) DSC scan are higher than the optimally cured state (single scan). Complete curing is important as many mechanical, chemical and physical properties of epoxy are influenced by the crosslinking level and the T_g. Correct T_g will help predicts the proper working temperature for the polymer and its composite. It is observed that the difference between the fully cured state and the optimally cured sample for the neat epoxy is 2ºC. Therefore, this curing cycle which produced a T_g close to that of completely cured epoxy can be accepted as the optimum. It is clear that 2% nanocomposites which was also cured using same curing cycle have T_g lower than the neat epoxy. This means that the presence of clay reduced the T_g of the epoxy. Unlike the neat epoxy, there is a difference in T_g of about 5 to 6ºC for the nanocomposite between the first and second DSC scan. However, no change in T_g was observed for the 2%-5min in both scan. This suggests that it might not be clay alone which was responsible for the lower T_g in the nanocomposite as revealed by the first scan. There may also have been the effect of processing parameters such as heat distribution.

Glass transition temperature of epoxy and its composite is linked to the crosslinking density. Lower T_g for nanocomposite have been reported by [13, 20, 21, 22, 23, 31, 34, 43], while other researchers [5, 17] have recorded increase in T_g. These authors have attributed the change in T_g to the modifying agent in the silicate clay which has the capability to change the crosslink density of the polymer.

It is noticed (table 4.2) that there was change in T_g in the first scan as the sonication time was varied. But for the repeated scan in which normalization had taken place, the change in sonication time did not produce any significant variation in the T_g of the nanocomposite. The result from first scan is thus the true representation of the glass transition temperature of the nanocomposite wherein the experimental conditions are seen. It suggests that for an ideally cured system, there may be no effect of sonication time. The second scan represents an ideal situation of perfect curing which is not achieved for the epoxy when Aradur [42] hardener is used.

4.3. Wide angle X-ray diffraction (WAXD)

Wide angle x-ray diffraction revealed that both intercalation and exfoliation or disorder intercalation were present in each of the nanocomposites. Figures 4.3a-c are representative x-ray diffraction spectra of pure epoxy, as received powder clay and the nanocomposites.

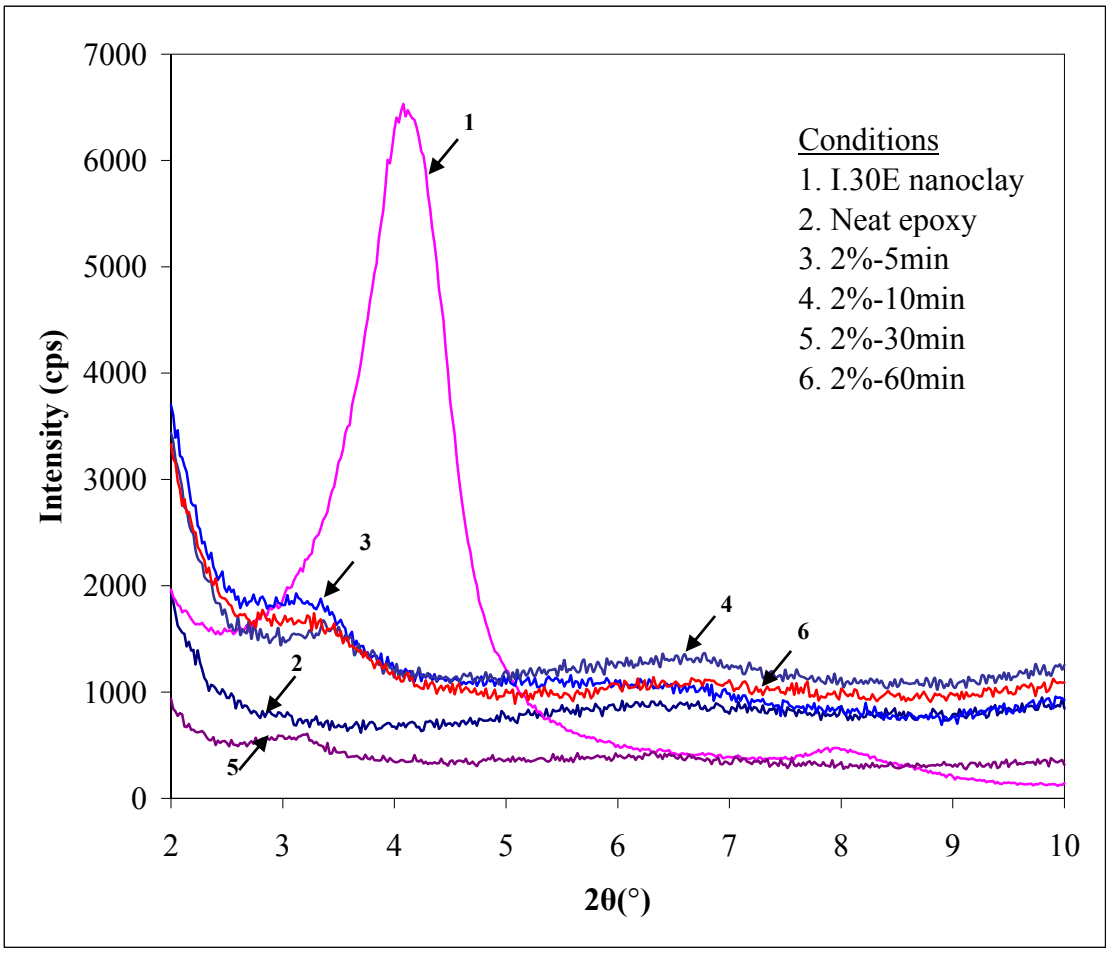

Figure 4.3a: X-ray diffraction spectrum of nanoclay, neat epoxy and 2% nanocomposite sonicated for 5, 10, 30 & 60 minutes.

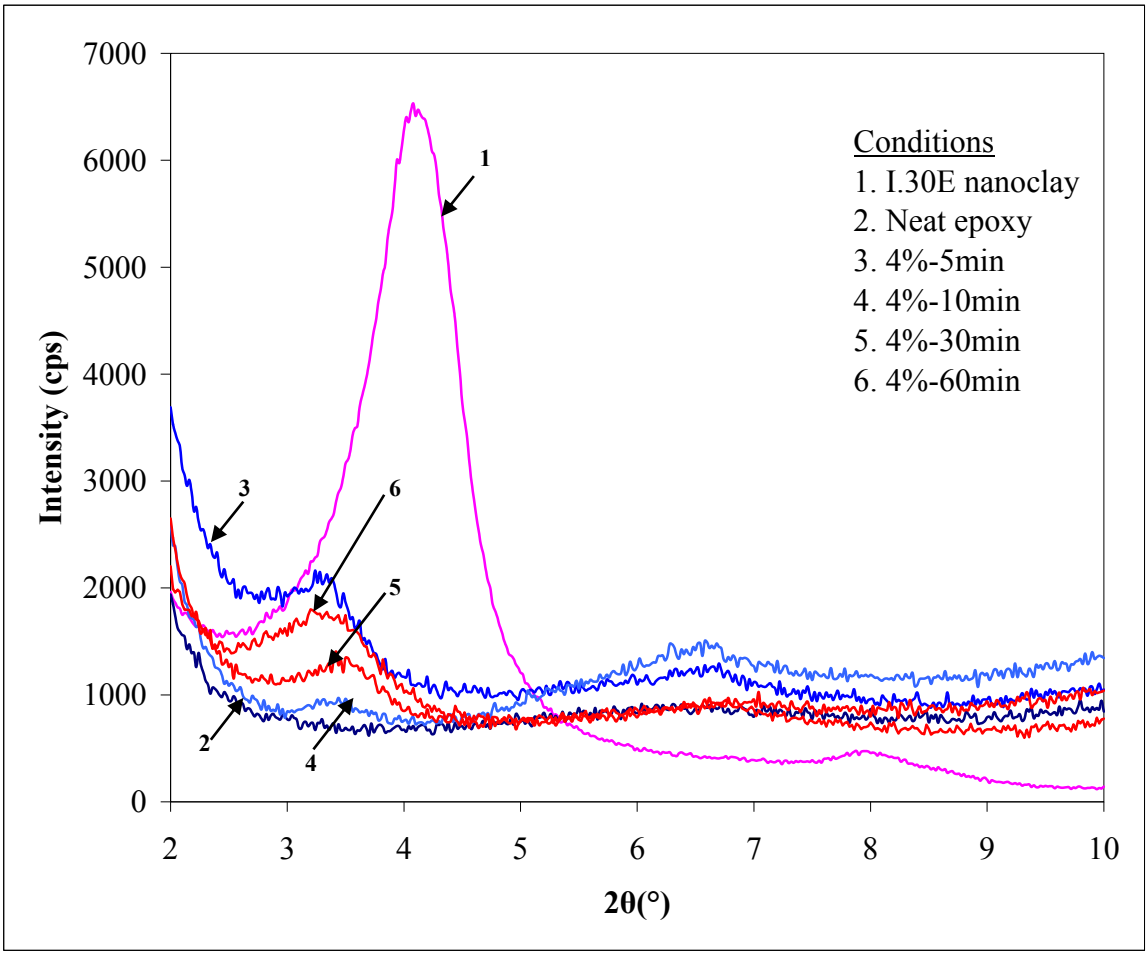

Figure 4.3b: X-ray diffraction spectrum of nanoclay, neat epoxy and 4% nanocomposites sonicated for 5, 10, 30 & 60 minutes.

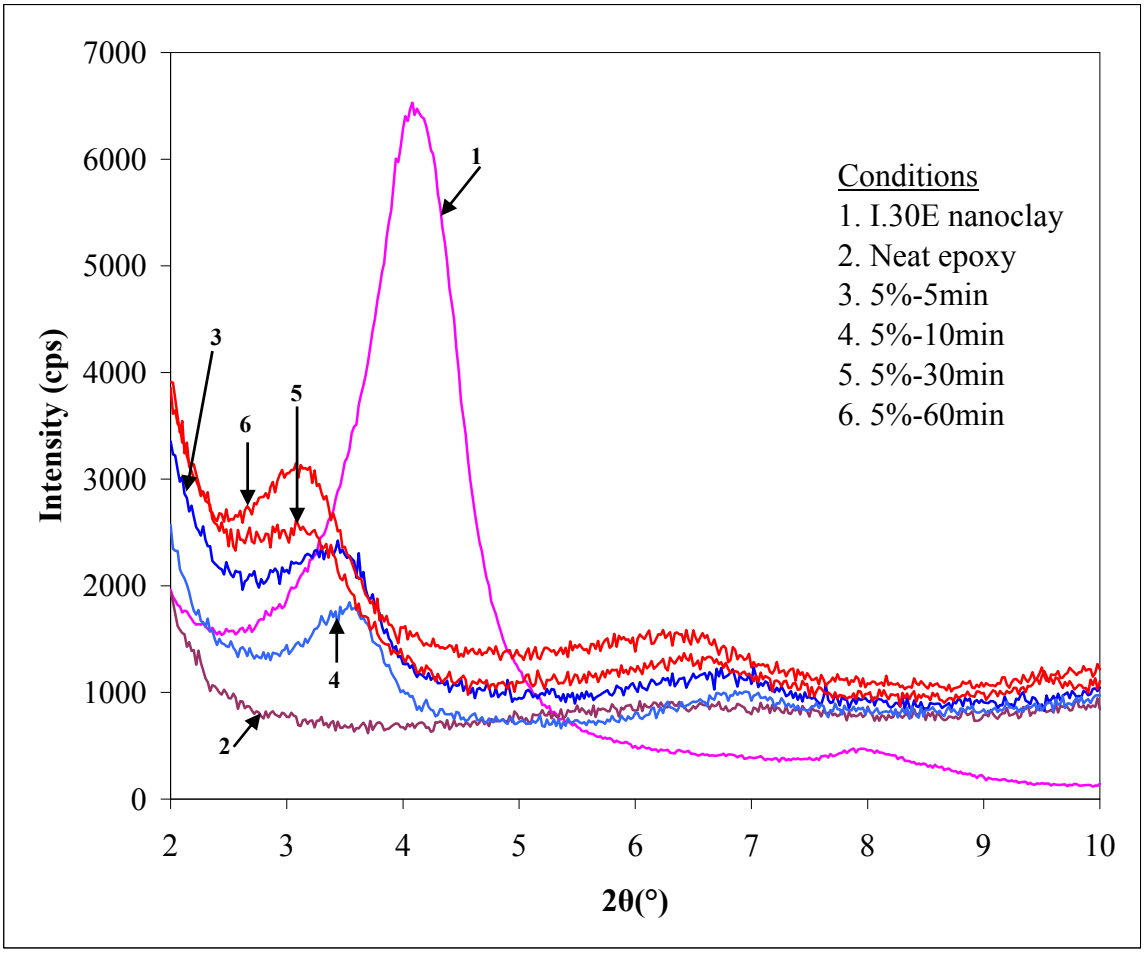

Figure 4.3c: X-ray diffraction spectrum of nanoclay, neat epoxy and 5% nanocomposites sonicated for 5, 10, 30 & 60 minutes.

It is seen from the results (figures 4.3a-c) that while the peak of the clay is prominent and sharp, indicating a highly ordered stack, the pure epoxy showed no peak confirming the amorphous nature of the material structure. Meanwhile, observable peaks are still present in the nanocomposites. These peaks are however lower than that of the nanoclay, and their angular positions (2θ's) are less than that of the nanoclay. Lower angular position means higher d-spacing. It signifies that epoxy polymer have diffused between the clay layers causing finite increase in the intergallery spacing.

As stated previously, at least five x-ray diffractions were conducted for each of the nanocomposite conditions with test specimens cut from different sections of the bulk sample in order to investigate the distribution of the basal spacing in the microstructure of the nanocomposite. From the angular positions obtained, d-spacings were calculated using Bragg's equation. The average values for both the peak angular positions and intergallery spacings are presented in table 4.3.

$$d = \frac{\lambda}{2\sin(\theta)} \qquad (4.1)$$

Bragg's equation, d is intergallery spacing,
λ is x – ray wavelength, and
θ is half bragg's angle.

Table 4.3: Mean Bragg's angle (2θ) and d-spacings for the nanoclay and nanocomposites.

	Mean 2θ(º)	**Mean d-spacing(Å)**
I.30E clay	4.19±0.11	21.1±0.6
2%-5min	3.26±0.32	26.7±2.8
2%-10min	3.34±0.08	26.4±0.7
2%-30min	3.22±0.16	27.7±1.2
2%-60min	3.25±0.16	27.2±1.4
4%-5min	3.29±0.17	26.9±1.4
4%-10min	3.41±0.03	25.9±0.2
4%-30min	3.37±0.10	26.2±0.8
4%-60min	3.20±0.19	27.7±1.7
5%-5min	3.44±0.19	25.6±1.5
5%-10min	3.51±0.07	25.2±0.5
5%-30min	3.18±0.19	27.8±1.6
5%-60min	3.19±0.13	27.8±1.2

From the result (table 4.3), it is observed that the sonication of I.30E nanoclay with epoxy caused its d-spacing to rise above the initial 21.1Å because epoxy resin diffused into the silicate interlayer spaces prior to crosslinking. The value of basal spacing obtained for the nanoclay in the present work is in close range with the values other researchers [12, 20, 22, 25, 27] have reported for similar clay.

4.3.1. General discussion of the XRD spectrum

It is seen (figures 4.3a-c) that the nanocomposite peaks are broad and of weak variance contrasting with the sharp peak of the clay. This smooth shoulder indicates that there is wide distribution of intergallery spacing within the nanocomposite. It also suggests that some of the silicate layers have gone into exfoliation as further shown in figure 4.3d. It is obvious furthermore that the peaks of the 2% nanocomposites are lower than those of the 4% and 5% nanocomposites. This is because the amount of clay powder present in the 2% nanocomposite is less than that in the 4% and 5% nanocomposites. Thus less clay particle is available before and after sonication for the x-ray beam to be diffracted. The difference in peak height is also seen between the 4% and 5% nanocomposites. The peaks of the 4% nanocomposites are generally lower than those of the 5%. Thus, higher peak intensity implies the presence of more orderly structure of clay particles. It means the amounts of clay particles which remain in organized stack after sonication are higher in the 4% and 5% than the 2% nanocomposite. Hence, the amount of clay present has effect on the intensity of the spectrum peak. The difference in intensity of spectrum with respect to clay amount agrees with the findings of [8, 23]

In figure 4.3d**,** x-ray diffraction spectra of 2%-60min, 4%-10min, 4%-30min & 5%-60min which show no peak are presented. These only represented rare cases; one out of the six tests conducted for each of the nanocomposites they represent.

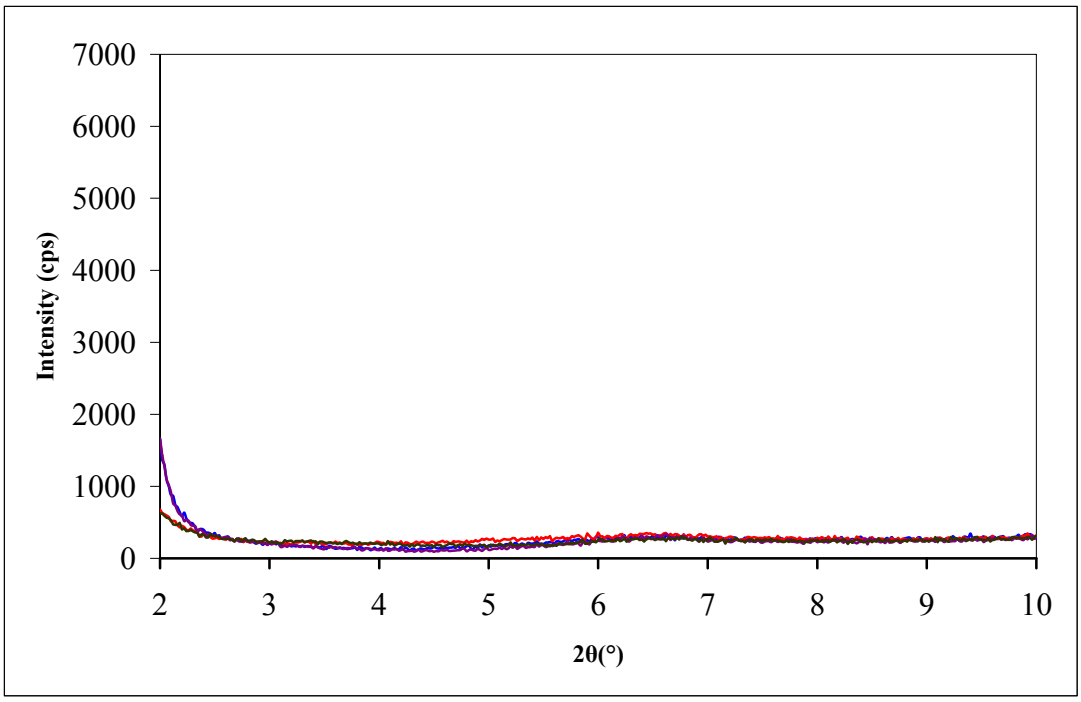

Figure 4.3d: X-ray diffraction spectra of 2%-60min, 4%-10min, 4%-30min & 5%-60min nanocomposites illustrating exfoliation.

These spectra suggest exfoliation or disorder intercalation, meaning that epoxy materials have diffused into the interlayer spacing resulting in extensive separation of the nanoclay layers. The spectra here are hardly distinguishable, all superimposing on one another. This is in contrast with intercalation in which spectrum shows peak and varies relative to intercalation level. Hence, it can be concluded that a mixture of intercalated and partially exfoliated/disorderly intercalated structure are present in some of the nanocomposites

synthesized in the current study. This, nonetheless, agrees with the finding of some authors who have shown that nanocomposite structure is usually a mix of intercalated and exfoliated structure. Hussein et al [20] found from TEM images that single delaminated layers representing exfoliation were also present in the predominantly intercalated structure of nanocomposites synthesized in their work. Luo and Daniel [1] reported that the sonication process they used for blending resulted in composites with partial exfoliation and intercalation and randomly dispersed exfoliated platelets and intercalated clusters.

The co-existence of the two types of structures in the present work is probably due to both time and clay volume effect. During sonication it was possible that more epoxy entered into the intergallery space of the clay as time was increased such that some of the layers that were initially intercalated would go into exfoliation or disordered intercalation. Also, the lower percentage clay fraction would have gone into exfoliation when sonicated for a longer time. This inference is supported by the spectra peaks of the intercalated nanocomposites. The peaks heights of the 2% nanocomposites as shown in figure 4.3a are so low and broad that some could hardly be noticed. These peaks suggest that few clay layers remained in orderly stack while most have already gone into exfoliation. Besides, homogeneity of mixture and position of clay particle during sonication could also be attributed to a mixture of micro structure. The sonication probe is 13 mm in diameter, positioned at the center of the clay-epoxy mixture in a beaker of 47 mm diameter. During sonication, it was observed that the clay particles swam to the edge of the free surface of the epoxy-clay mixture. When sonication only lasted for few minutes, these particles were only partially swollen within the epoxy. Conversely, clay particles in the immediate neighbourhood of the probe were totally swollen by the epoxy. These two phenomena would result into a mixture of structure.

Several other factors including epoxy viscosity, clay exchange capacity and balancing of inter and extra gallery polymerization rate can also be attributed to formation of either intercalated or exfoliated structure [20].

4.3.2. Effect of sonication time on the d-spacing

The effect of sonication time on the interlayer spacing was studied by varying the sonication time from 5 to 60 minutes for the three cases of clay loadings (2%, 4% and 5 %) considered in the current work. The results of this investigation are illustrated in figures 4.4a-c. The generalized trend of change is shown in figure 4.4d.

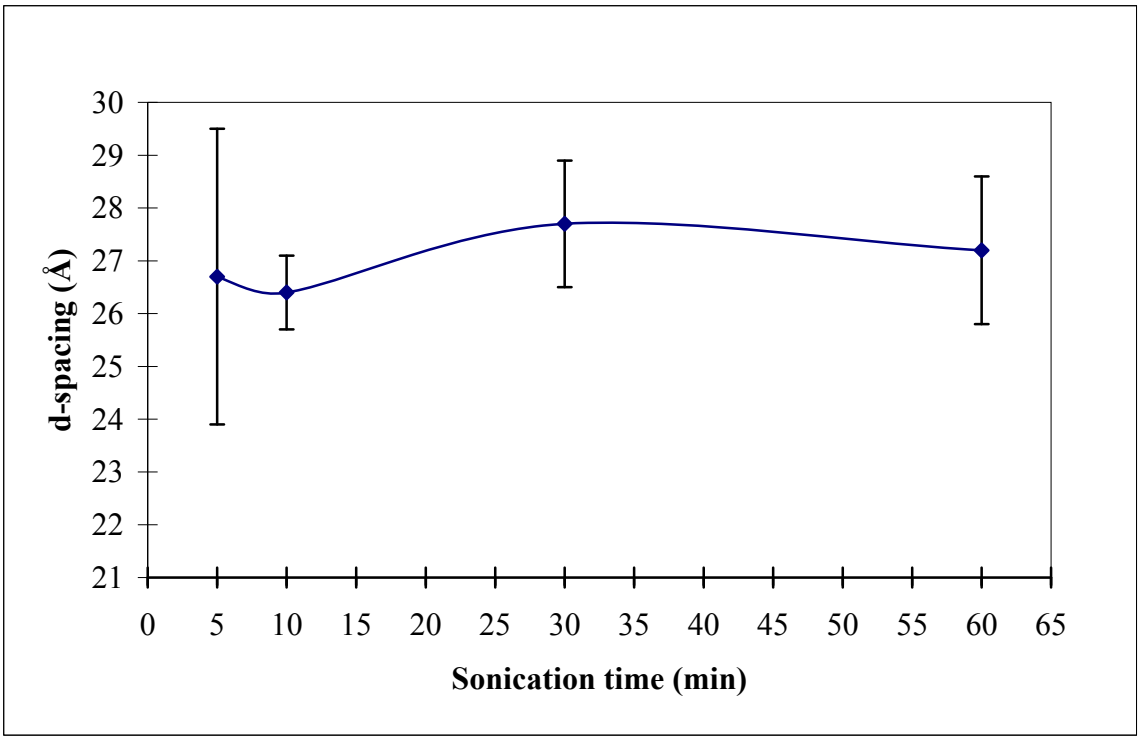

Figure 4.4a: Effect of sonication time on the d-spacings of 2 wt% nanocomposites.

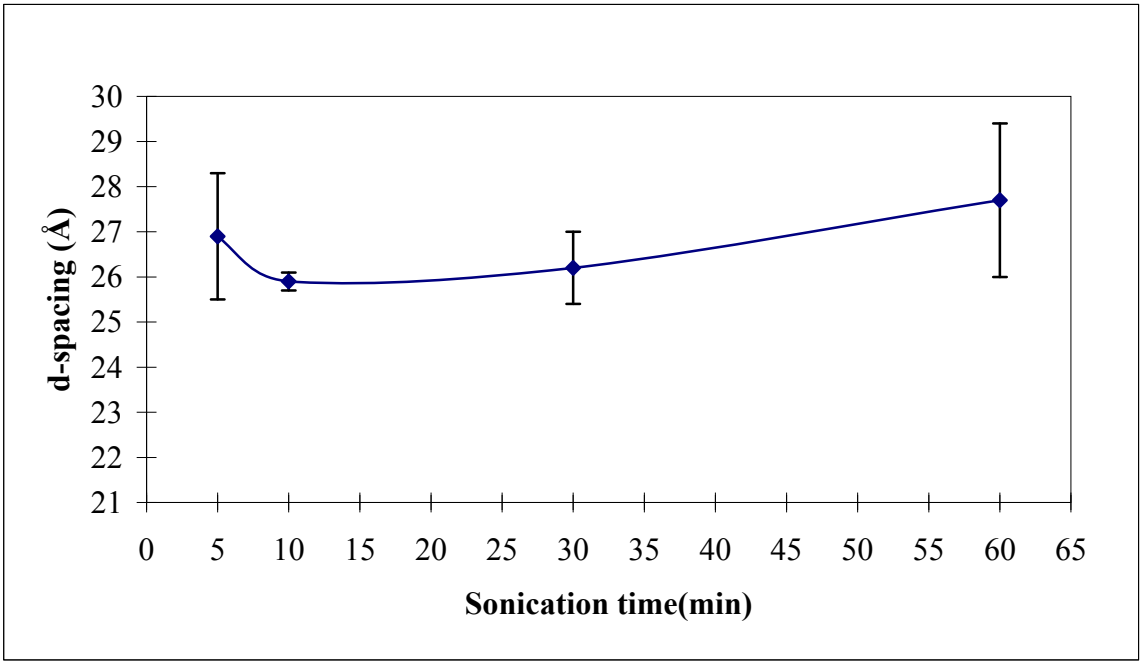

Figure 4.4b: Effect of sonication time on the d-spacings of 4 wt% nanocomposites.

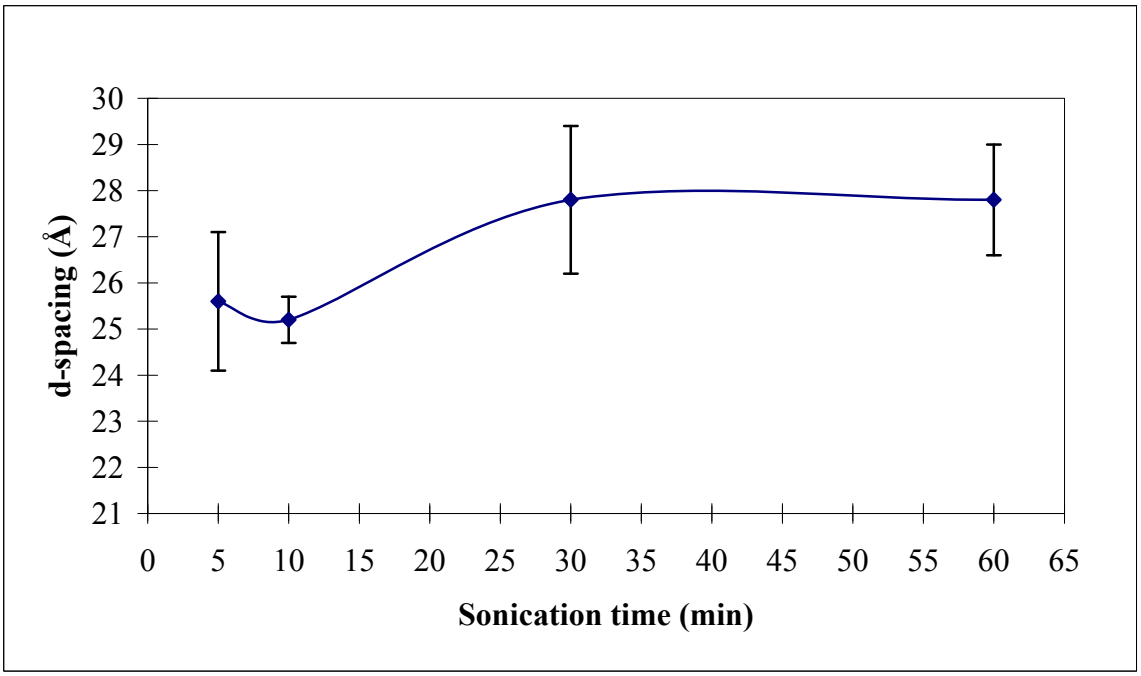

Figure 4.4c: Effect of sonication time on the d-spacings of 5 wt% nanocomposites.

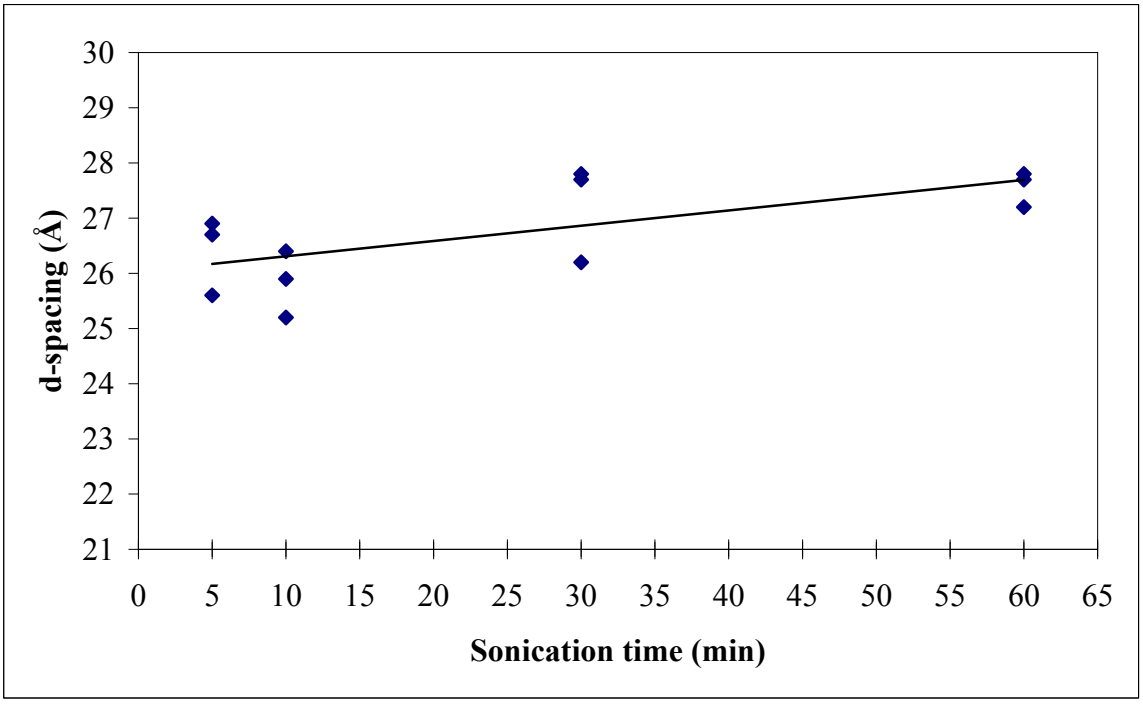

Figure 4.4d: Variation of d-spacing with sonication time.

It is noted that change in sonication time for each clay concentration also produced change in the d-spacing. However, this change was not proportional to the change in the sonication time. For the 2% nanocomposite (figure 4.4a), sonication times of 5, 10, 30 and 60 minutes produced the mean intergallery spacings of 26.7±2.8, 26.4±0.7, 27.7±1.2 and 27.2±1.4Å, respectively. The increase in sonication time from 5 to 10 minutes caused a decrease of 0.3 Å in the average value of d-spacing. The maximum d-spacing value is found for 30 minute sonication time. The increase in d-spacings at 30 and 60 minute sonication times signifies that more epoxy moved into the intergallery layer of the clay. From statistic point, the intergallery distribution in the nanocomposites with 10, 30 and 60 minutes sonication time are better than that of the 5 minutes sonication time, as evidenced by the standard deviation. It can be concluded that the optimum sonication time for 2% nanocomposite was 30 minutes.

For the 4% nanocomposites in figure 4.4b, the increase in sonication time from 5 to 10 minutes caused the mean d-spacing to decrease by 1.0 Å. But the d-spacing increased with increase in the sonication time from 10, 30 to 60 minutes. Although, the mean numerical value of 26.2±0.8 Å for the 4%-30minute was less than 26.9±1.4 Å for the 4%-5min, the standard deviation shows that the scatter in the 4%-5min was high. In another term, there is more uniformity in the micro structural distribution in the 4%-30min nanocomposite than the 4%-5min nanocomposite. Since the maximum average d-spacing is shown by the 4% nanocomposite sonicated for 60 minutes, the optimum sonication for this is 60 minutes. The increase in sonication time from 5 to 60 minutes increased the intergallery spacing by 0.8 Å.

The trend which was observed in 4% nanocomposite is also seen in 5% nanocomposites (figure 4.4c). Increasing the sonication time from 5 to 10 minutes caused an initial drop in the mean intergallery spacing from 25.6±1.5 Å to 25.2±0.5Å. However, the 30 and 60 minute sonication times produced the same average intergallery spacing of 27.8Å, suggesting that, on the average, the same amount of epoxy migrated into the interlayer spacing of the clay during these sonication times. It was noted however that the scatter in the 60 minutes sonication time was less than that of 30 minutes.

It was noted also that the same trend is shown by the nanocomposites for all clay amount when sonication time was changed from 5 to 10 minutes: the d-spacing always dropped to lower value. However, the distribution of intergallery spacing in the 10 minute sonication time was better than the 5, 30 and 60 minutes sonication time. It signifies a more uniform distribution of intercalated sites. The general trend of d-spacing with sonication time for all

percentage weights indicates that d-spacing increase with sonication time (figure 4.4d). This correlation can be expressed by the equation:

$$d = 0.0277t + 26.032 \qquad \text{for } 5 \leq t \leq 60 \qquad (4.2)$$

where d is in Å and t is in min

The effects of sonication time on intergallery space have been investigated by Lam et al [14] and Bashir [32]. Lam et al. [14] found that increasing sonication time did not change the interlayer spacing of the nanocomposite synthesized from Nanolin DK1 clay and Araldite GY251 epoxy. In the current work, the d-spacing changed with variation in sonication time, but the values of the d-spacing remain within the same range. Bashir [31] showed that increase in sonication time from 30 minutes to 60 minutes increased the d-spacing of 4 wt% Cloisite 20A-polyester nanocomposites by 2.6Å. For the current work, the increase in sonication time from 30 to 60 minutes changed the d-spacing by 1.5 Å. It should be mentioned that both the resins and clays used by Bashir or Lam et al are different from those utilized in the present work.

4.3.3. Effect of clay loading on the d-spacing

For each of the sonication time of 5, 10, 30 and 60 minutes, the amount of clay mixed with epoxy was varied from 2 to 4 to 5%. The effects of clay loading on the interlayer spacings of resulting nanocomposites are illustrated in figures 4.5a through 4.5d. The generalized trend is indicated by figure 4.5e

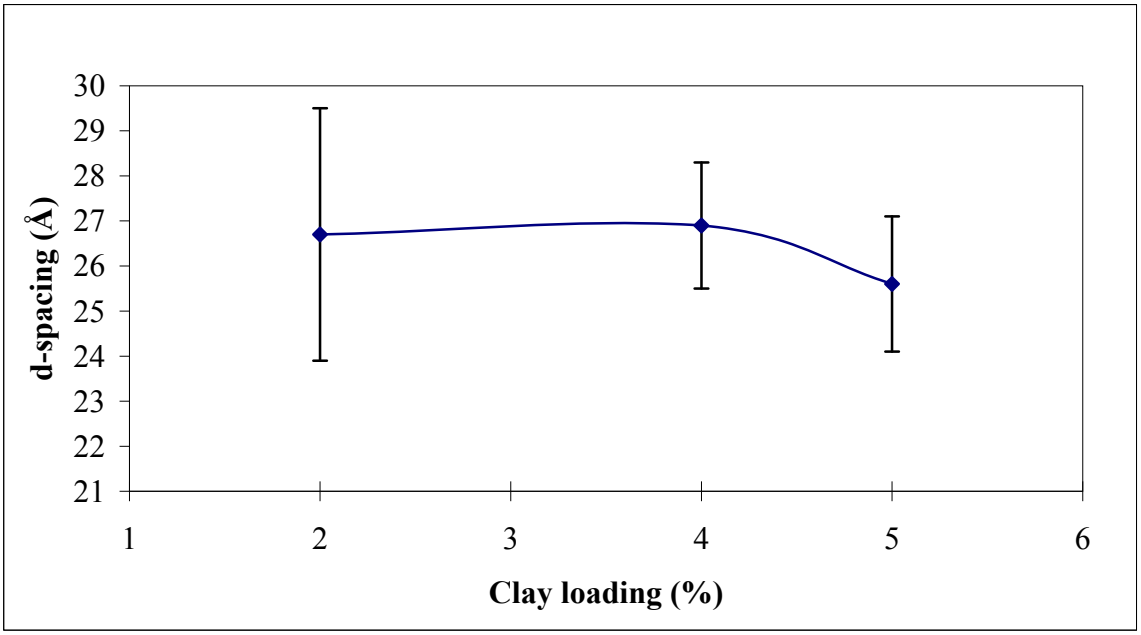

Figure 4.5a: Effect of clay loading on the d-spacings of nanocomposites sonicated for 5 minutes.

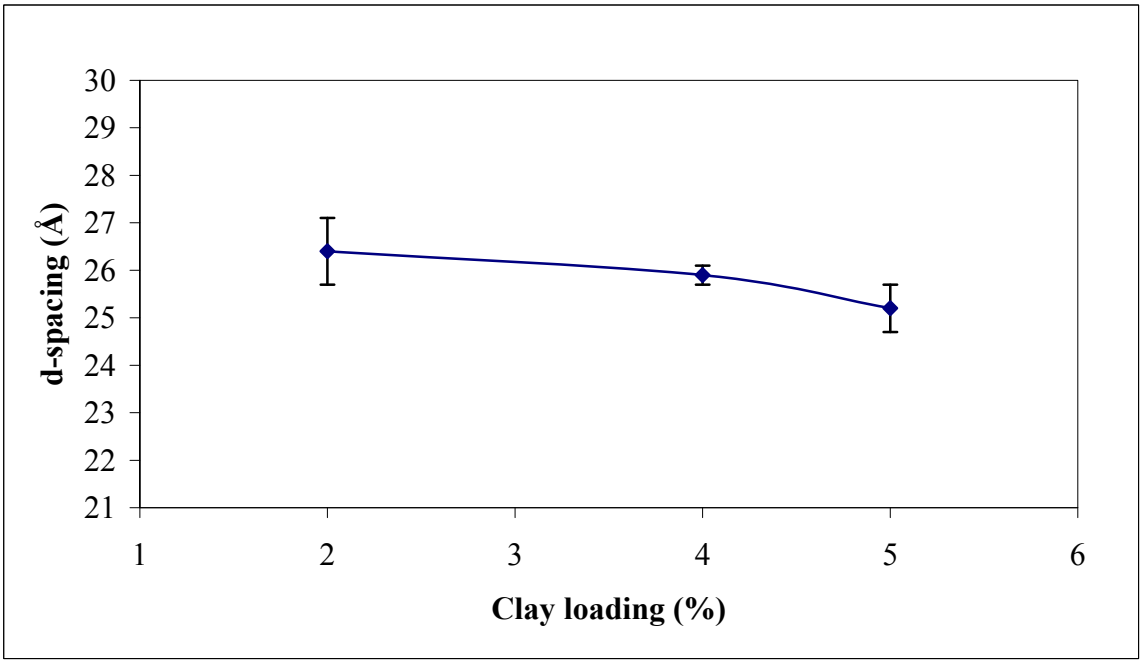

Figure 4.5b: Effect of clay loading on the d-spacings of nanocomposites sonicated for 10 minutes.

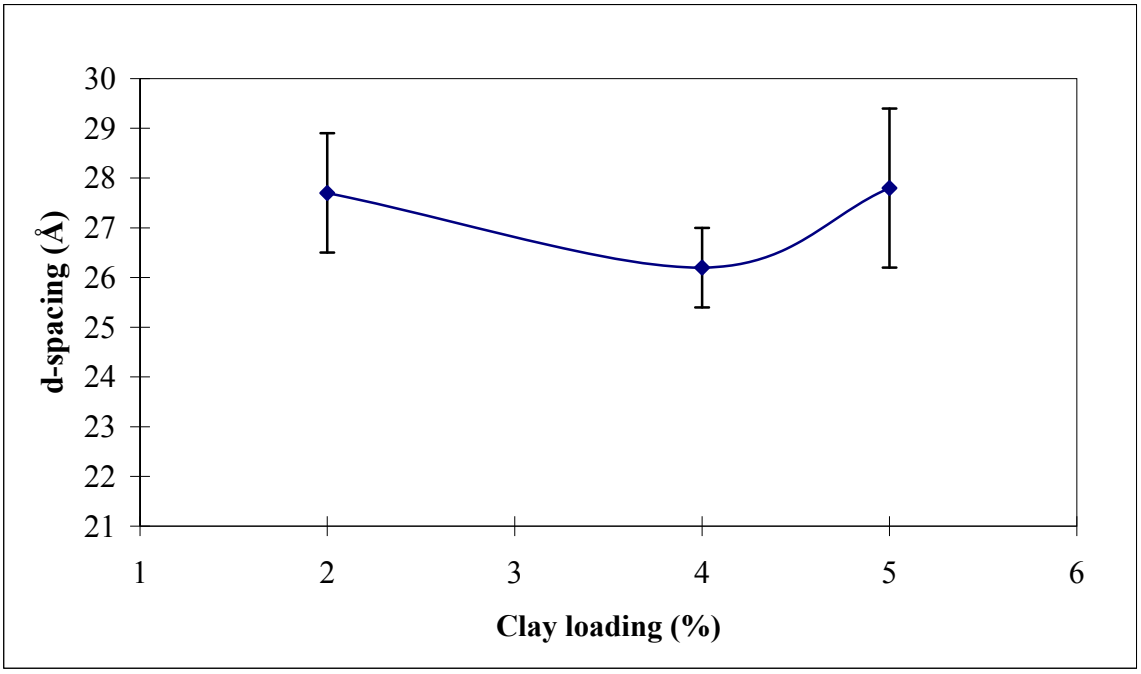

Figure 4.5c: Effect of clay loading on the d-spacings of nanocomposites sonicated for 30 minutes.

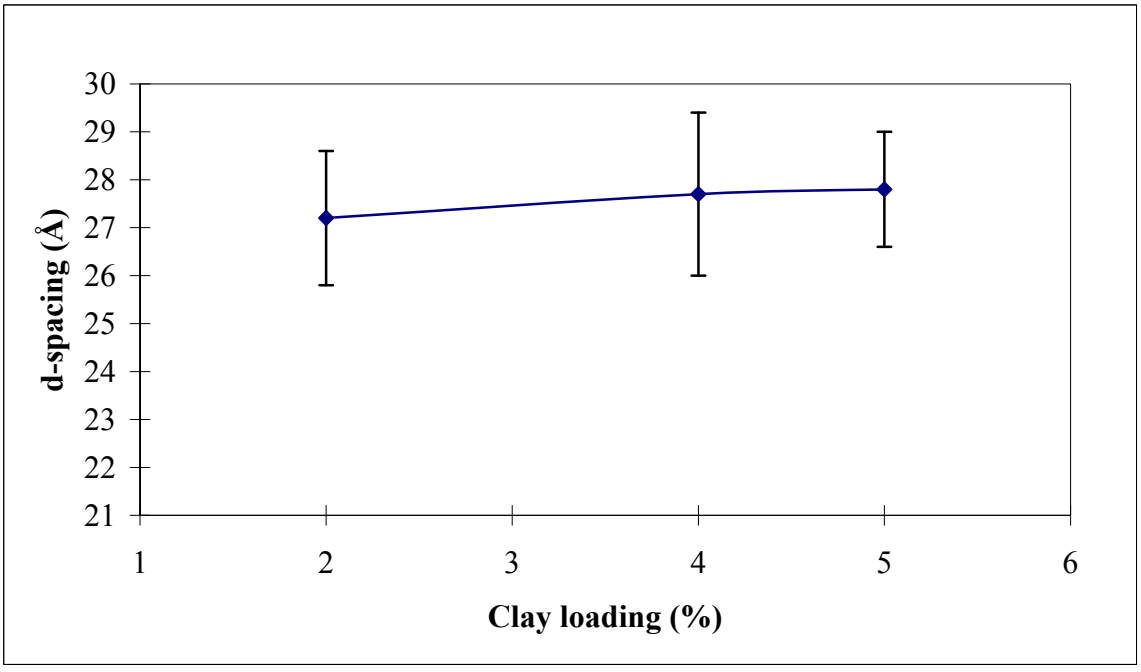

Figure 4.5d: Effect of clay loading on the d-spacings of nanocomposites sonicated for 60 minutes.

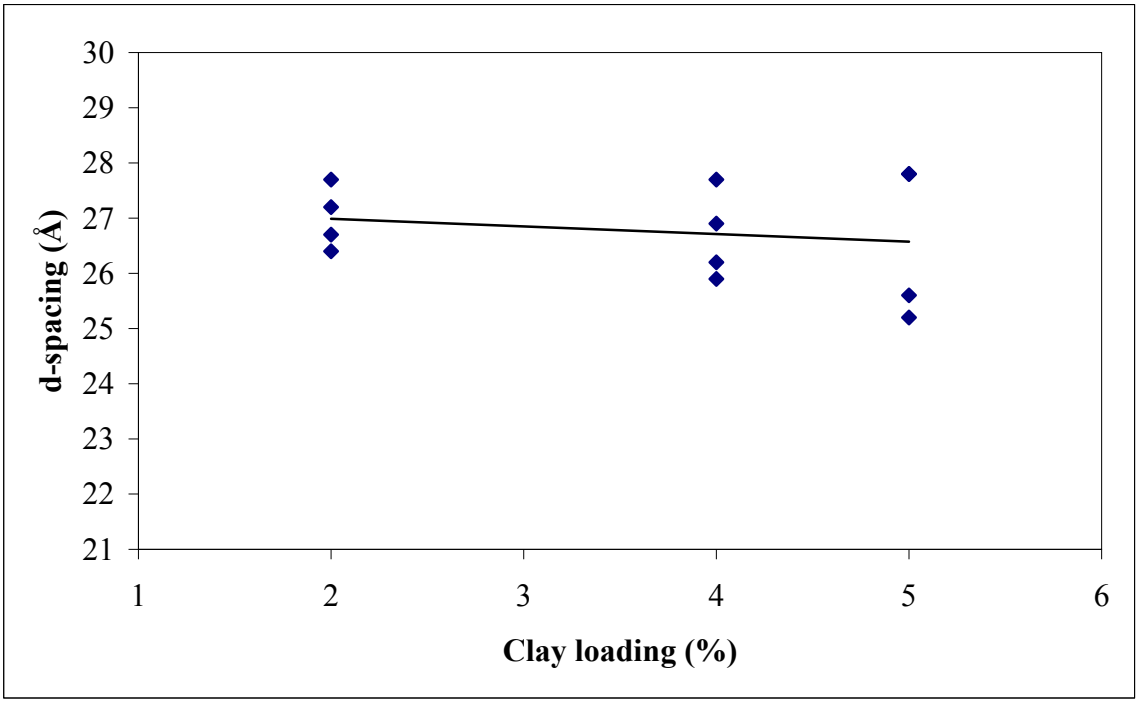

Figure 4.5e: Variation of d-spacings with clay loadings.

For the sonication time of 5 minutes (figure 4.5a), the mean d-spacing increased by 0.2Å as the amount of clay increased from 2% to 4%. With further increase in the amount of clay to 5%, the d-spacing dropped to 25.6Å. At 10 minute sonication time (figure 4.5b), intergallery spacing dropped from 26.9 Å by 0.5Å when the clay loading was increased from 2% to 4%. At 5% clay loading for the same sonication time of 10 minutes, the d-spacing further dropped to 25.2 Å. For the 30 minute sonication time represented by figure 4.5c, the initial d-spacing of 27.7 Å for 2% clay amount dropped to 26.2 Å for 4%, but jumped again to 27.8 Å when clay fraction was increased to 5%. As seen in figure 4.5d, at 60 minute sonication time, intergallery distance increased from 27.2 to 27.7 Å when the clay loading was raised from 2 to 4%. From 4% to 5% clay loading, the d-spacing increased by just 0.1 Å.

From the results (figure 4.5a-d), the relationship between the intergallery spacing and the clay amount is a combination of increase and decrease in interlayer spacing as the clay amount was increased. For instance, while the 10-minute sonication time showed an obvious inverse relationship between the d-spacing and the clay amount, the 60-minute sonication time showed increasing trend in d-spacing with respect to increased clay amount, although the change in d-spacing from 4% to 5% was only 0.1 Å for the 60-minute sonication time. Increase in the interlayer spacing at higher clay amount can be attributed to the presence of more cationic exchange ion which increased the intergallery crosslinking reaction. On the other hand, the gain could be offset by the increase in mixture viscosity which would hinder the migration of epoxy to the interlayer of the clay platelets resulting in low intergallery spacing. However, the plot for the generalized trend (figure 4.5e) shows that increase in clay loading generally lowered the d-spacing. The trend can be expressed by the following relation:

$$d = 27.263 - 0.1375x \qquad \text{for } 2 \leq x \leq 5 \qquad (4.3)$$

where d is in Å and x is in %

Avila et al. [42] reported that the basal spacing of I.30E clay in DGEBA based epoxy increased from 13.6 to 13.8 Å when the clay fraction was increased from 5% to 10%. This was 1.4% increase in basal spacing as against the 100% increase in clay loading. They explained that this was due to matrix saturation limit. Oh [31] found that the difference in clay loading insignificantly affects the d-spacing of the type of nanocomposites prepared in his study. However, Hussain et al [20] and Jinwei et al [22] showed that increase in clay concentration decreased the interlayer spacing. According to Hussein et al. [22], as the organoclay concentration increases, the viscosity of the mixture also increases, and hence the

separation of clay layers became more difficult. The d-spacing that can be achieved may be dependent on other factors than sonication time and clay amount. The degree of exfoliation and intercalation depends on the type or nature of clay, its surface modification and balancing of the intra and extra gallery polymerization rates [20, 22].

4.4. Effect of sonication time and clay loading on nanocomposite tensile properties

In the current work tensile tests were conducted on at least six specimens of each type of nanocomposite and pure epoxy to investigate their stress-strain behaviour under uniaxial tensile loading according to ASTM standard D638M-93. Representative stress-strain curves obtained from these tests are given in figures 4.6a-c, respectively for 2, 4 and 5% clay loadings.

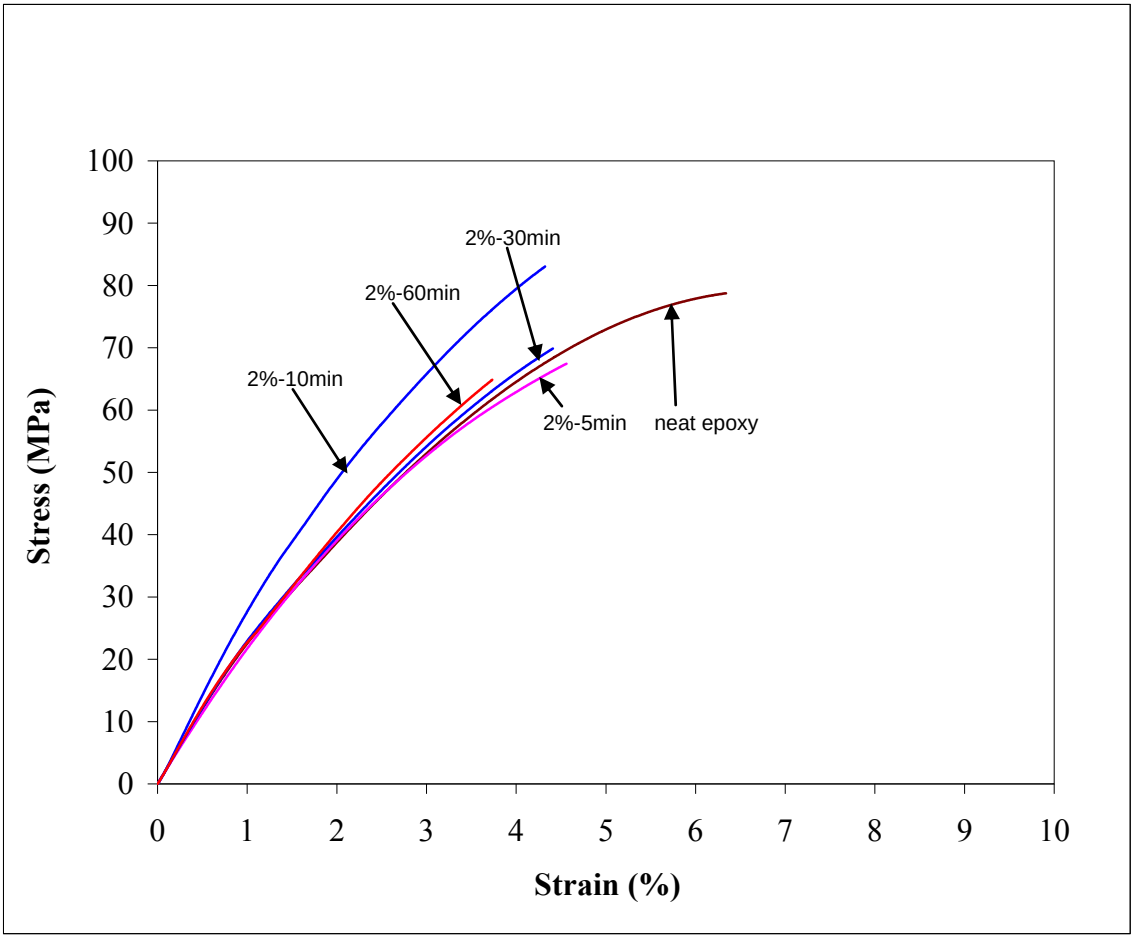

Figure 4.6a: Representative stress-strain curves for unfilled epoxy and 2% nanocomposites sonicated for 5, 10, 30 & 60 minutes.

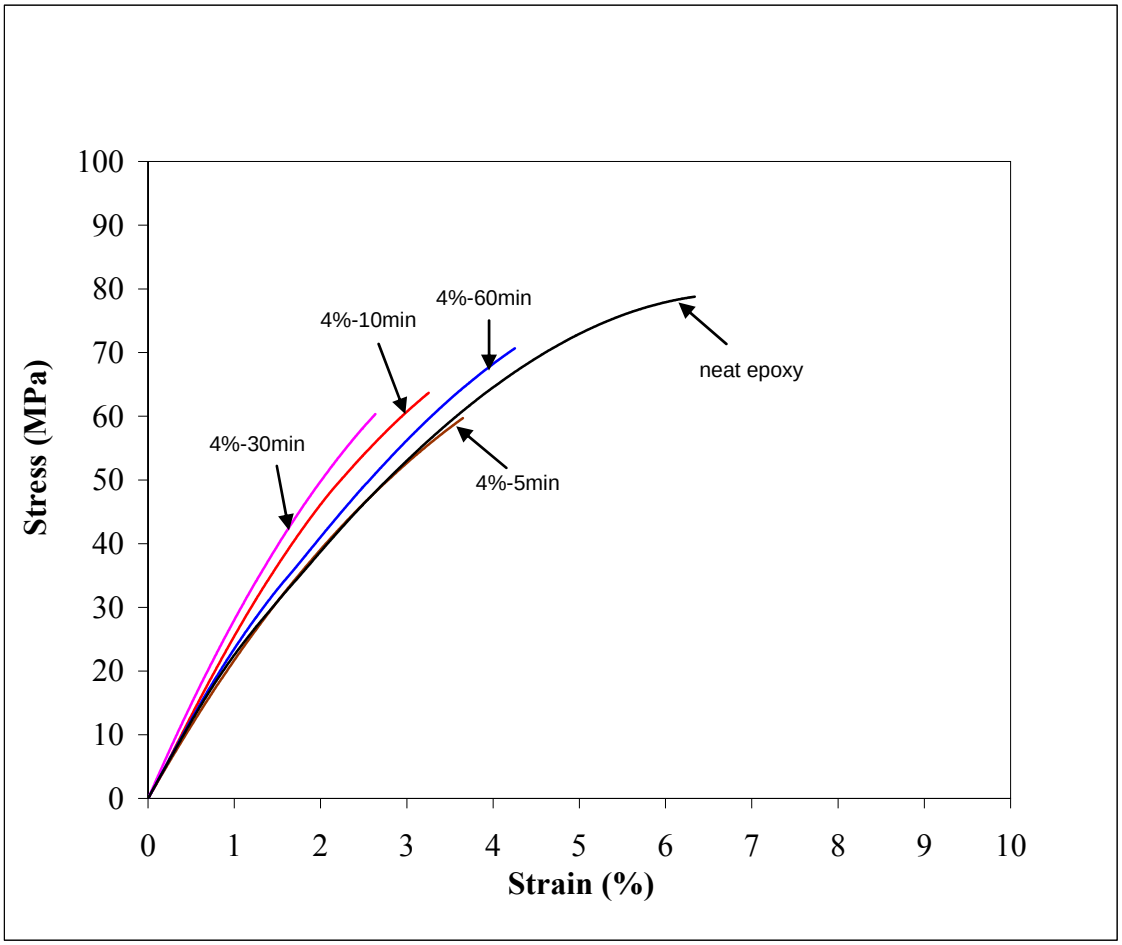

Figure 4.6b: Representative stress-strain curves for unfilled epoxy and 4% nanocomposites sonicated for 5, 10, 30 & 60 minutes.

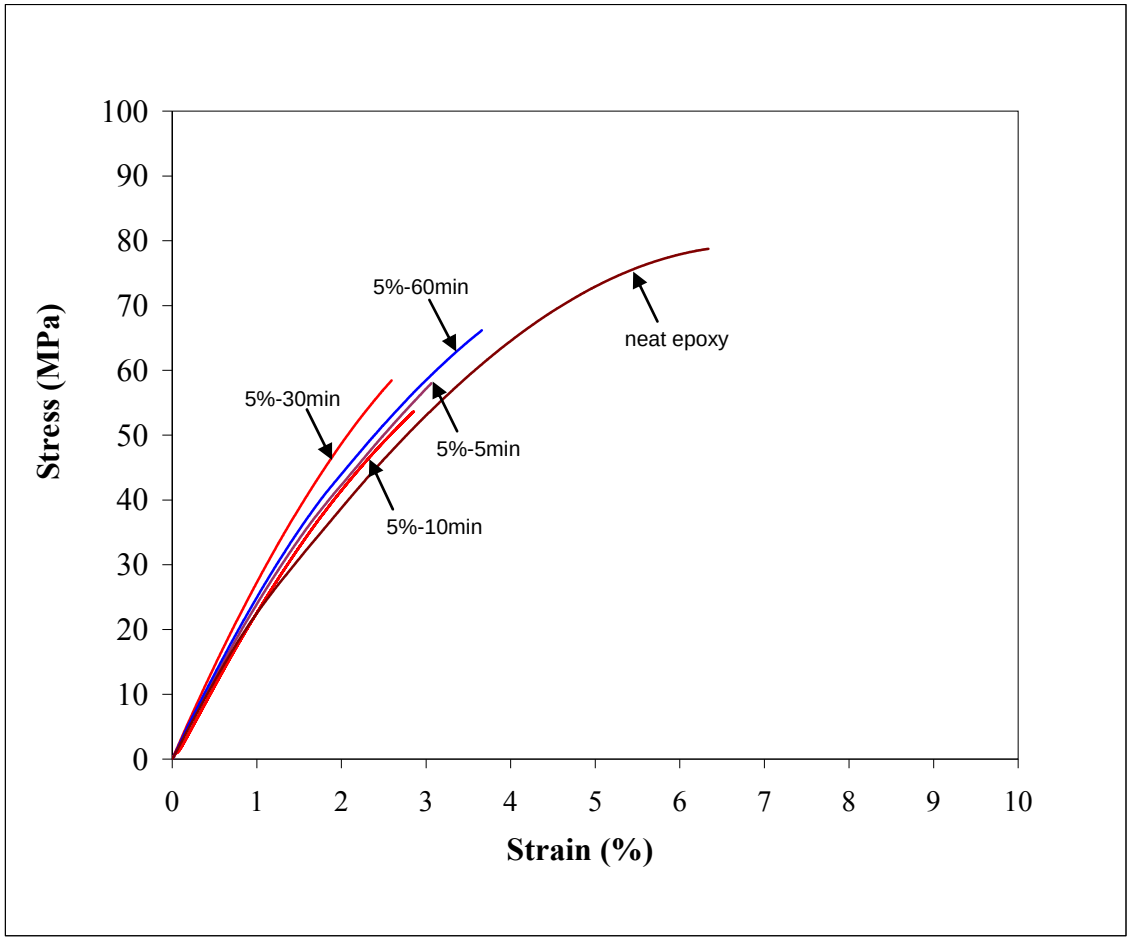

Figure 4.6c: Representative stress-strain curves for unfilled epoxy and 5% nanocomposites sonicated for 5, 10, 30 & 60 minutes.

4.4.1. Determination of stress, strain and modulus of elasticity

Tensile strengths were obtained by dividing the maximum load by the average cross-sectional areas of the tensile specimens. The tensile strengths were found to be same as the fracture strengths of the nanocomposite specimens. The modulus of elasticity of a material is a measure of its resistance to elastic deformation. In a stress-strain diagram, the elastic modulus is computed from the region where the stress is proportional to the strain. For

polymers, the elastic modulus is not easily defined by the characteristic stress-strain curve. Therefore, either secant or tangent modulus is applied to find the elastic modulus. The region of elastic modulus is not obvious in the stress-strain curves obtained in the current study as well. Hence, elastic moduli for both neat epoxy and nanocomposites were measured in accordance with the procedure specified in [39]. The initial linear portion of the load-extension curves were extended (figure 4.7). From a segment of the tangent line, load was divided by the average cross sectional area of the material and the stress obtained was used to compute the modulus of elasticity by dividing this stress by the corresponding strain in the chosen segment. Fracture strain values were derived directly from the stress-strain curves.

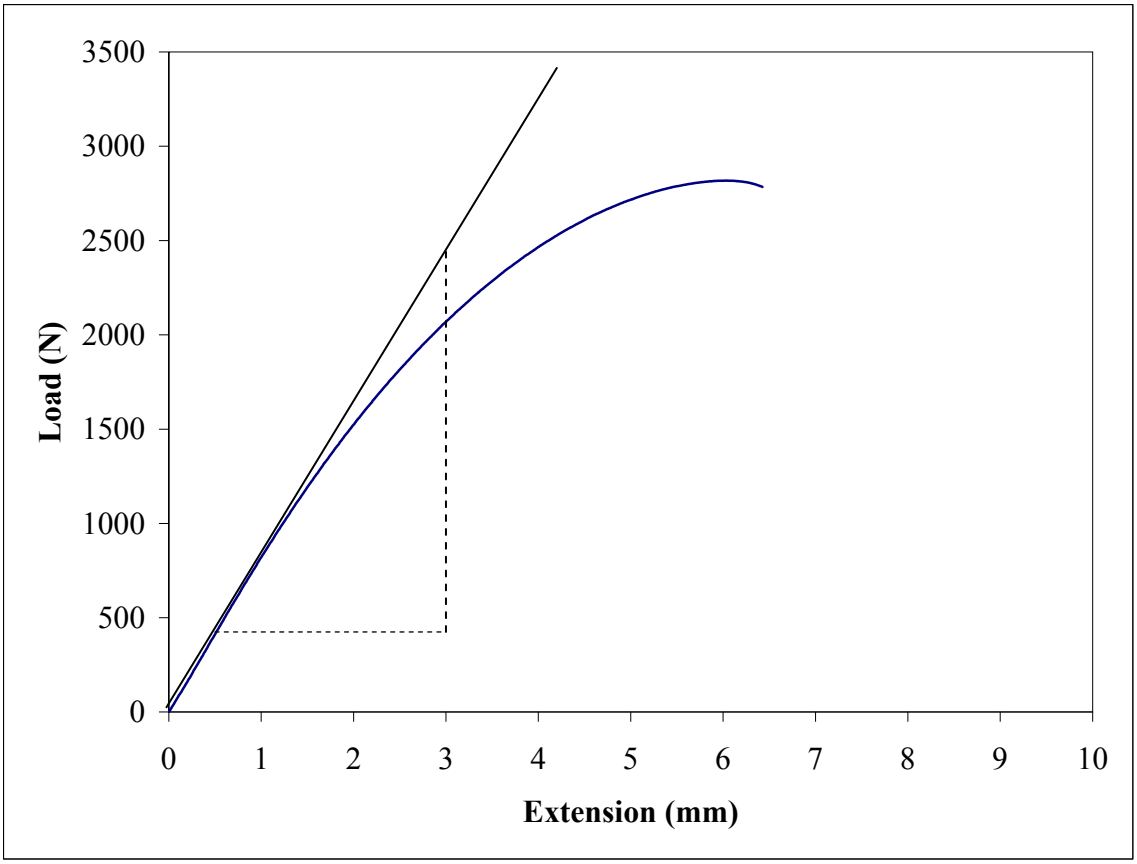

Figure 4.7: Load-extension curve for the determination of elastic modulus, E.

In table 4.4, the average values of at least six tests for the tensile properties of the neat epoxy and epoxy-clay nanocomposites are summarized. Table 4.5 shows the percentage change in the tensile properties with respect to the neat epoxy. Negative values indicate decrease in the measured tensile properties.

Table 4.4: Mean tensile properties of neat epoxy and nanocomposites.

Specimens	**Mean Ultimate Strength, S_{ut} (MPa)**	**Mean Elastic Modulus, E (GPa)**	**Mean Fracture Strain, ε_f (%)**
neat epoxy	80 ±0.9	2.3±0.18	6±0.54
2%-5min	64.7±5.1	2.25±0.07	4.6±0.59
2%-10min	82.9±1.2	2.96±0.08	4.5±0.12
2%-30min	69.7±1.5	2.41±0.02	4.5±0.17
2%-60min	64.9±1.1	2.5±0.05	3.9±0.11
4%-5min	58.8±2.7	2.3±0.17	3.5±0.60
4%-10min	63.±6.4	2.7±0.03	3.45±0.66
4%-30min	58.6±7.3	2.85±0.12	3.35±1.3
4%-60min	70.6±1.5	2.45±0.04	3.9±0.70
5%-5min	58.1±5.2	2.6±0.10	3.1±0.74
5%-10min	53.7±3.6	2.5±0.19	2.6±0.32
5%-30min	58.5±6.5	2.6±0.07	2.6±0.18
5%-60min	65.6±8.1	2.6±0.37	3.7±0.84

Table 4.5: Percentage change in the tensile properties of nanocomposites relative to the neat epoxy.

Nanocomposite	**Change in Ultimate Strength, S_{ut} (%)**	**Change in Elastic Modulus, E (%)**	**Change in Fracture Strain, ε_f (%)**
2%-5min	-19.1	-2.2	-23.3
2%-10min	3.6	28.7	-25.0
2%-30min	-12.9	4.8	-25.0
2%-60min	-18.9	8.7	-35.0
4%-5min	-26.5	0.0	-41.7
4%-10min	-21.3	17.4	-42.5
4%-30min	-26.8	23.9	-44.7
4%-60min	-11.8	6.5	-35.0
5%-5min	-27.4	13.0	-48.3
5%-10min	-32.9	8.7	-56.7
5%-30min	-26.9	13.0	-56.7
5%-60min	-18.0	13.0	-38.3

The results of the tensile tests given in table 4.4 indicate that the unfilled epoxy has an average tensile strength of 80 MPa. The mean fracture strain was found to be 6% and the average modulus of elasticity was 2.3 GPa. It is noticeable from the results given in tables 4.4 and 4.5 that the tensile strength of the nanocomposites are lower than the neat epoxy

except for the 2% nanocomposites which showed a marginal increase of 3.6 % in tensile strength at 10-minute sonication time. The results obtained here are comparable to those reported in other research works [19, 20, 27]. The characteristic curves for both the neat epoxy and nanocomposites represent a brittle behaviour. Nevertheless, the strain values illustrate that the nanocomposites are more brittle than the neat epoxy. In the sections which follow, the tensile properties obtained are related to the different sonication times, clay loadings and the d-spacings.

4.4.2. Effect of sonication time on nanocomposites tensile properties

One of the objectives of the current work was to investigate the effect of sonication time on the tensile properties of epoxy-clay nanocomposites. For epoxy-clay nanocomposite in particular, observed changes in properties are usually related to the microstructure that is defined by exfoliation or intercalation. The variation in sonication duration was observed in section 4.3.1 to have effect on the separation and distribution of clay within the epoxy matrix. Accordingly, the resulting micro structure to which many mechanical properties, including tensile strength, are linked would be influenced by the sonication time. The effect of sonication time on the tensile properties, namely, tensile strength, modulus of elasticity and elongation (strain) at break is presented in the following section. Each line on a plot represents a different clay loading.

(a) Tensile strength, S_{ut}

The variation of tensile strength with sonication time for epoxy-clay nanocomposite is shown in figure 4.8a.

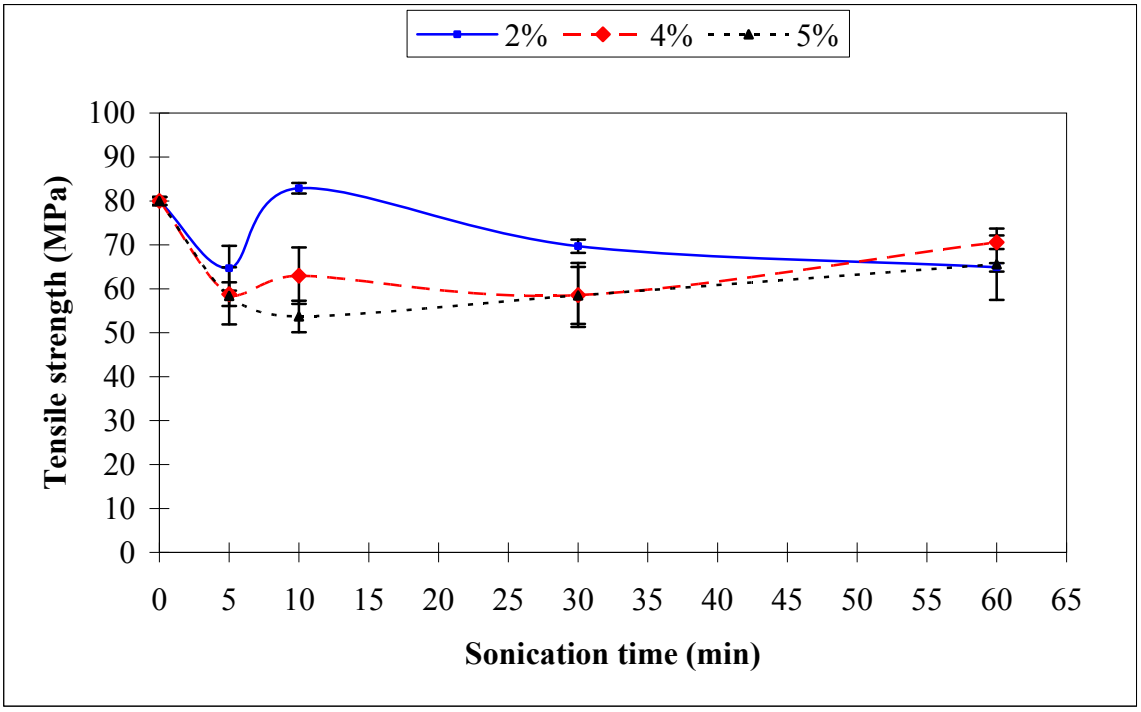

Figure 4.8a: Effect of sonication time on nanocomposites tensile stresses for the different clay loadings.

It is observed (figure 4.8a) that the 2% nanocomposite sonicated for 10 minutes shows a moderate increase of 3.6% in tensile strength. But this increase is insignificant when compared to the neat epoxy and the overall trend of decrease shown by entire samples of nanocomposites. The value of tensile strength and the corresponding percentage change were already tabulated in tables 4.4 and 4.5. While the tensile strength for the 2% nanocomposite continuously decreased after 10 minutes, the 5% nanocomposites increased in strength after 10 minute. The generalized trend of tensile strength variation with sonication time is presented in figure 4.8b.

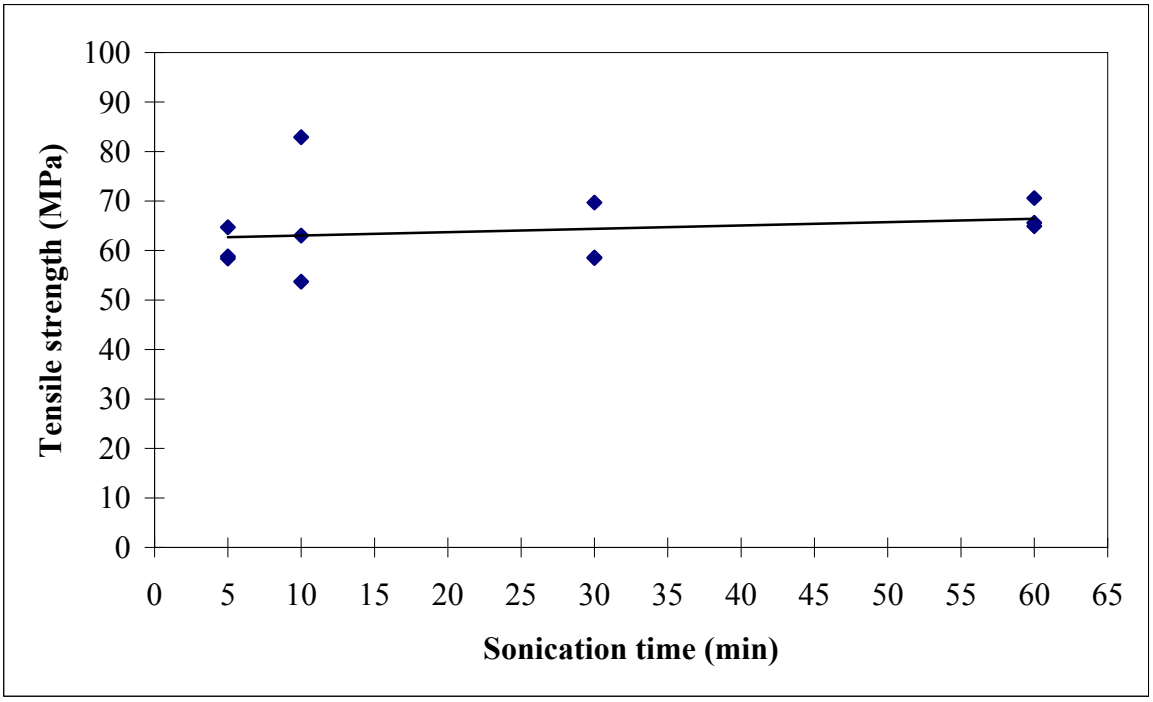

Figure 4.8b: Variation of tensile strengths with sonication times

The trend illustrates that increment in the sonication time caused the tensile strength of the nanocomposites to increase, and this can be described by the following equation:

$$S_{ut} = 0.0676t + 62.343 \qquad (4.4)$$

where S_{ut} is in MPa and t is in min

(b) Fracture strain, ε_f

The fracture strain-sonication time relationship is illustrated in figure 4.8c. The fracture strains are lower than that of the neat epoxy. While sonication time changed from 5 to 30 minutes for the 2% nanocomposite, nearly same average strain of 4.5% was maintained. At 60 minutes, it dropped to 3.9%. For 4% nanocomposite, the 5 and 10 minute sonication time

produced same average strain level of nearly 3.5%. The strain dropped to 3.35% at 30 minutes and rose again to 3.9% at 60 minutes. At 5% clay loading, 5 minutes of sonication time produced 3.1% strain. With the sonication time rising to 10 minutes, the strain dropped to 2.6%. This strain value was maintained at 30 minutes but rose to 3.1% when the sonication time was 60 minutes. The overall trend (figure 4.8d) is similar to that obtained for the tensile strength. It indicates that fracture strains remain nearly the same or only marginally increased with increase in sonication time. The generalized correlation between the strain and sonication time can be given in the following equation:

$$\varepsilon_f = 0.0032t + 3.558 \qquad (4.5)$$

where ε_f is in % and t is in min

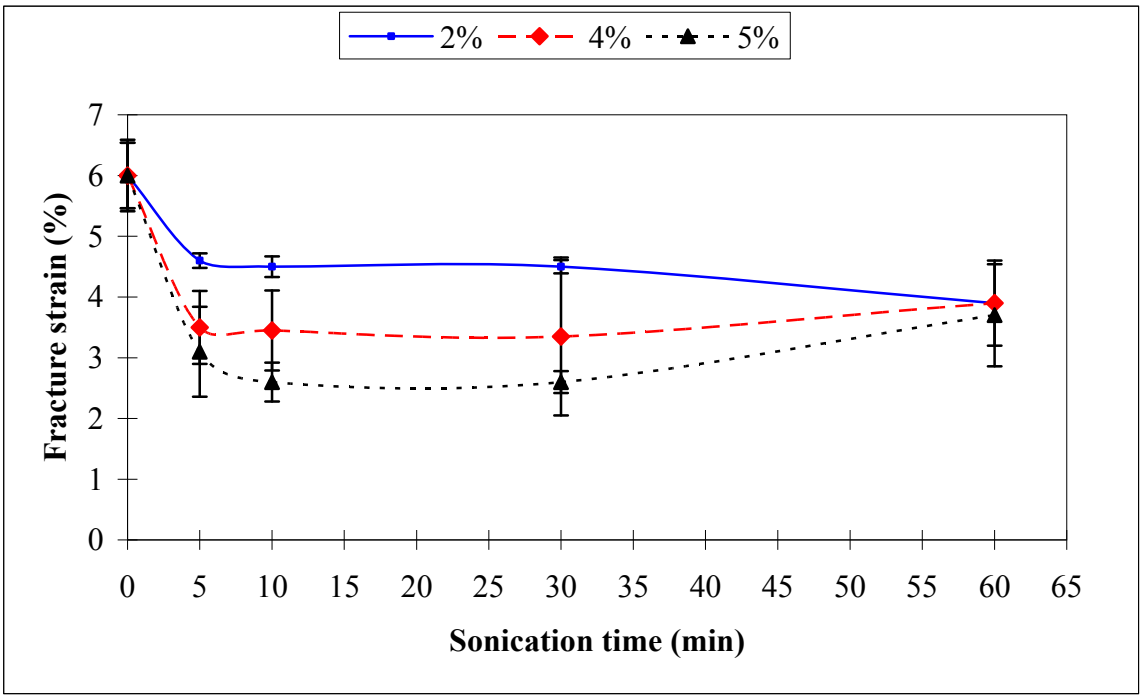

Figure 4.8c: Effect of sonication time on nanocomposites fracture strains for the different clay loadings.

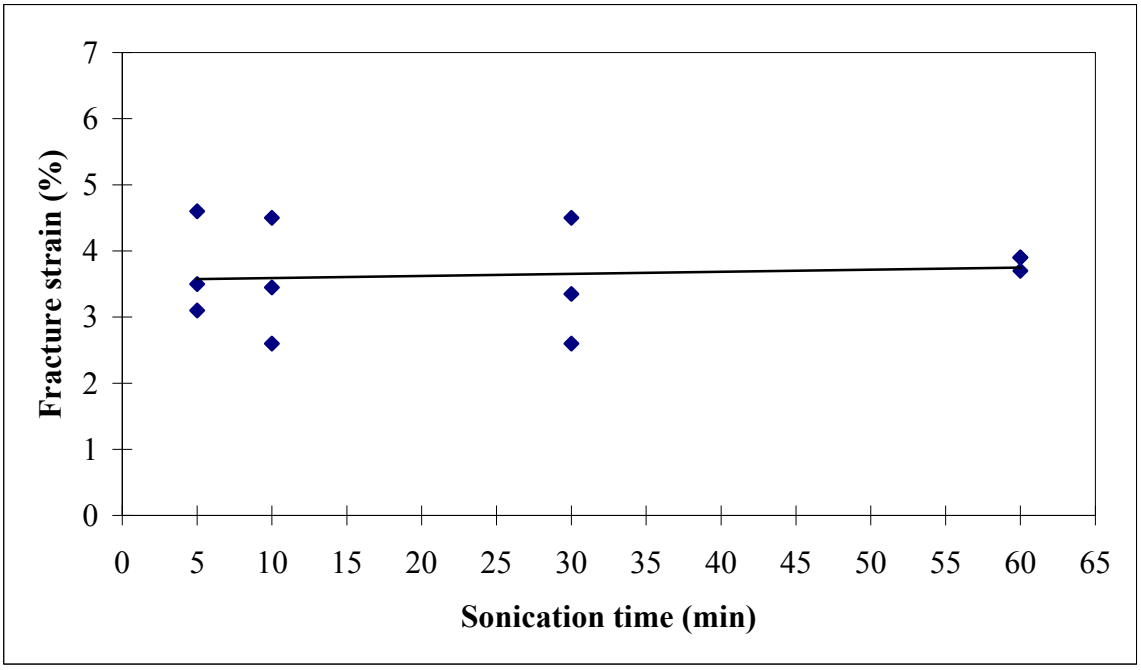

Figure 4.8d: Variation of fracture strain with sonication time.

(c) Modulus of elasticity, E.

As would be expected, the modulus of elasticity of a polymer is affected when the polymer is blended with a nanoclay material. The process and parameters of blending may also have effect on the modulus. The effect of sonication time on the modulus of the epoxy at all clay loadings was investigated. The elastic modulus of almost all the nanocomposite specimens tested in the current study are higher than that of the neat epoxy as shown in figure 4.8e and table 4.5. It is noted that the sonication of epoxy and clay results in enhanced modulus of elasticity. The general pattern of variation of modulus of elasticity with sonication time is illustrated in figure 4.8f and it shows that the sonication time generally has slight decreasing effect on the modulus. This can be represented by the following relation:

$$E = 2.5612 - 4 \times 10^{-5}\,\mathrm{x} \qquad (4.6)$$

where E is in GPa and x is in min

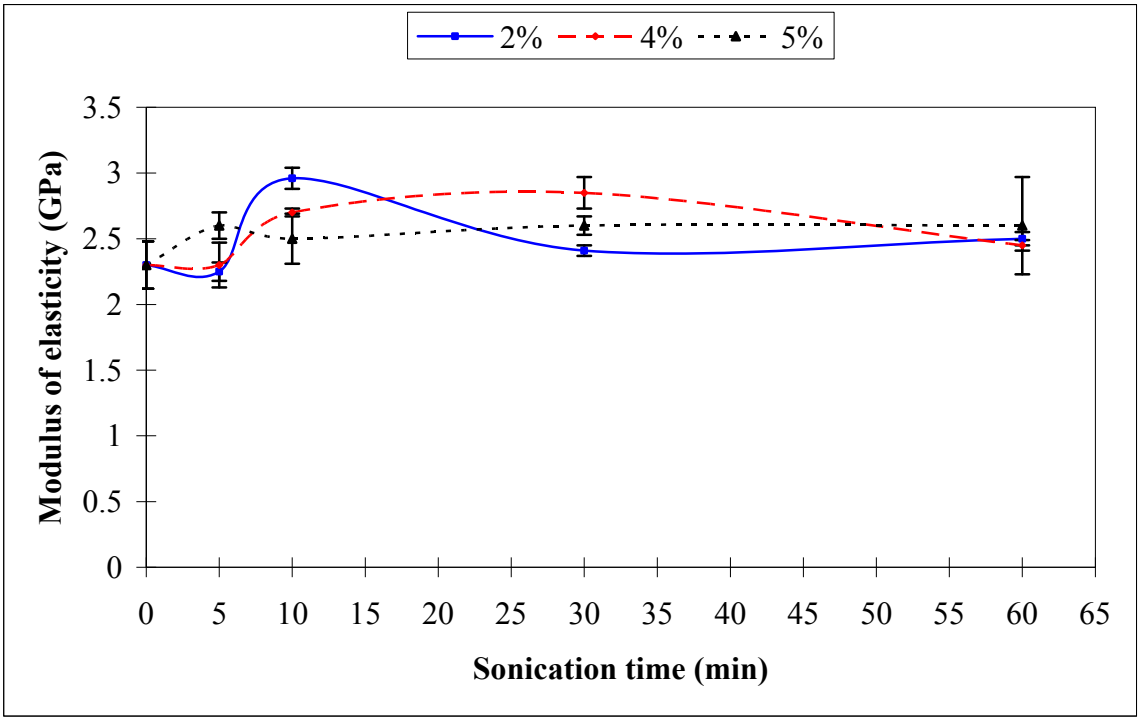

Figure 4.8e: Effect of sonication time on nanocomposites moduli of elasticity for the different clay loadings.

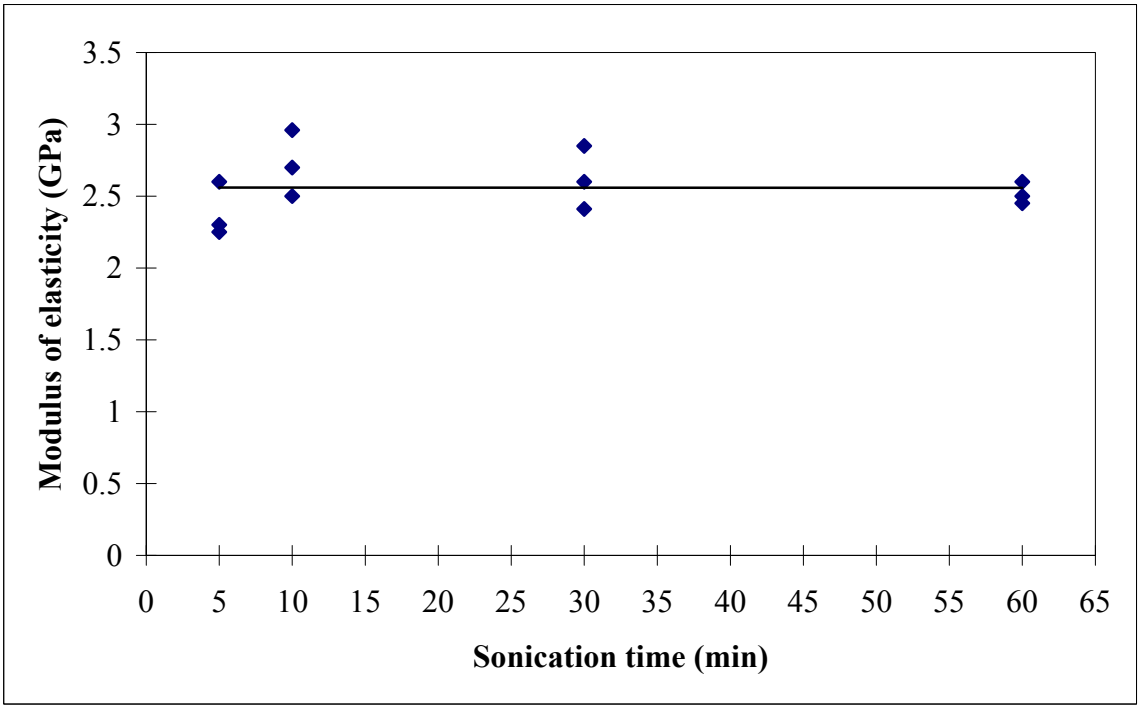

Figure 4.8f: Variation of modulus of elasticity with sonication time.

4.4.3. Effect of clay loading on nanocomposites tensile properties

The effect of clay amount on the tensile properties for the nanocomposites is presented in figures 4.9a-c and a general discussion of the result is afterwards presented.

(a) Tensile strength, $S_{ut.}$

The correlation between tensile strength and sonication time is illustrated in figure 4.9a. The general trend which is shown in figure 4.9b indicates that as the clay amount increased, the tensile strength decreased below that of the neat epoxy. The reduction in strength seems to be directly proportional to clay loading and can be expressed by the equation below:

$$S_{ut} = 79.569 - 4.18x \qquad (4.7)$$

where S_{ut} is in MPa and x is in %

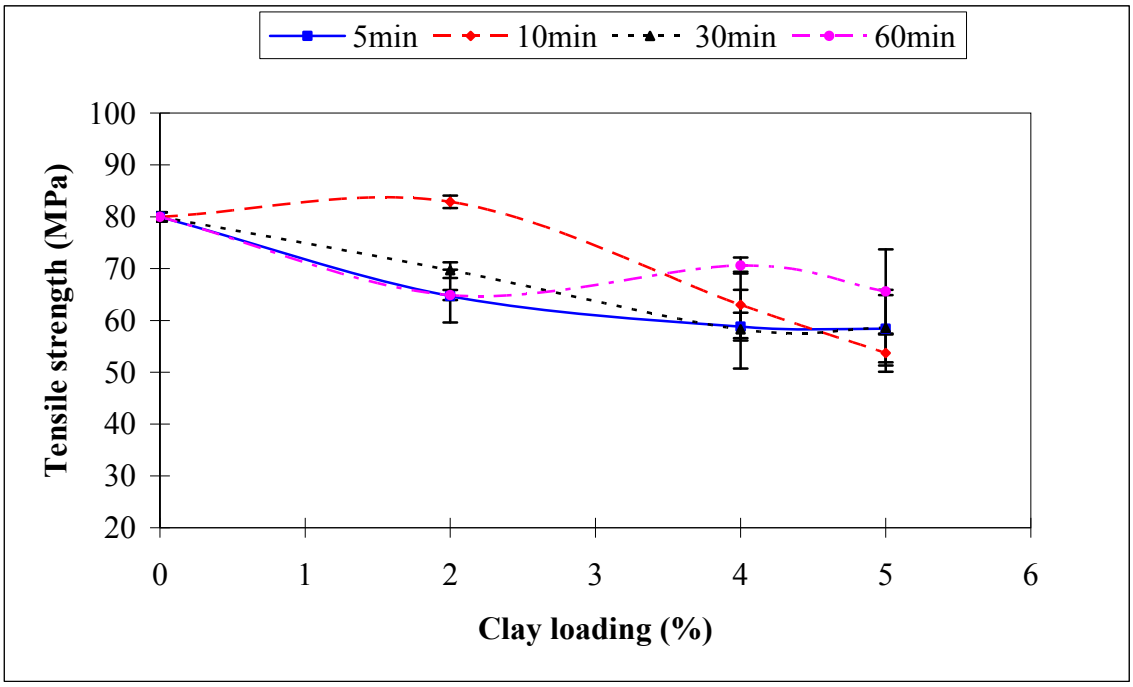

Figure 4.9a: Effect of clay loading on nanocomposites tensile strengths for the different sonication time.

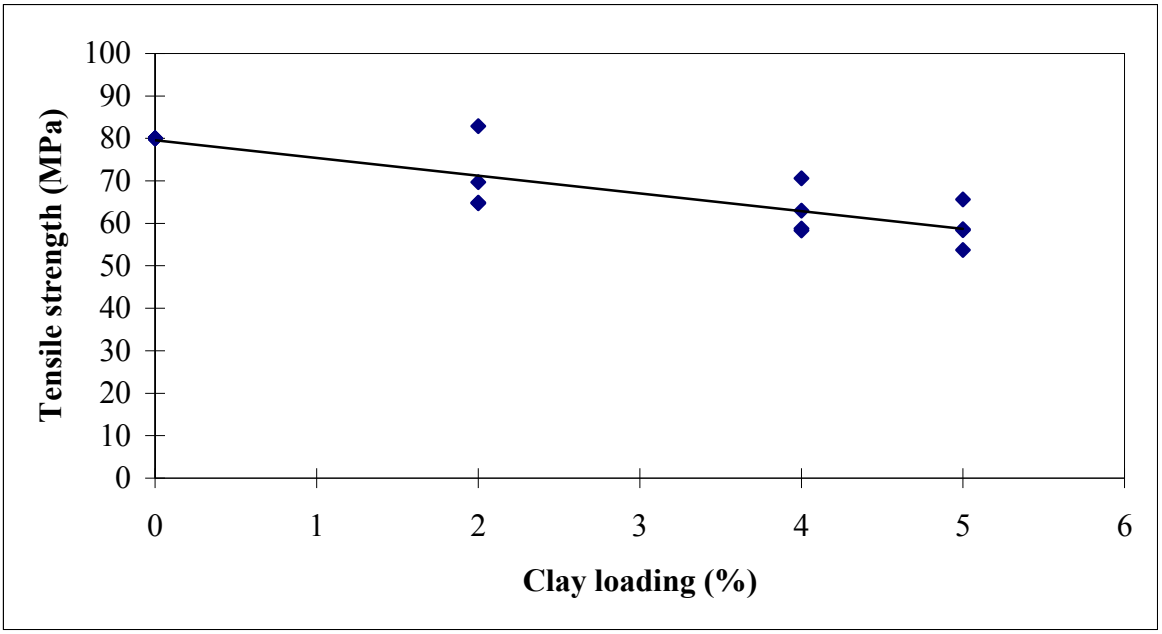

Figure 4.9b: Variation of tensile strength with clay loadings.

(b) Fracture strain, ε_f

Figure 4.9c shows the relationship between fracture strain and clay loading.

Error! Not a valid link. Figure 4.9c: Effect of clay loading on nanocomposites fracture strains for the different sonication times.

It is observed that the initial fracture strain of 6% for the pure epoxy dropped as clay amount increased at a given sonication time. For the 60 minutes sonication time, the strain remained almost constant as the clay amount increased from 2% through 5%. The variation in numerical value and percentage change in strain as clay amount increased were already shown in table 4.4 and 4.5. Figure 4.9d illustrates that the general variation of fracture strain with clay loading is similar to that of the ultimate strength. Increase in clay loading results in reduction of both fracture strain and ultimate tensile strength. The overall trend of variation of fracture strain with clay loading is described in the following equation

$$\varepsilon_f = 5.8335 - 0.5826\,x \qquad (4.8)$$

where both ε_f and x are in %

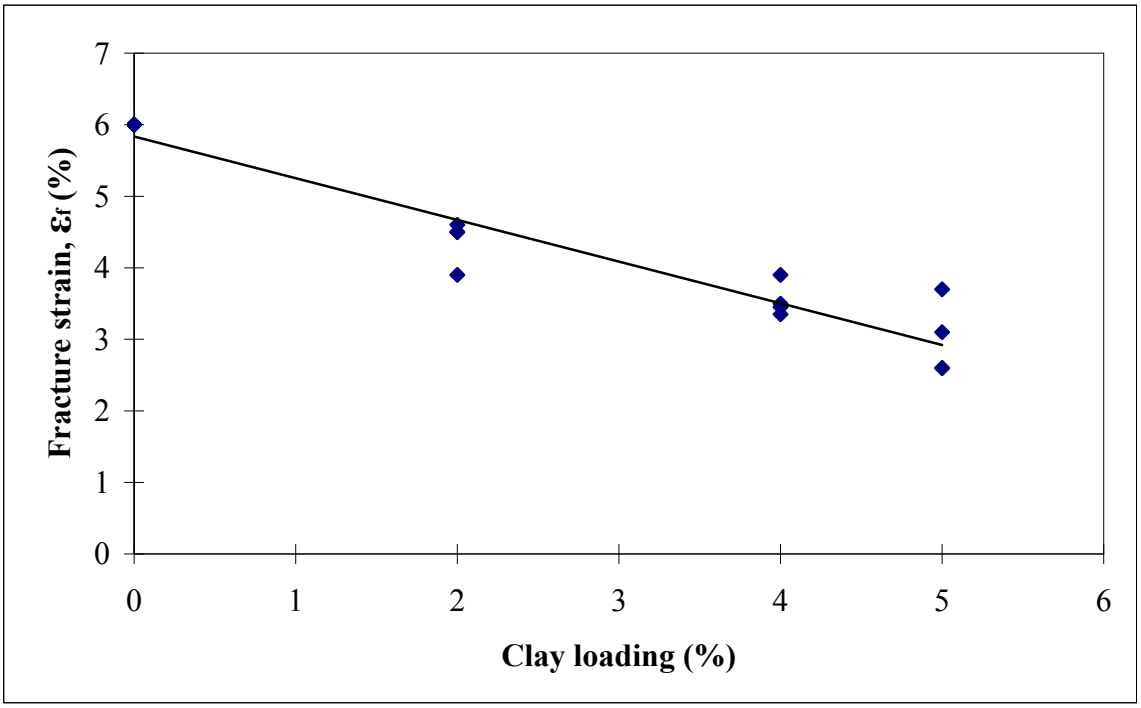

Figure 4.9d: Variation of fracture strains with clay loadings.

(c) Modulus of elasticity, E

The relationships between clay loadings and elastic moduli are shown in figure 4.9e. The elastic moduli of nanocomposites are higher than that of the neat epoxy except in two cases where the elastic modulus is of the same value on the average with that of the neat epoxy. A maximum modulus of elasticity of 2.96 GPa was recorded in the 2% nanocomposite at a sonication time of 10 minutes. The general trend (figure 4.9f) indicates that modulus of elasticity was increased as clay loading increased. The correlation between the modulus of elasticity and the clay loading can be represented by the following equation:

$$E = 0.0536x + 2.3477 \qquad (4.9)$$

where E is in GPa and x in %

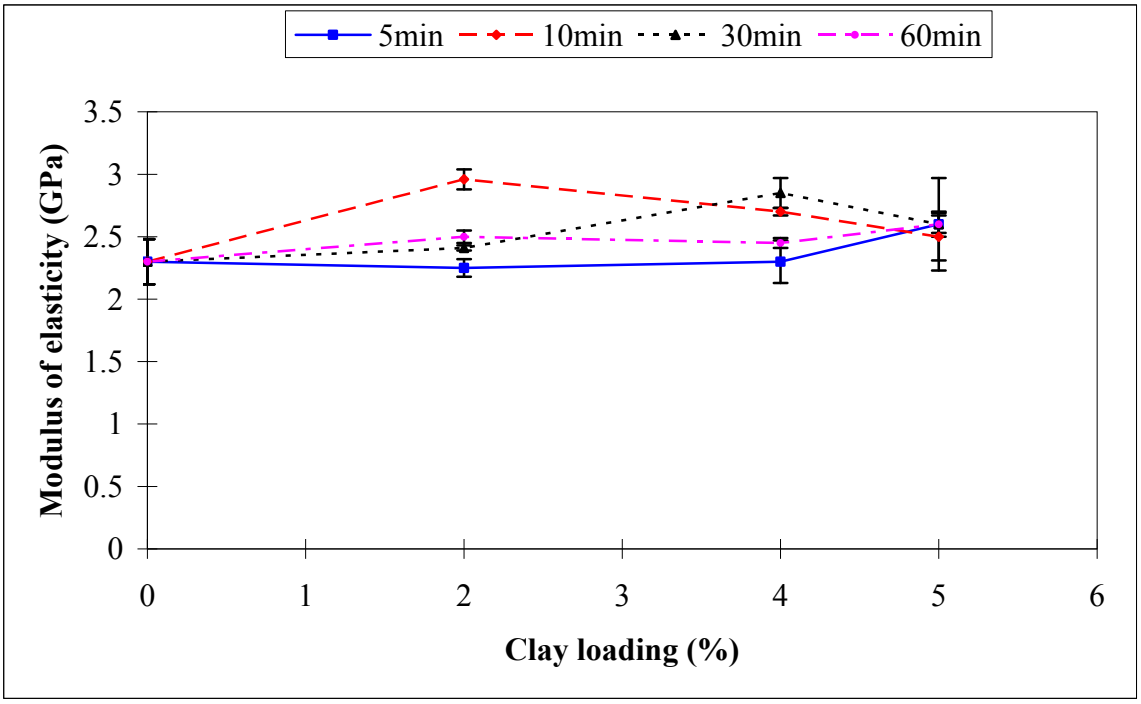

Figure 4.9e: Effect of clay loadings on nanocomposites modulus of elasticity for the different sonication time.

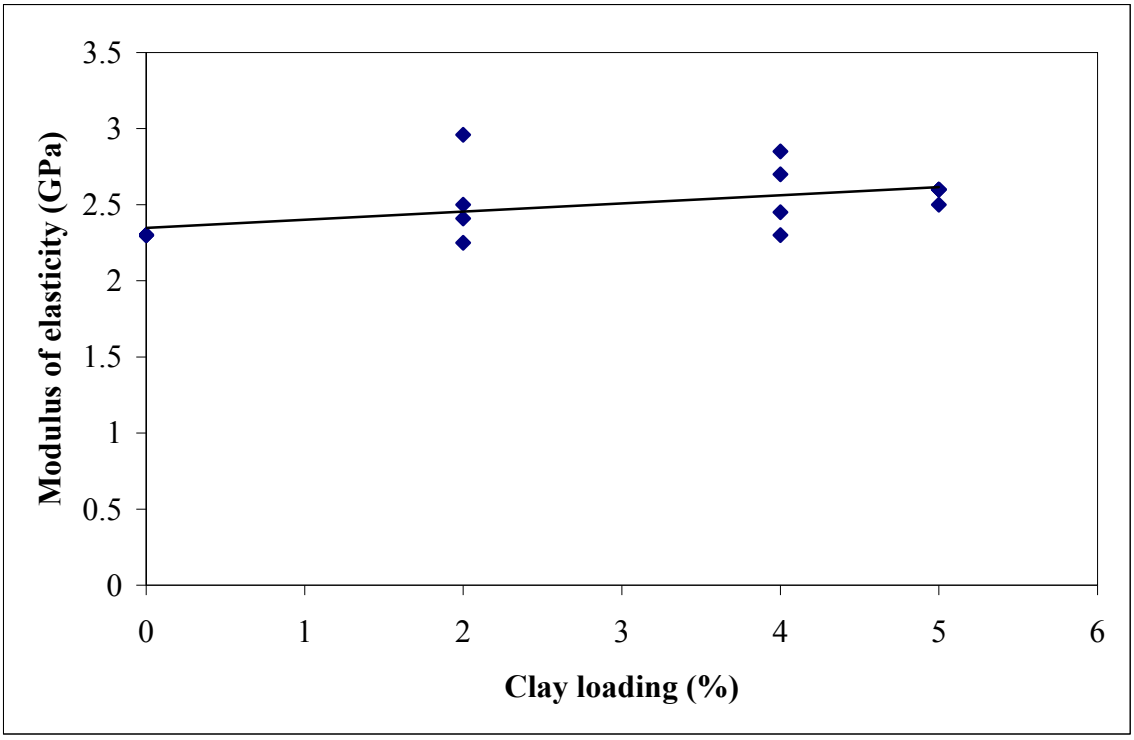

Figure 4.9f: Variation of modulus of elasticity with clay loading.

Tensile strength decreases in polymer-clay nanocomposite because of clay agglomeration that create stress concentration areas from which cracks initiate resulting in premature failure. Drop in fracture strain is due to reduced mobility in the polymer chain as a result of clay particles attachment with the polymer chain. The clay usually has higher stiffness compared to the polymer matrix. This will usually lead to higher modulus of nanocomposite. Thus, as clay loading is increased, the polymer chain may become more restricted resulting in higher modulus. Nonetheless, this is dependent on the amount of interaction between the clay and polymer, as high modulus in epoxy-nanoclay composites is also attributed to good surface interaction between clay and epoxy matrix. The clay firm attachment to the epoxy chain constrains its movement resulting in higher stiffness.

4.4.4. Effect of d-spacing on nanocomposites tensile properties

The general agreement among researchers is that the interlayer spacing resulting from mixing nanoclay with epoxy controls or has relation with the properties, especially the tensile properties.

(a) Tensile strength, S_{ut}

Figures 4.10a-c illustrate the relationships between the measured interlayer spacings and the tensile strength of the epoxy-clay nanocomposite synthesized in the present work. The trend of variation for all clay loadings and sonication times is represented in figure 4.10d.

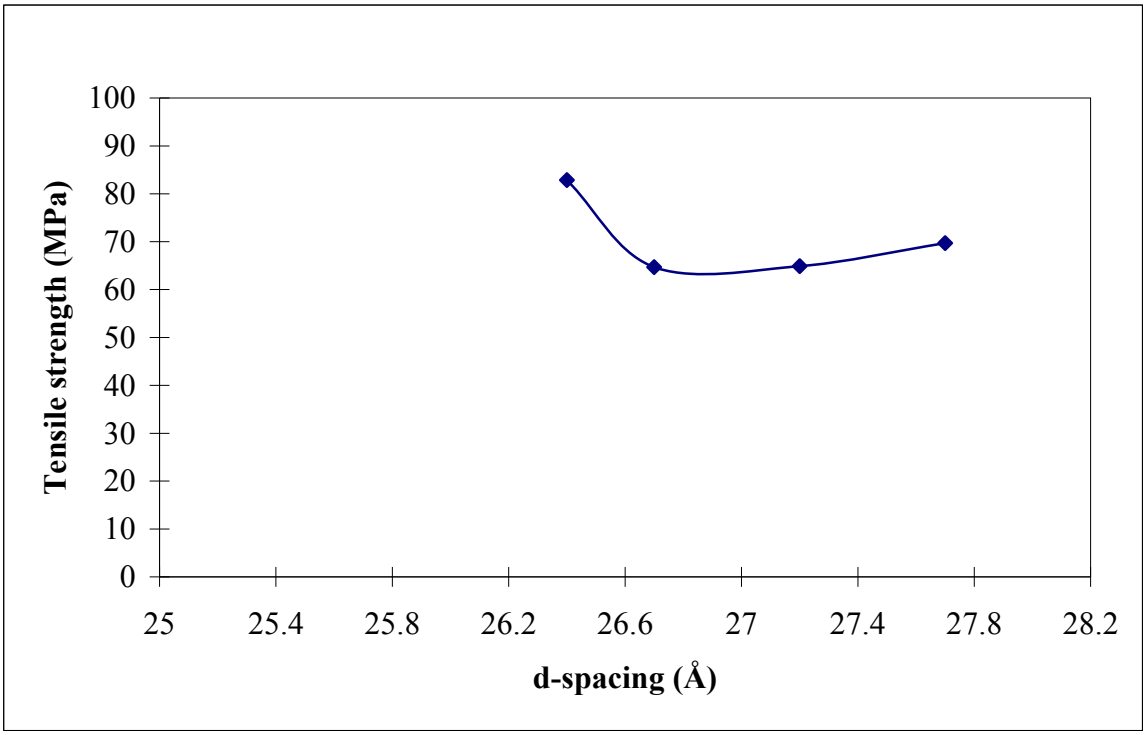

Figure 4.10a: Effect of d-spacing on the tensile strength of 2% nanocomposites.

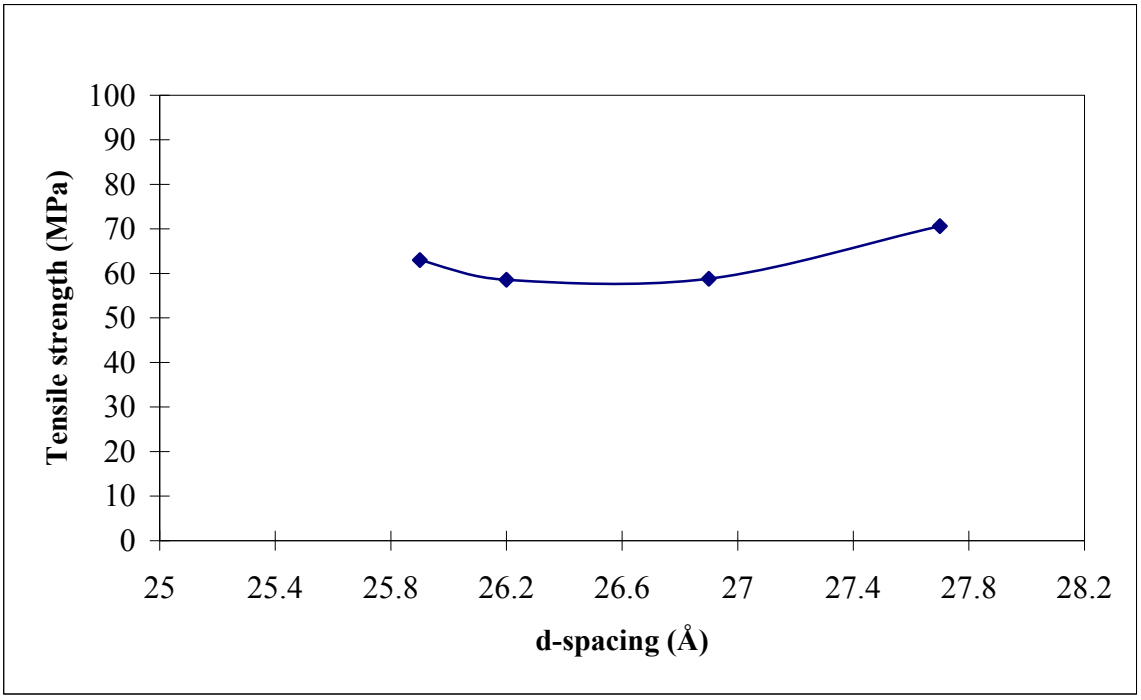

Figure 4.10b: Effect of d-spacing on the tensile strength of 4% nanocomposites.

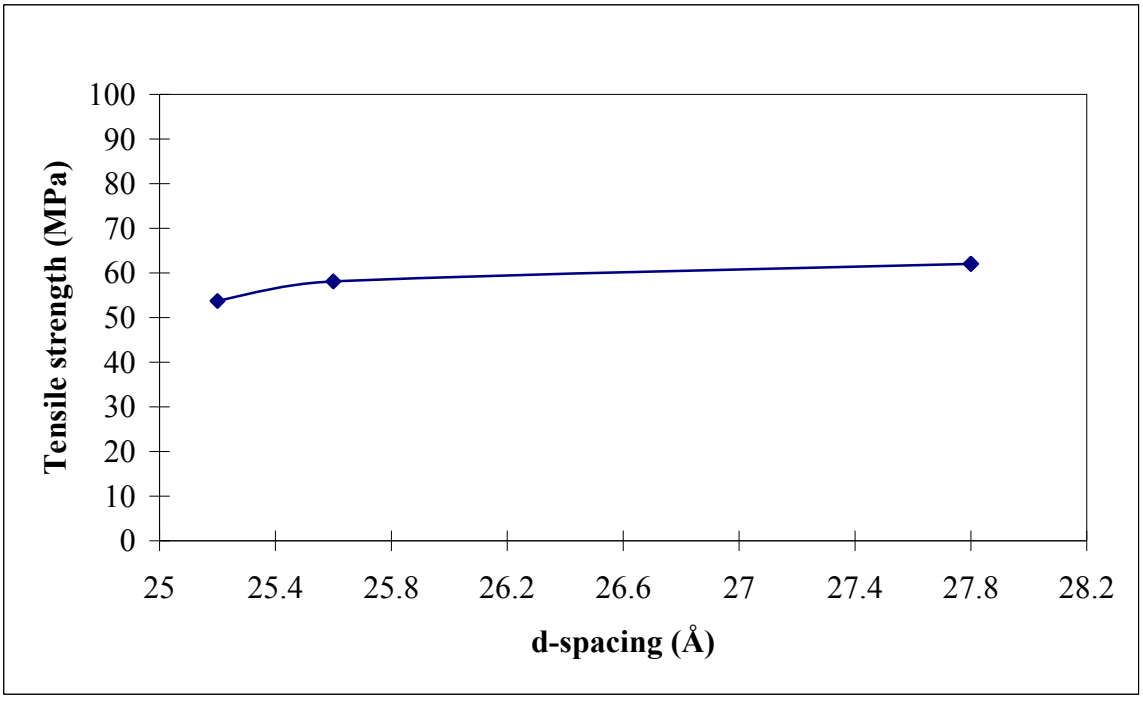

Figure 4.10c: Effect of d-spacing on the tensile strength of 5% nanocomposites.

The order of the sonication time for the plot in figure 4.10a is 10, 5, 60 and 30 minutes for 26.4, 26.7, 27.2 and 27.7 Å, respectively. The 10-minute sonication time possesses the lowest d-spacing of 26.4 Å, yet the highest tensile strength of 83 MPa. With 26.7 Å at 5-minute sonication time, the tensile strength was 64.7 MPa. As the d-spacing increased to 27.2 Å at 60-minute sonication time, the tensile strength also rose to 64.9 MPa, and at 30-minute sonication time when the d-spacing was 27.7 Å, the tensile strength increased to 69.7 MPa as well. The trend observed here is that an increase in d-spacing results in an improvement in tensile strength.

In figure 4.10b, the d-spacing obtained for the 4% nanocomposite are plotted against their corresponding tensile strength. Similar trend as seen in the 2% nanocomposite are also obvious here. The nanocomposites show an increasing trend in tensile strength as the d-spacing increased. The order of the plot is 10, 5, 10 and 60 minutes. The 10-minute sonication time has a tensile strength of 63 MPa at a d-spacing of 25.9 Å. At 26.2 Å for 30 minutes, the strength was 58.8 MPa. With increase in the d-spacing by 0.7 Å at 5 minute sonication time, the tensile strength was raised by 0.2 MPa. At 60-minute sonication time, the d-spacing was 27.7 Å and the corresponding tensile strength was 70.6 MPa.

The 5% group as illustrated in figure 4.10c also shows that higher d-spacing possessed better tensile strength. The order of the d-spacings is 25.2, 25.6, 27.8 and 27.8 Å for 10, 5, 60 and 30 minute sonication time, respectively. The corresponding tensile strengths are 53.7, 58.1, 65.6 and 58.5 MPa.

Figure 4.10d below represents the trend of variation of tensile strength with d-spacing. It can be concluded that tensile strength generally increases with increase in the d-spacing. This general relation is expressed in the following equation:

$$S_{ut} = 2.978d - 15.59 \qquad (4.10)$$

where S_{ut} is in MPa and d is in Å

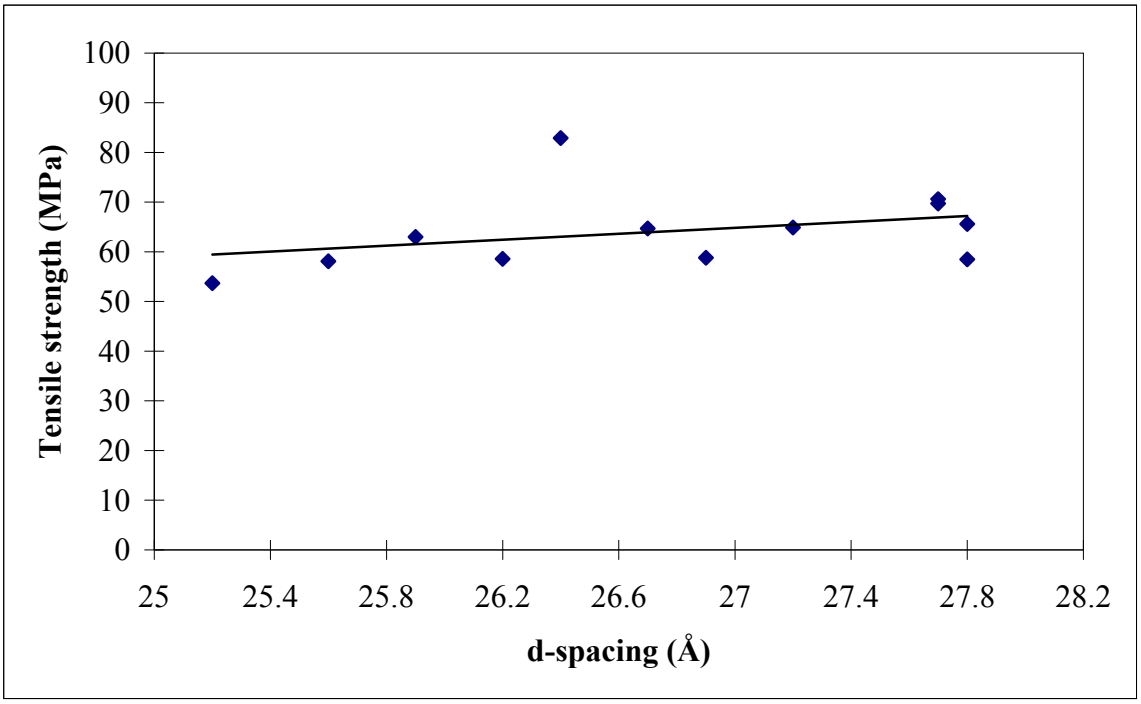

Figure 4.10d: Variation of tensile strength with d-spacing for all sonication times and clay loadings.

(b) Modulus of elasticity, E

The relationships between elastic modulus and d-spacing are depicted in figures 4.11a-c and the general trend of variation is shown in figure 4.11d.

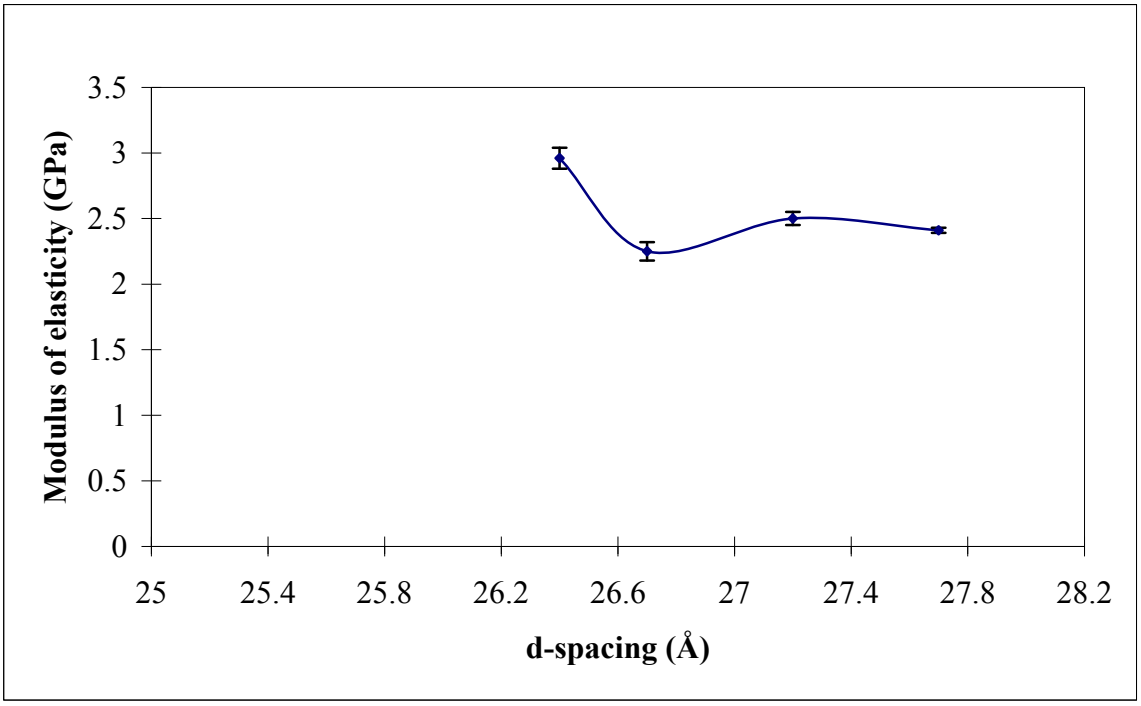

Figure 4.11a: Effect of d-spacing on the modulus of elasticity of 2% nanocomposite

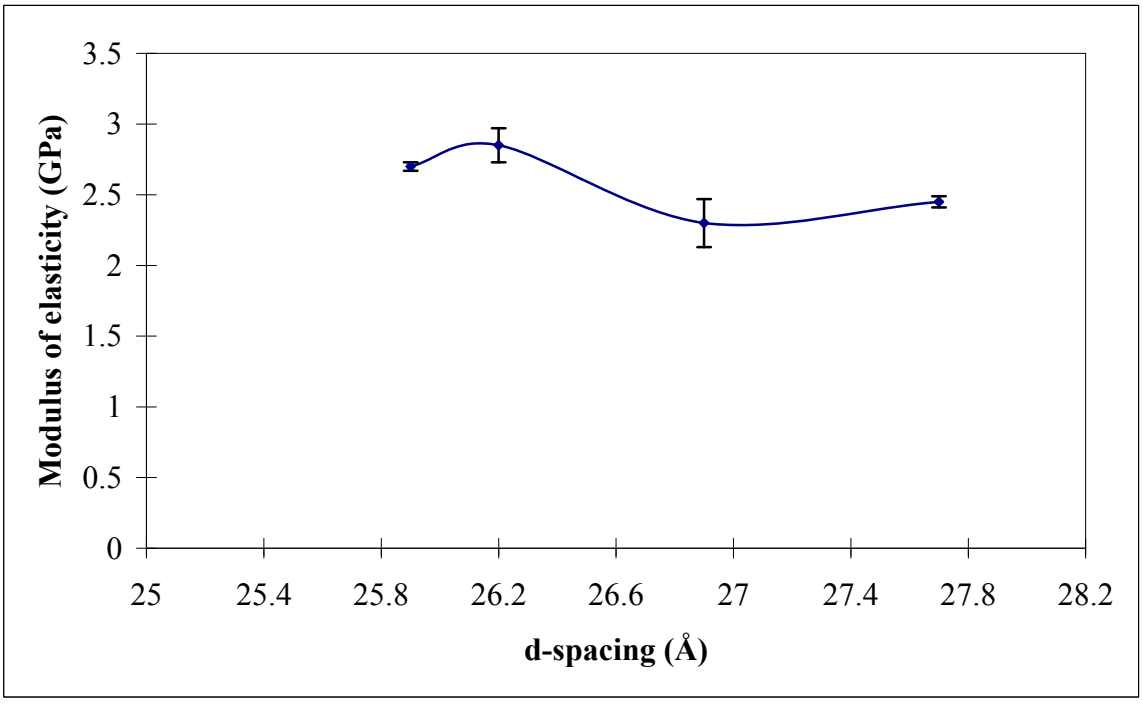

Figure 4.11b: Effect of d-spacing on the modulus of elasticity of 4% nanocomposite.

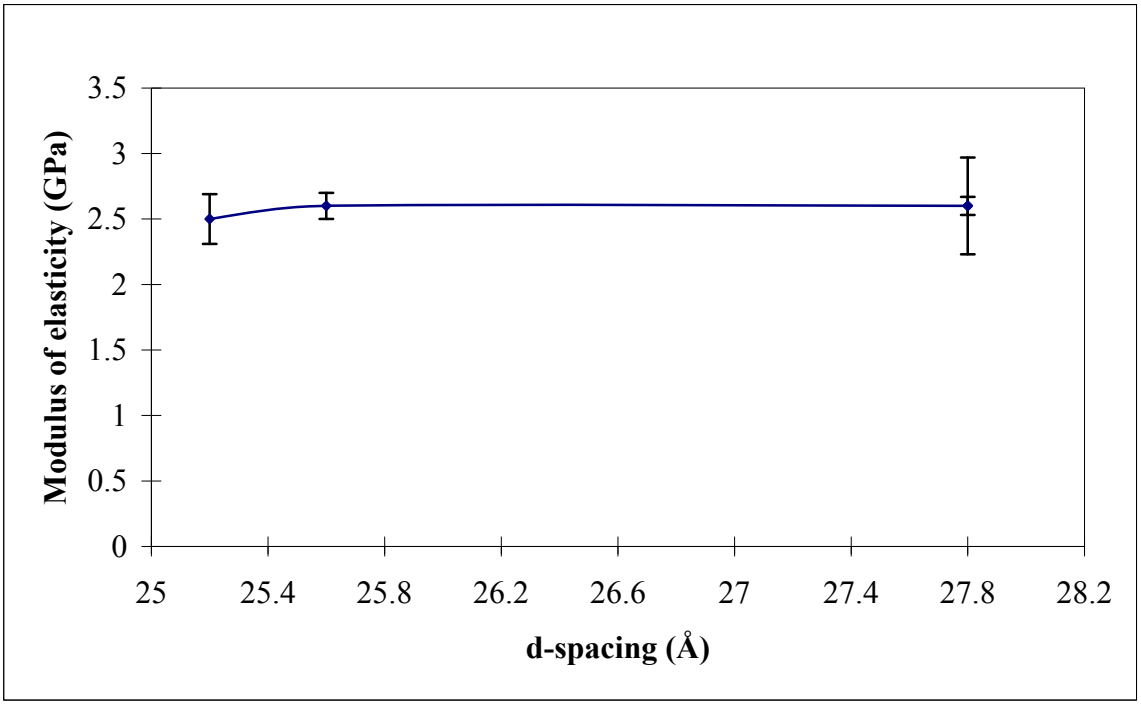

Figure 4.11c: Effect of d-spacing on the modulus of elasticity of 5% nanocomposite.

In figure 4.11a, the relationship between d-spacing and modulus of elasticity is shown for 2% nanocomposite. The order of sonication time for the d-spacing is 10, 5, 60 and 30 minutes. Initially at an interlayer spacing of 26.4 Å, the modulus of elasticity was 2.96 GPa. As the d-spacing climbed to 26.7 Å, the modulus, however, dropped to a lower elastic modulus value of 2.25 GPa. With further rise in the d-spacing to 27.2 Å, the elastic modulus once again rose to 2.5 GPa. With increase in the intergallery spacing by 0.5 Å, from 27.2 to 27.7 Å, the modulus however dropped from 2.5 to 2.41 GPa.

The intergallery distance obtained for 4% nanocomposite and the corresponding modulus of elasticity is illustrated in figure 4.11b. The fluctuation which was seen for 2% nanocomposite is also observed here. The 10 minute sonication time has the lowest interlayer

spacing of 25.9 Å and the corresponding modulus of elasticity was 2.7 GPa. This value of modulus of elasticity rose to 2.85 GPa when the intergallery spacing was 26.2 Å at 30 minute sonication time. At 5 minute sonication time when the d-spacing further rose to 26.9 Å, the elastic modulus however dropped to 2.3 GPa. The elastic modulus once again climbed to 2.45 GPa at 60 minutes as the d-spacing increased to 27.7 Å.

For 5% nanocomposite, the interlayer spacing-elastic modulus correlation is plotted in figure 4.11c. It appears that the effect of increasing intergallery spacing on the elastic modulus is minimal. At 25.2 Å for 10 minute sonication time, the modulus of elasticity was 2.5 GPa. Although the d-spacing increased to 25.6, 27.8 and 2.78 Å, respectively for 5, 60 and 30 minutes, the elastic modulus increased but remained at 2.6 GPa.

The general relationship between elastic modulus and d-spacing for all sonication times and clay loadings are depicted in figure 4.11d and can be expressed in the following equation:

$$E = 4.2784 - 0.0642\text{x} \qquad (4.11)$$

where E is in GPa and d is in Å

It can be concluded, hence, that the modulus of elasticity decreases as d-spacing rises.

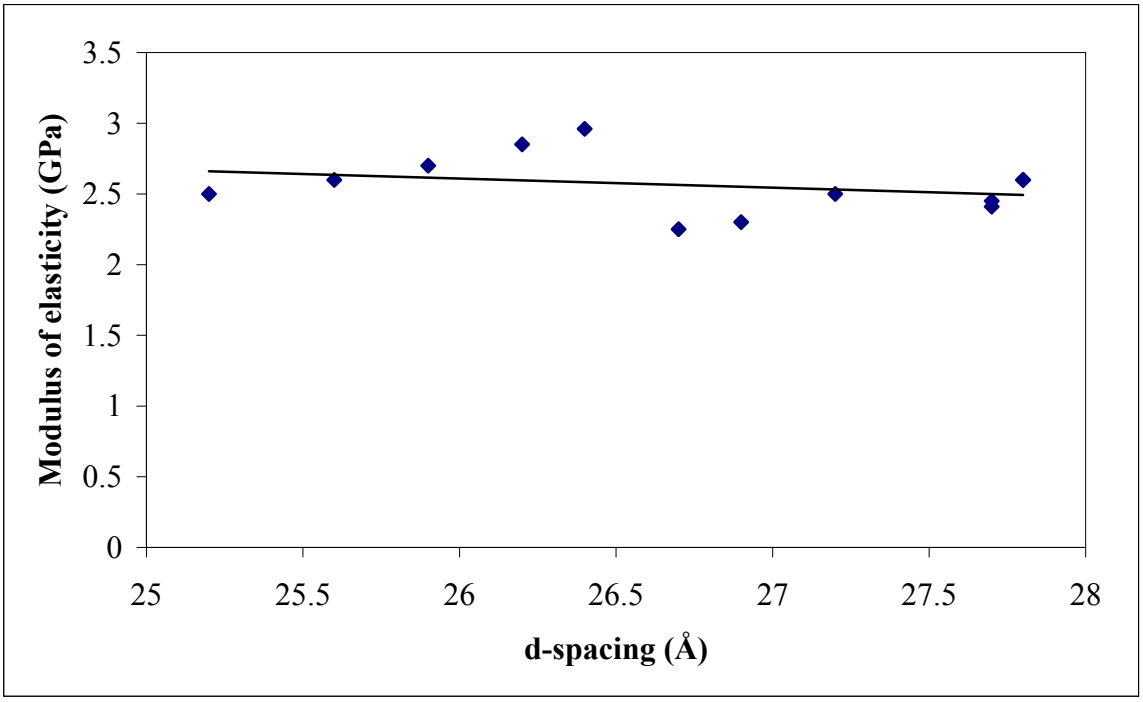

Figure 4.11d: Variation of modulus of elasticity with d-spacing for all sonication times and clay loadings

From the results (figure 4.10a-4.11d) it can be concluded that the increase in interlayer spacing results in better tensile strength. For the modulus of elasticity, the generalized observation is that increase in the intergallery spacing resulted in slight decrease of modulus of elasticity. Increase in tensile properties as the intergallery spacing rises can be attributed to increase in the volume to surface area ratio. When d-spacing increases, it means two opposing clay platelets have moved further apart due to ingression of polymer matrix between them, yet the surface area remains the same. It signifies that more polymer chains have entered into the intergallery surface making maximum possible interaction with the platelet surface. Luo and Daniel [1] performed a theoretical modeling of the interlayer space to predict its effect on nanocomposite modulus. They showed that higher composite modulus

was obtained by increasing the d-spacing. They acknowledged however that this effect would be marginal because of the effect of reduced aspect ratio of platelets.

4.4.5. General discussion of the tensile properties

The first direct effect of sonication time is probably on the nanocomposites micro-structure as was revealed by x-ray diffraction. As it was seen in the variation of d-spacing with respect to sonication time (figures 4.4a-c), the pattern of variation in the intergallery spacing as sonication time was changed followed an increasing trend. Since the amount of clay layer separations attained was taken to represent the microstructures of the samples, the trend observed in the relationship between sonication time and d-spacing as revealed by x-ray diffraction may also be reflected in other properties which are dependent on the microstructure, as it was observed in the variation of the tensile strength with respect to d-spacing. It should be mentioned that correlating the micro structural identity with mechanical properties has its limitation. By and large, only the intercalated phase has been related to other measured properties because it is the quantifiable phase of the micro structure. However, some levels of exfoliation or disordered intercalation have been achieved in the nanocomposites. Such exfoliation or disordered intercalation which can not be quantified in numerical value would have combined to influence the tensile properties of the nanocomposites. In addition, the interlayer spacing is an experimentally measured property which was likely affected by such parameters as clay volume and sonication time. It is, thus, not an independent parameter as it was illustrated in figures 4.10a-c to 4.11a-c. As it is explained later in the section, the tensile properties could have been affected by other factors other than the sonication time, interlayer spacing and clay amount, such as, voids and

clay agglomeration. The presence of these factors can be used to explain why nanocomposite with lower d-spacing possessed better tensile properties or those with same interlayer spacing had dissimilar tensile properties, as it was observed in the present work. Nonetheless, voids and clay agglomerates are also influenced by sonication time and clay amount. For instance, the longer the sonication time, the more foam is produced in the epoxy-clay blend and hence, the more difficult the degassing process. Also, the higher the clay loading, the higher the chance for nanoclay to form agglomeration, especially at lower sonication time.

In general, the trend of the results obtained in the current work shows that blending epoxy with clay under different sonication times and clay loadings caused decrease in the tensile strength of the material. Yet, the material becomes stiffer causing the Young's modulus to be higher as a result of interaction between the clay and epoxy regardless of sonication time. Increased modulus is attributed to the constraint in the movement of the polymer chain by clay layers. Such increase is brought about by the good interfacial interaction between the polymer-clay blend. Increased elastic modulus has also been linked to the high modulus of the clay [27]. It is observed that almost all the 2% nanocomposites have higher tensile strength and fracture strain than their 4% and 5% counterparts sonicated for the same duration. This suggests that increase in clay amount will further lower the tensile strength and fracture strain. This agrees with what was reported by a number of other researchers [2, 18, 20]. With increased clay amount, the number of sites with clay agglomeration will increase due to the presence of more clay particles, as evidenced by SEM images in section 4.5.1. Higher clay contents increased the viscosity of the blend which hampered complete

degassing process. Thus, this produces more voids in the cured nanocomposite with higher clay contents resulting in early failure.

The drop in the tensile strength observed in the synthesized nanocomposites can also be attributed to voids resulting from the epoxy-clay blending process. As was reported in section 4.1, mixing clay with epoxy produced bubbles and foams. After sonication, the blend was stirred again with stirring rod to burst the bubbles and foam before it was taken for degassing, it was still impossible to remove all the bubbles through the degassing before the outset of crosslinking, especially in the nanocomposites with high clay fractions. The crosslinking start times of the nanocomposites were less than that of the neat epoxy because of the onium ions presence in the clay which catalyzed the curing process. So, these remaining bubbles later constituted themselves into internal microscopic voids which became potential failure initiation sites in the cured nanocomposite as shown in the SEM images in section 4.5.1. Bozkurt et al [44] found that the void content of the nanocomposites increased with increase in the amount of clay in the epoxy matrix. It was observed that voids could also be created due to air trapped in material during pouring into mould. Clays which remained unbroken or aggregated as shown by the fractographic images in section 4.5.1 may have caused poor interfacial interaction between the epoxy and clay. These form stress concentration sites where failure can also begin. The tensile test results obtained in the current work are similar to what was observed by Hussein et al. [20]. The authors used a combination of mechanical stirrer and ultrasonicator to mix different percentage of I.30E clay with epoxy. Only nanocomposite with 1% clay volume marginally increased in tensile strength by 3%. Both the 2% and 5% nanocomposite decreased in tensile strength by 8% and

22%, respectively. They concluded that the low tensile strength observed was due to clay stack forming stress concentration effect which ultimately reduced the adhesion strength at nanoclay matrix interface. Qi et al. [27] investigated the tensile properties of DGEBA based epoxy mixed with 2% I.30E clay under mechanical stirrer for 2 hours. They recorded a decrease in tensile strength, failure strain and the Young's modulus of the material. Only at 10% wt they recorded a 12.2% increase in modulus. Yasmin et al. [19] processed nanocomposites from Cloisite 30B clay and Araldite 6010 using the three-roll mill. The tensile strength of the materials was reduced by more than 60 %. They concluded that the low tensile strength was process related. The authors observed that the epoxy-clay blend was highly viscous and foamy with the addition of clay. Likewise in the current work, foaming and high viscosity became a serious challenge as clay amount increased. Also, Isik et al [2] observed that the tensile strength of nanocomposites prepared from the epoxy resin Araldite M and Cloisite 30B nanoclay decreased with increasing amount of the montmorillonite clay. This they attributed to higher stress concentration effect of clay agglomerates at high clay contents. They explained further that non-exfoliated clay particles form larger agglomerates, and thus clay–polymer surface interactions decrease. Velmurugan and Mohan [18] have also reported low tensile strength but higher modulus of elasticity for the nanocomposites synthesized in their work. They observed from their study that for the nanocomposites containing 5 or higher wt% of clay, the degassing problem becomes critical. Hence they affirmed that the reduced tensile strength was due to voids resulting from incomplete degassing, causing specimen failure at relatively low strains under tensile loading. They claimed that the improvement of elastic modulus was due to the exfoliation/intercalation of nanoscale clay particles in the matrix that restricted the mobility

of polymer chains under loading and also due to the good interfacial adhesion between the particles and the epoxy matrix.

The current results however contrast with the results obtained by Ho et al. [8] and Samandari et al. [9]. Ho et al. [8] reported increase in tensile strength of the nanocomposites produced by addition of up to 7wt% of clay to epoxy. However, the tensile strength of the 2wt% nanocomposite was inexplicably lower than the neat epoxy. Samandari et al. [9] found that increase in clay quantity increased the tensile strength and modulus of elasticity of the nanocomposite they prpepared. But while the tensile strength continuously rises with up to 10 % of clay, the modulus of elasticity decreased after 6% clay addition. They concluded that the changes observed were due to the type of the surface treatment of that clay.

It can be concluded from the results obtained in the present work that nanocomposites tensile properties are more affected by clay loadings than sonication times.

4.5. Effect of sonication time and clay loading on nanocomposite hardness

Table 4.6 below summarizes the measured Vickers hardness for the neat epoxy and nanocomposites. Each hardness value is an average of ten indentations with indentation positions being at least 5 mm apart. In the sections which follow, these results are analyzed in relation to the sonication times and clay loadings.

Table 4.6: Average hardness, standard deviation and percentage change in the hardness of epoxy-clay nanocomposites.

	Mean hardness	**Standard deviation**	**%change**
Neat epoxy	19.15	0.15	
2%-5min	19.11	0.14	-0.47
2%-10min	19.16	0.16	0.05
2%-30min	19.08	0.18	-0.62
2%-60min	19.4	0.21	1.23
4%-5min	19.82	0.35	3.22
4%-10min	19.52	0.11	1.66
4%-30min	19.56	0.16	1.89
4%-60min	19.49	0.08	1.52
5%-5min	19.30	0.08	0.81
5%-10min	19.22	0.08	0.38
5%-30min	19.18	0.29	0.14
5%-60min	19.36	0.09	1.09

4.5.1. Effect of sonication time on nanocomposite hardness.

Four cases of sonication time were considered in the present work; 5, 10, 30 and 60 minutes. Figure 4.12a illustrates the effect of sonication time on nanocomposites hardness for each of the nanoclay loadings.

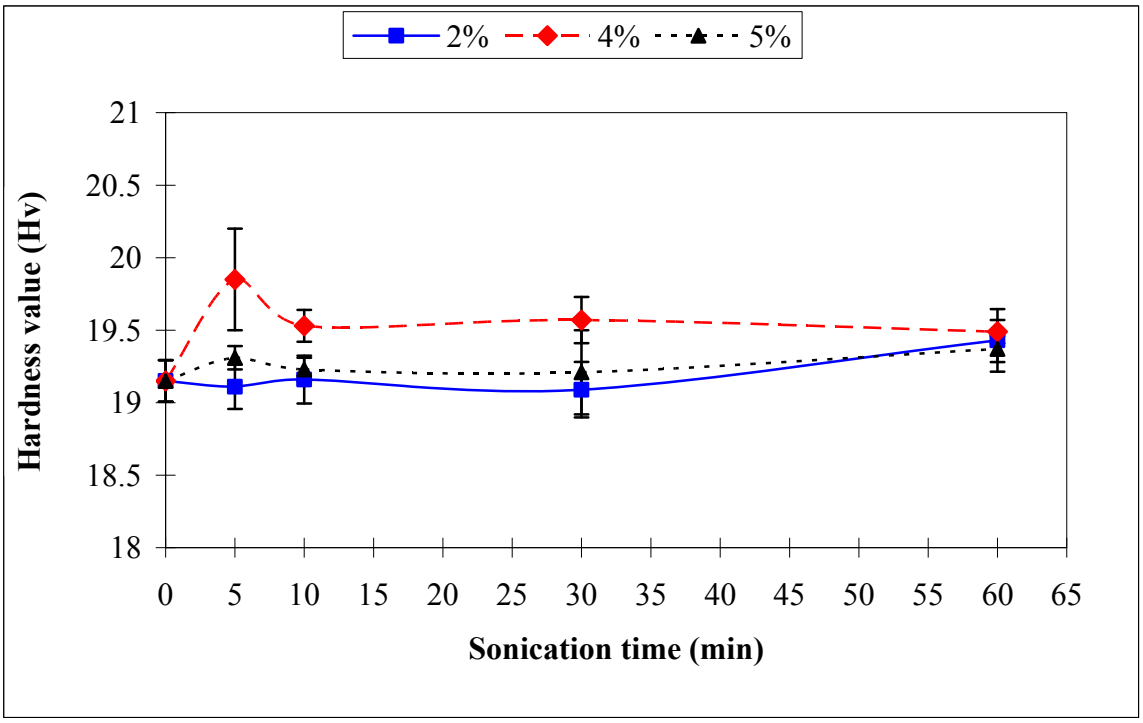

Figure 4.12a: Effect of sonication time on nanocomposites hardness for the different clay loadings.

The figure shows that there is no significant change in hardness with increased sonication time for clay contents. The highest increase in hardness by 1.2% for the 2% nanocomposite is at 60-minute sonication time. Also, maximum improvement in hardness values of 3.2% and 1.1% were seen for the 4% and 5% nanocomposites, respectively at 5 and 60 minutes. In general, the hardness values remain fairly constant at all sonication times. However, one interesting observation is that at 10-minute sonication time, the nanocomposite was always

above that of the neat epoxy. This trend was also shown by the 10-minute sonication time in d-spacing when the correlations between d-spacing and tensile properties were made. Lam et al [14, 45] have investigated nanocomposite hardness with respect to time. They [45] synthesized nanocomposite from Nanolin DK1 clay and Araldite GY251 to investigate its micro-hardness. The authors showed that at 1 hour sonication time, 2% nanocomposites micro-hardness value was increased above the neat epoxy. They reported that the optimum sonication time achieved for 4% nanocomposite was at 10 minutes [14].

4.5.2. Effect of clay loading on nanocomposites hardness.

The hardness values of the nanocomposite for the three cases of clay amount (2, 4 and 5%) are illustrated in figure 4.12b.

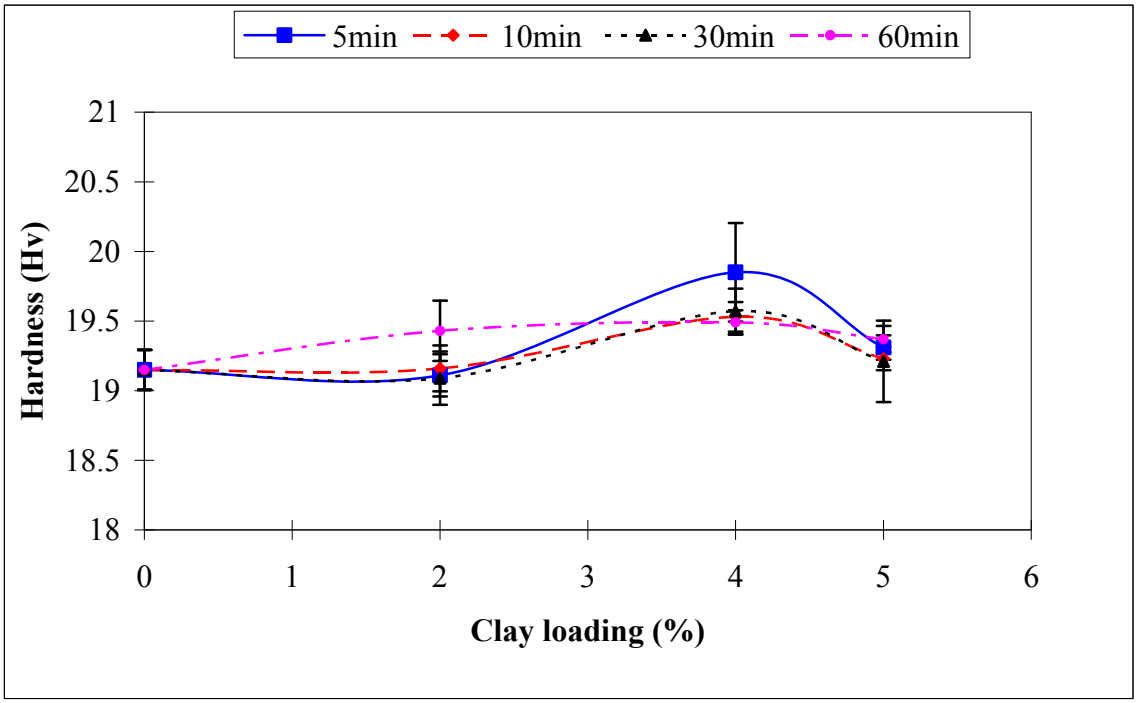

Figure 4.12b: Effect of clay loading on the nanocomposite hardness for the different sonication times.

It is clear (figure 4.12b) that the 4% clay loading showed the highest increase in hardness at all sonication time. The increases are 3.22%, 1.66%, 1.89 and 1.5% at 5, 10, 30 and 60 minutes sonication time, respectively. Strictly speaking, the 2% nanocomposite hardness fluctuates with change in the sonication time, while for the 4% and 5% nanocomposites, the hardness values are marginally higher than the neat epoxy irrespective of sonication time (refer to table 4.6). It can be concluded from these results that the amount of clay has marginal effect on nanocomposite hardness. Lam et al [14] found that the micro-hardness of nanocomposite synthesized from Araldite GY251 and Nanolin DKI series (S_iO_2) began to decline after 10 minute of sonication time at 4% clay loading. Ho et al [9] reported for the nanocomposite they produced from the blend of Araldite GY 251 and Garamite 1958 clay that with increase in clay amount, the hardness continues to increase. The hardness value was fluctuating above 5% clay loading, yet was still above the neat epoxy.

4.6. Fractographic Analysis and Energy Dispersive Spectroscopy

4.6.1. Fractographic Analysis.

Scanning electron microscopy (SEM) of the fractured surfaces of all synthesized tensile samples was conducted to see the differences in the microstructure of the samples and possibly make correlations between the observed properties and the microstructure. Micrographs of the fractured surfaces of nanocomposite samples and pure epoxy are presented in figures 4.13 through 4.25. Low and high magnifications of each sample are presented. The former gives a general idea of the structure, while the latter allows a close and detailed view.

Figures 4.13a-c are SEM micrographs of the neat epoxy. Figure 4.13a gives a general view of the fractured surface. Three distinct regions are identified on this micrograph: A, B and C, each identifying different fracture feature. The fractograph shows that a crack has initiated at point A and propagated through region B and C before the specimen finally fractured. There seems to be an existing flaw at point A. As force was applied during testing, this crack began to advance in the direction of B and C. In region B, the crack was advancing at slow rate which is why this area has smooth appearance. Higher crack propagation rate has resulted in coarse surface at C. This particular region dominates the fracture surface. Further magnifications of region C are presented 4.13b and 4.13c. The fracture surface in 4.13b shows that the region C consists of dimple like feature. A high magnification (x4000) of one of these dimple-like features shown in figure 4.13c reveals a very smooth surface. This structure is a characteristic of fracture resulting from uniaxial tensile failure of brittle materials. Therefore, the dominant failure mechanism in the epoxy is a brittle failure. This is supported by the representative stress-stain curve presented in figures 4.6a-c.

For the nanocomposites, the surfaces are rough both at low and high magnifications. Similar SEM images as presented here for both the neat epoxy and nanocomposite were reported by a number of other researchers [8, 15, 20, 27, 44]. Crack initiation sites are also readily visible in figures 4.14a, 4.16a, 4.17a, 4.18a, 4.19a, 4.20a, 4.21a and 4.25a. It is clear that crack initiated at either clay agglomeration or void sites. This could be indicative of the reason why the strength of the nanocomposite is lower than that of the neat epoxy in the current work. The regions of slow and fast crack propagation are also noticeable. While the region of fast crack propagation in the neat epoxy is smooth as seen in figure 4.13c, those of

the nanocomposites are rough due to the presence of clay. Secondary cracks observed on the nanocomposites fractured surfaces are due to high local stresses caused by clay agglomerations or voids. The microstructures of the nanocomposites suggest that the addition of clay to the epoxy makes it more brittle resulting in the observed lower fracture strain. Hussein et al [20] reported that aggregates behave as stress concentrators in polymer matrix to initiate crack under tensile load at low strain.

In addition, cavities are left by clay which disengaged from the surface of the matrix. Clay agglomerates and particles dotted the surfaces of the nanocomposites (figures 4.14-25) which are not seen in the SEM of unfilled epoxy. Such sites became weak areas in nanocomposites causing premature failure; thus lower tensile strengths and fracture strains. Qi et al [27] explained that the cavities present in nanocomposites could have been left by either entrapped voids or clay particles/aggregates that had fallen away from the resin following failure under tensile loading.

The sizes of clay agglomerates are smaller in the nanocomposite sonicated for longer time. This suggests that continuing sonication could help further break down clay particles. This can be inferred from the comparison of the micrographs of figures 4.14e, 4.15e, 4.16e and 4.17e for 2%-5min, 2%-10min, 2%-30min and 2%-60min, respectively. Approximate particles size as estimated from these micrographs are 20 μm and 15 μm for 2%-5min and 2%-10min, respectively. Micrographs for other clay loading have also shown similar trends. That is, the size of the clay particles progressively get smaller as the sonication duration was increased. Therefore, in the current study SEM images suggest that the distribution of clay

particles in the epoxy material increased with increased sonication time. This position is corroborated by the distribution of interlayer spacing in section 4.3. It was observed that in most cases the nanocomposite with high sonication time possessed low standard deviation signifying better distribution of intercalated sites. On the other hand, small size agglomerate may also mean that at higher sonication time, smaller sizes of clay aggregate sites are present in the nanocomposite. Sites that have been reported so far from the SEM images as representing clay particles or agglomeration have been confirmed by Energy Dispersive Spectroscopy (EDS) and the results are presented in the next section.

It is worth mentioning that exfoliation or intercalation can not be deducted from SEM images. It is a comparative analytical tool for nanocomposite structure. However, from the quality of the micrographs, the level of clay distribution could be roughly deducted. The presence of voids in nanocomposite is confirmed in figures 4.16a-b and 4.24a. These voids hence become potential crack initiation sites which result in premature failures of nanocomposite. It is important to point out also that the microstructures of the nanocomposites present several features. These different features are due to different clay concentrations, the distribution of the clay in the epoxy matrix and the interaction of clay with the epoxy, etc.

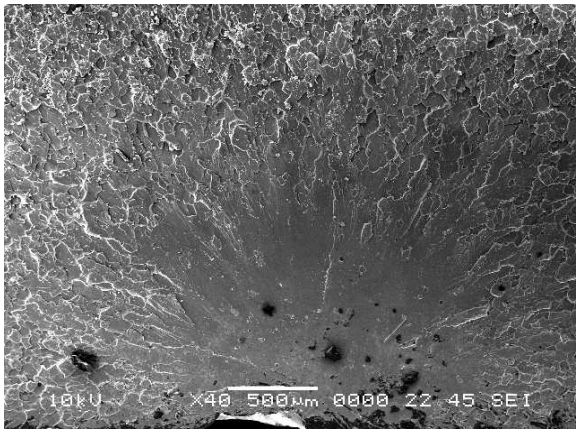

(a)

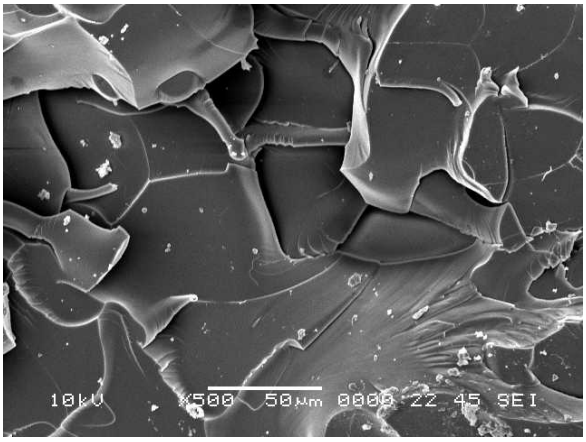

(b)

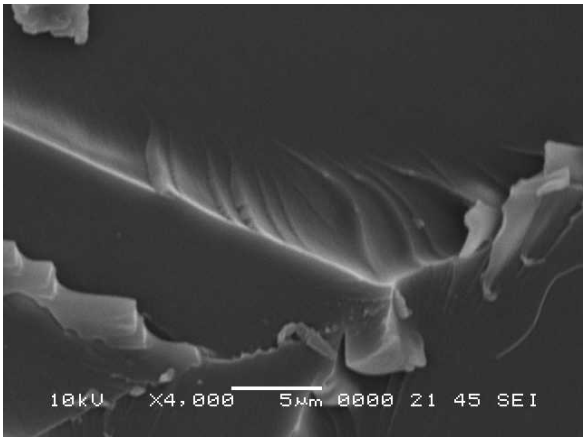

(c)

Figures 4.13: SEM images of neat epoxy showing (a) **A**, crack initiation; **B**, slow crack propagation, and **C**, fast crack propagation region; (b) magnification of point **C** (x500); (c) higher magnification of **D** (x4000)

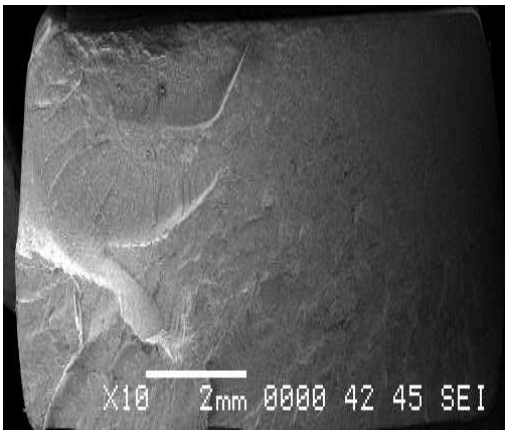

(a)

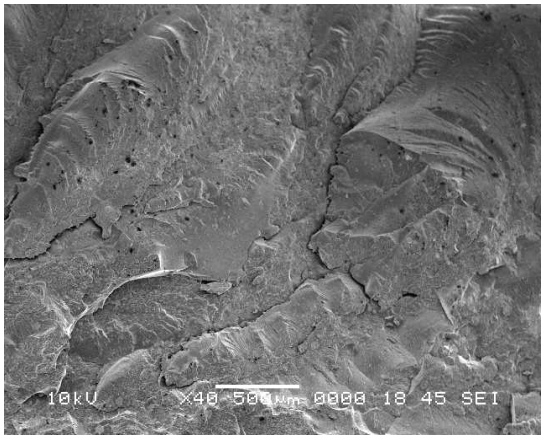

(b)

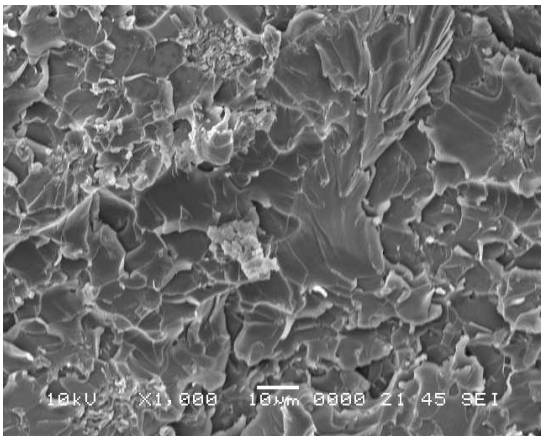

(c)

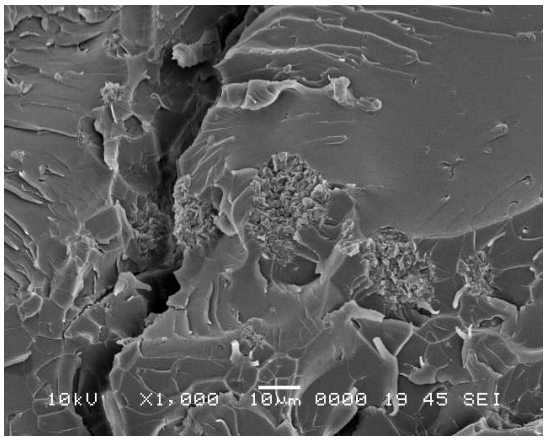

(d)

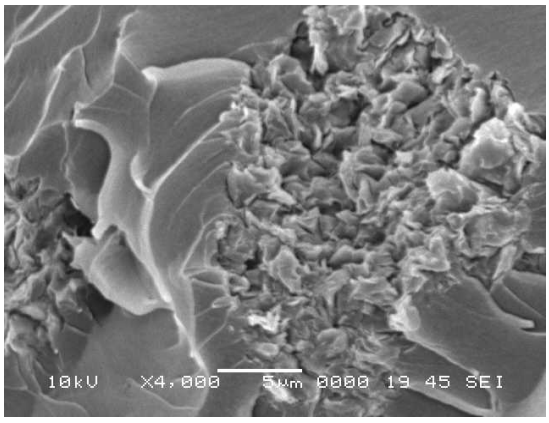

(e)

Figures 4.14: SEM micrographs of 2%-5min nanocomposites illustrating: (a) crack initiation site, **A;** (b) general feature at low magnification (x40); (c) general features at high magnification (x1000); (d) secondary crack, **B**; (e) clay particle or agglomerate, **C**.

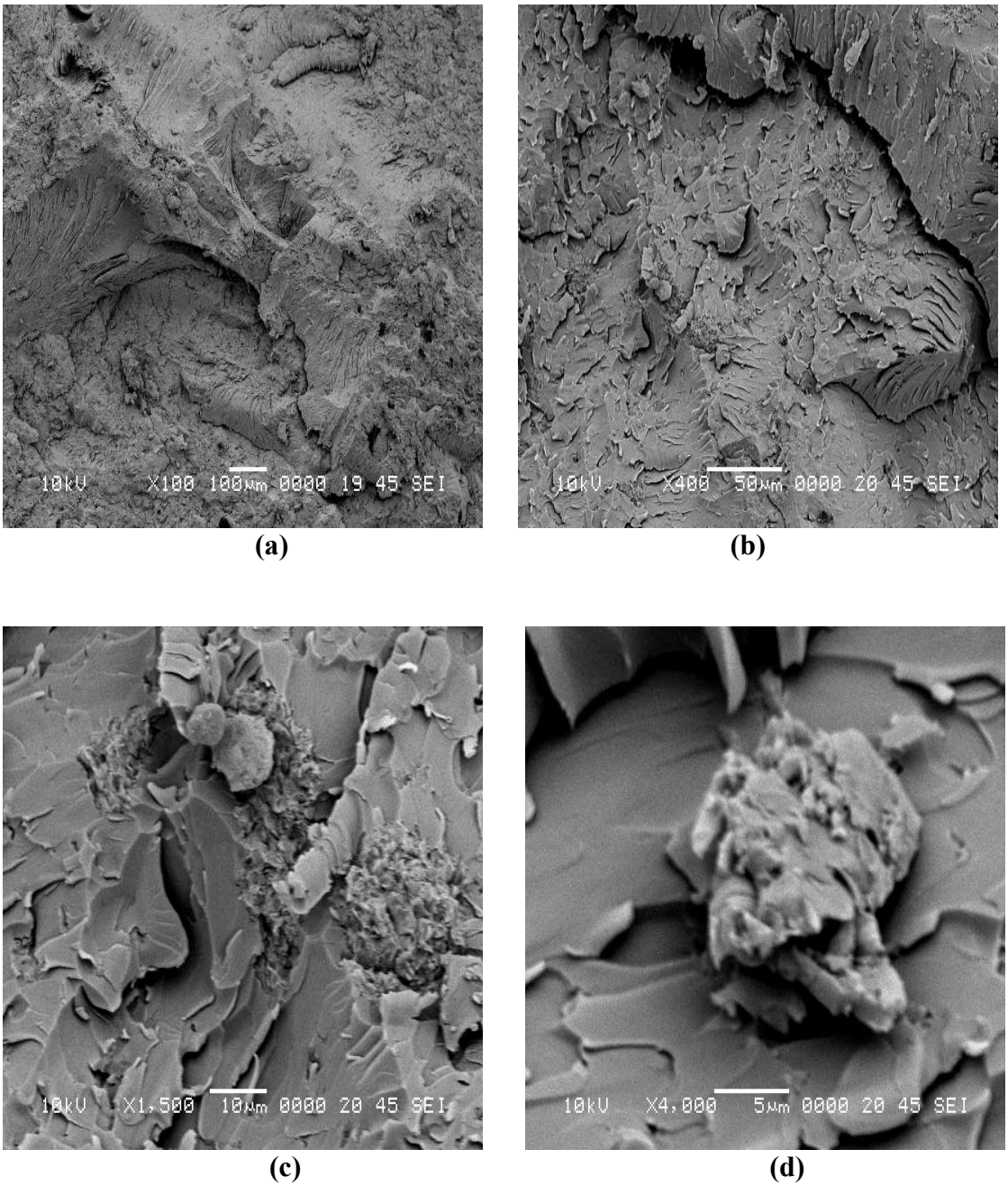

(a) **(b)**

(c) **(d)**

Figure 4.15: Different magnifications of SEM images of fractured surface of 2%-10min nanocomposite [(a) x100, (b) x400, (c) x400, (d) x4000] showing different micro structural feature, secondary cracks, **A**& **B,** and clay sites, **C**& **D.**

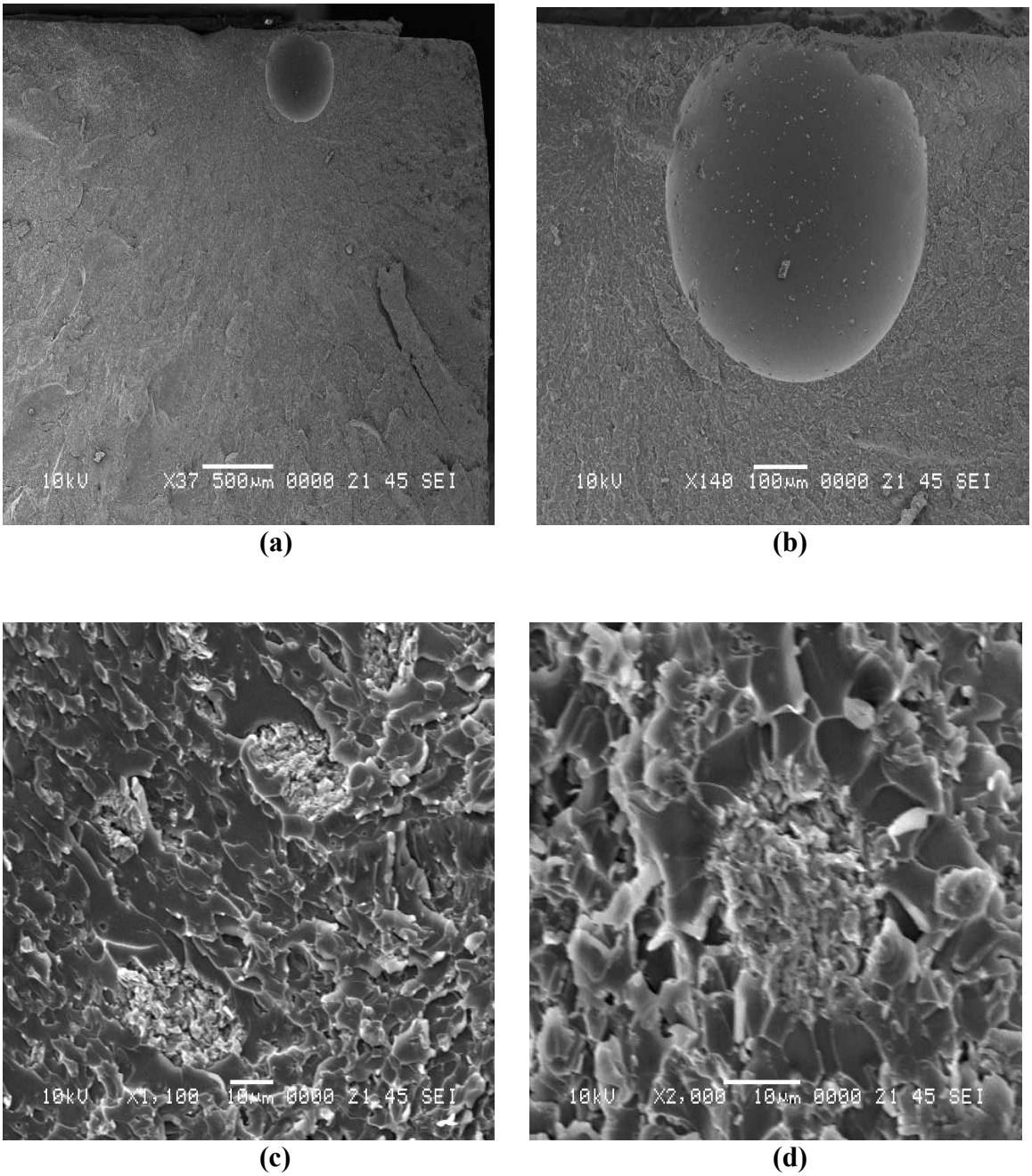

Figure 4.16: SEM image of fractured surface of 2%-30min nanocomposite showing: (a) void and slow crack propagation region; (b) magnification of the void, **A**; (c) distribution of clay agglomeration, **B**; (d) high magnification (x2000) of clay agglomeration, **C**.

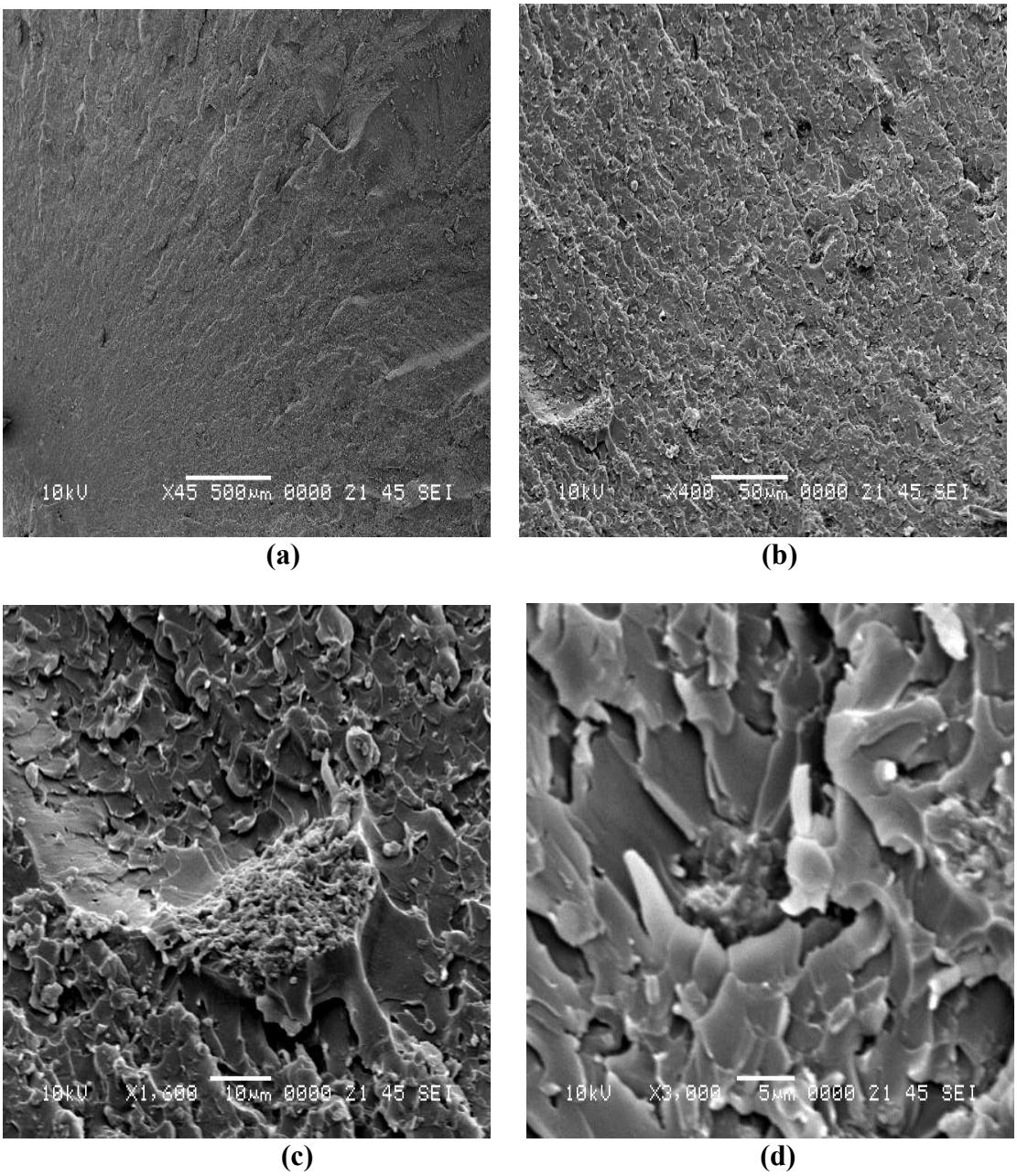

Figure 4.17: SEM micrographs of the fractured surface of 2%-60min nanocomposite illustrating: (a) crack initiation site, **A**, (b) low magnification (x400) representative microstructure, (c) clay site, **B,** (d) high magnification (x3000) of the representative microstructure.

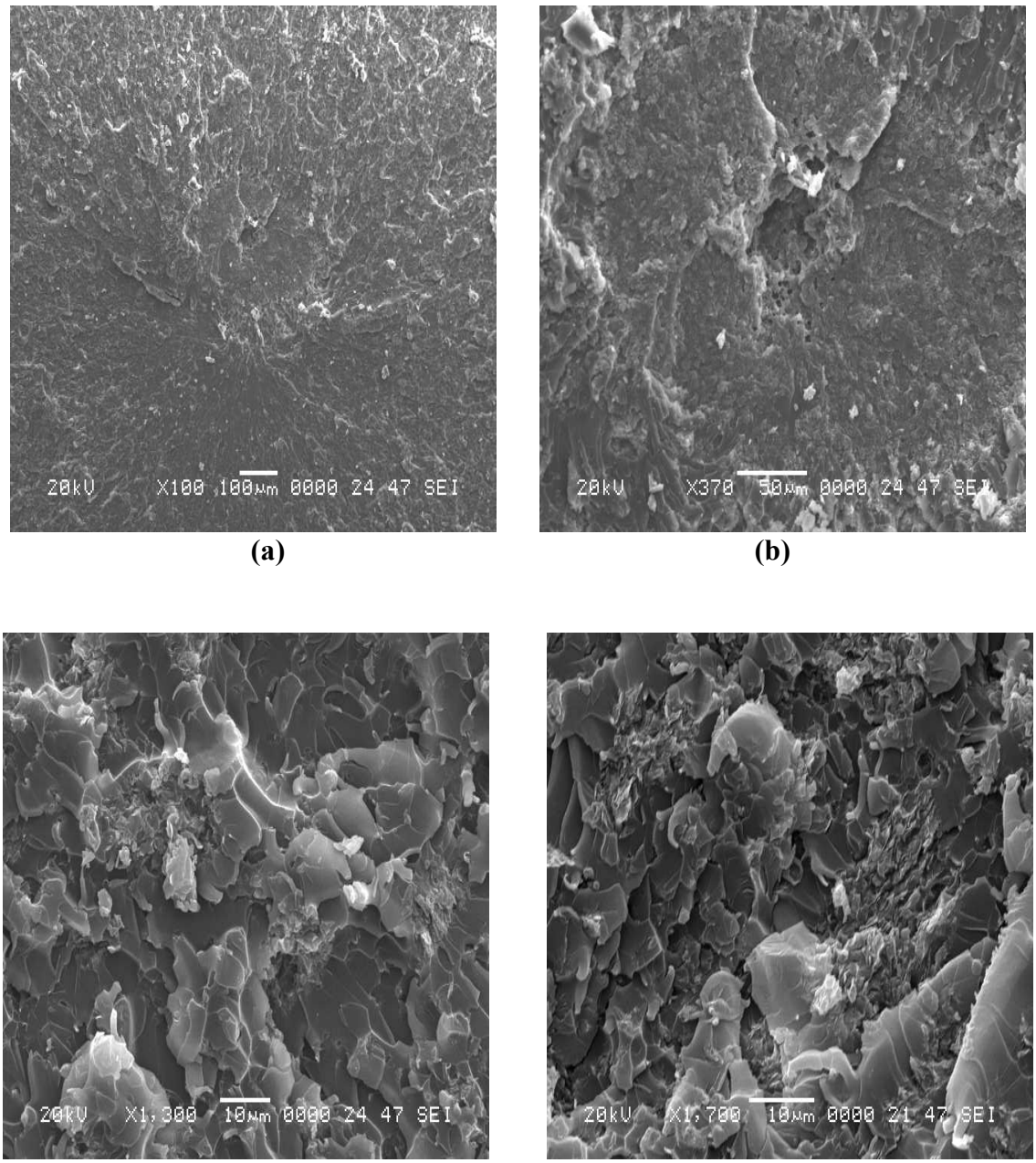

(a) **(b)**

(c) **(d)**

Figure 4.18: SEM images of the fractured surface of 4%-5min nanocomposite (a) crack initiation site, **A**; (b) Clay disengagement site or cavity, **B**; (c) & (d) two different representative microstructures at x1300 and x1700 magnifications, respectively.

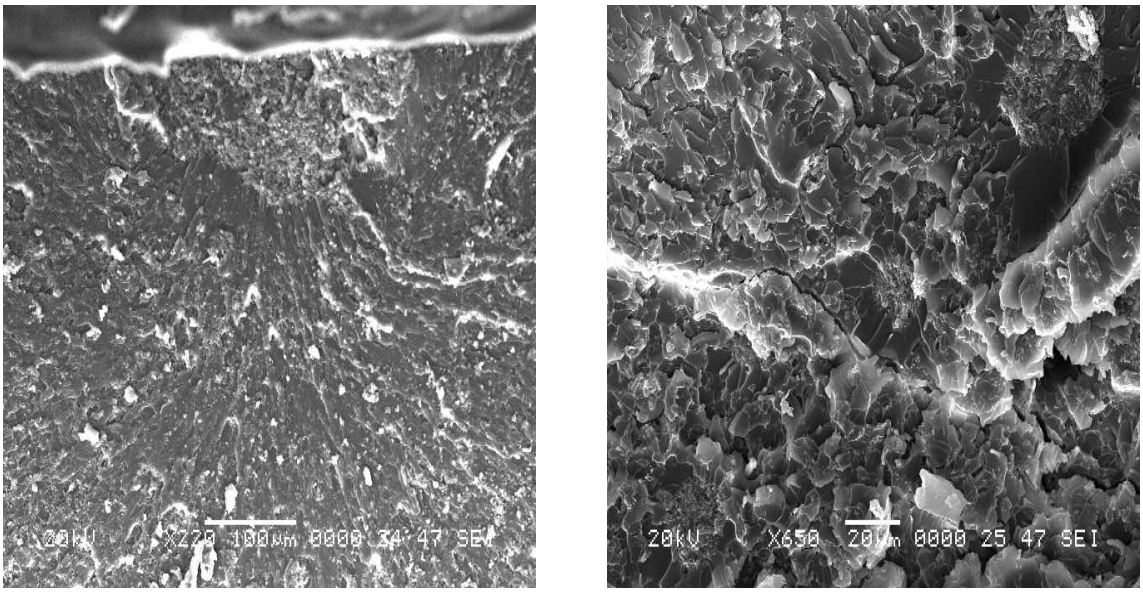

(a) **(b)**

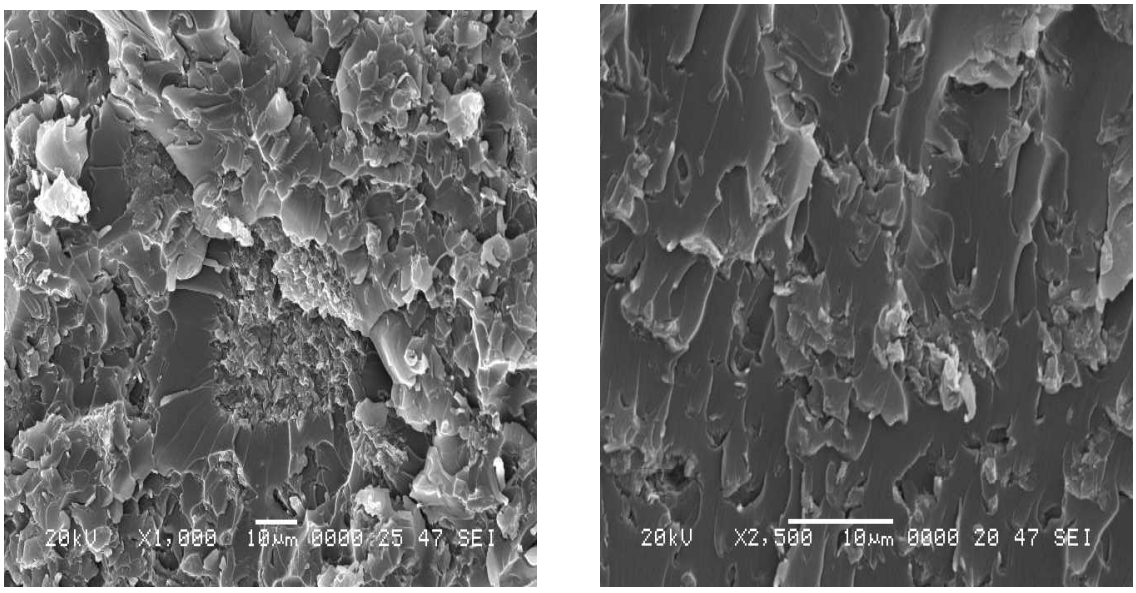

(b) **(d)**

Figure 4.19: SEM images of the fractured surface of 4%-10min nanocomposite showing: (a) crack initiation site, **A;** (b) secondary crack, **B**; (c) & (d) different magnifications illustrating representative structure at high magnifications.

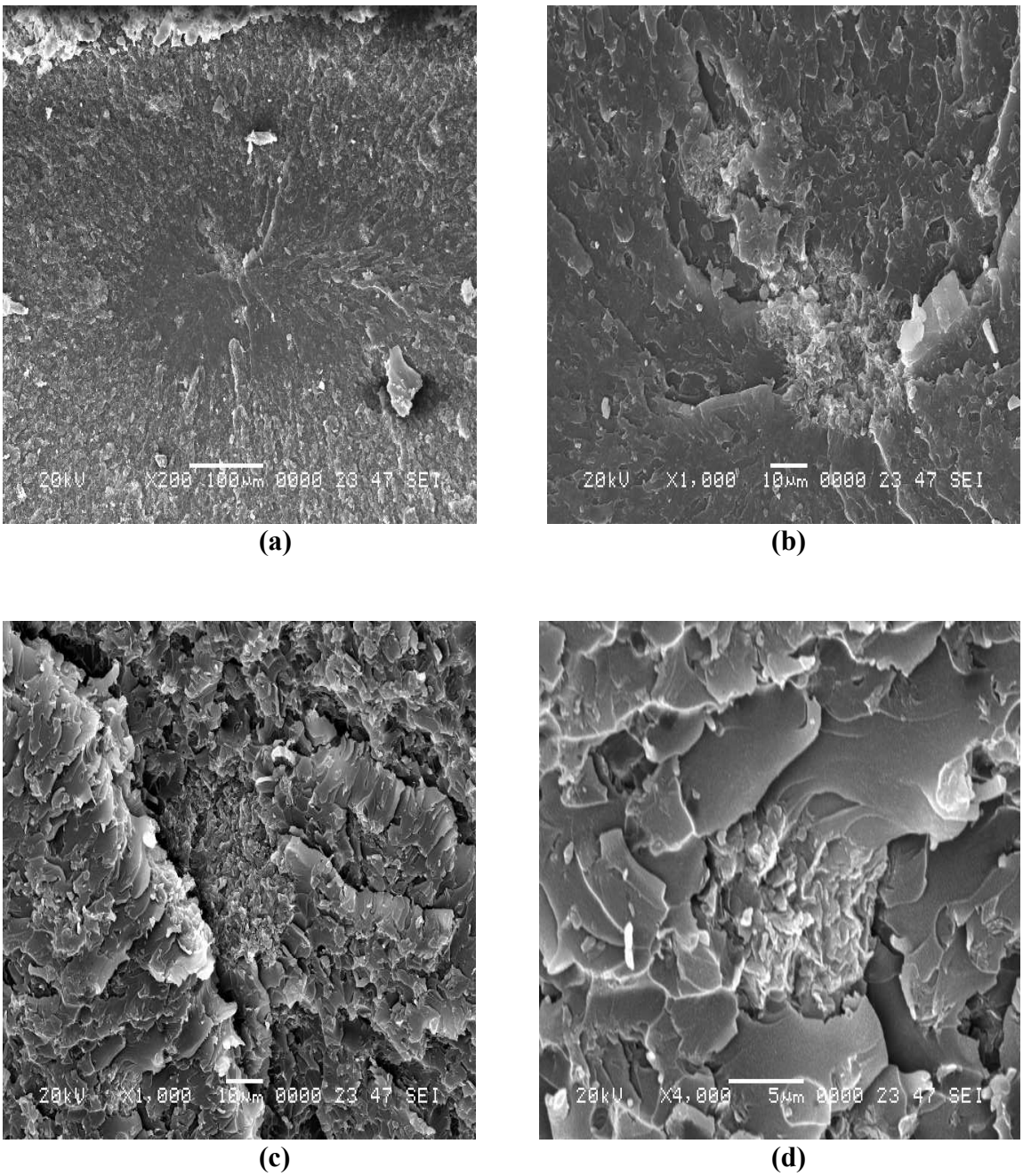

Figure 4.20: SEM image of the fractured surface of 4%-30min nanocomposite showing: (a) crack initiation site **A**; (b) magnification of the crack initiation site; (c) secondary crack, **B**; (d) clay particle or agglomeration site, **C**.

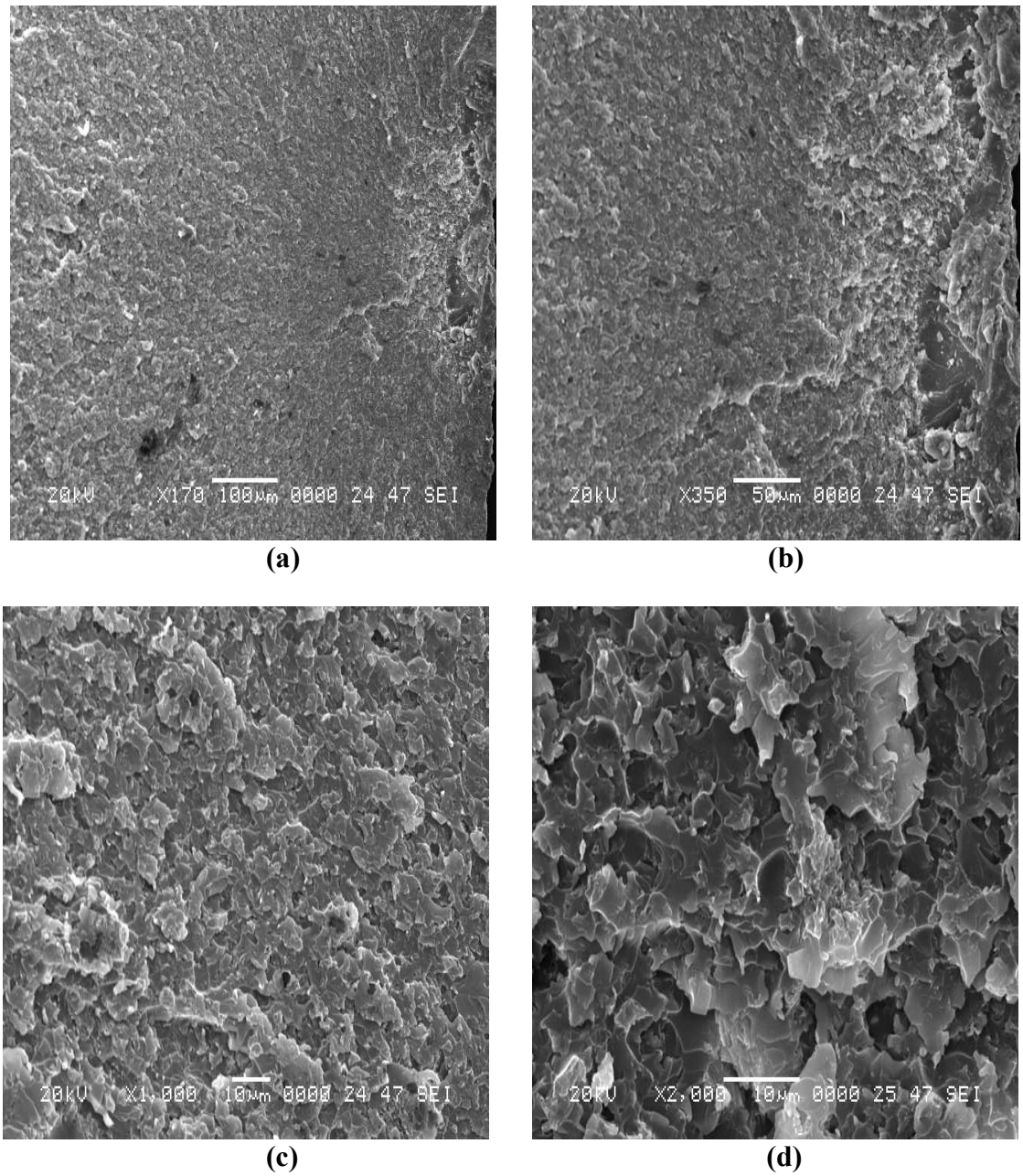

Figure 4.21: SEM images of the fractured surface of 4%-60min nanocomposite illustrating: (a) & (b) crack initiation site; (c) & (d) two different magnifications [x1000 and x2000, respectively] of its representative microstructure.

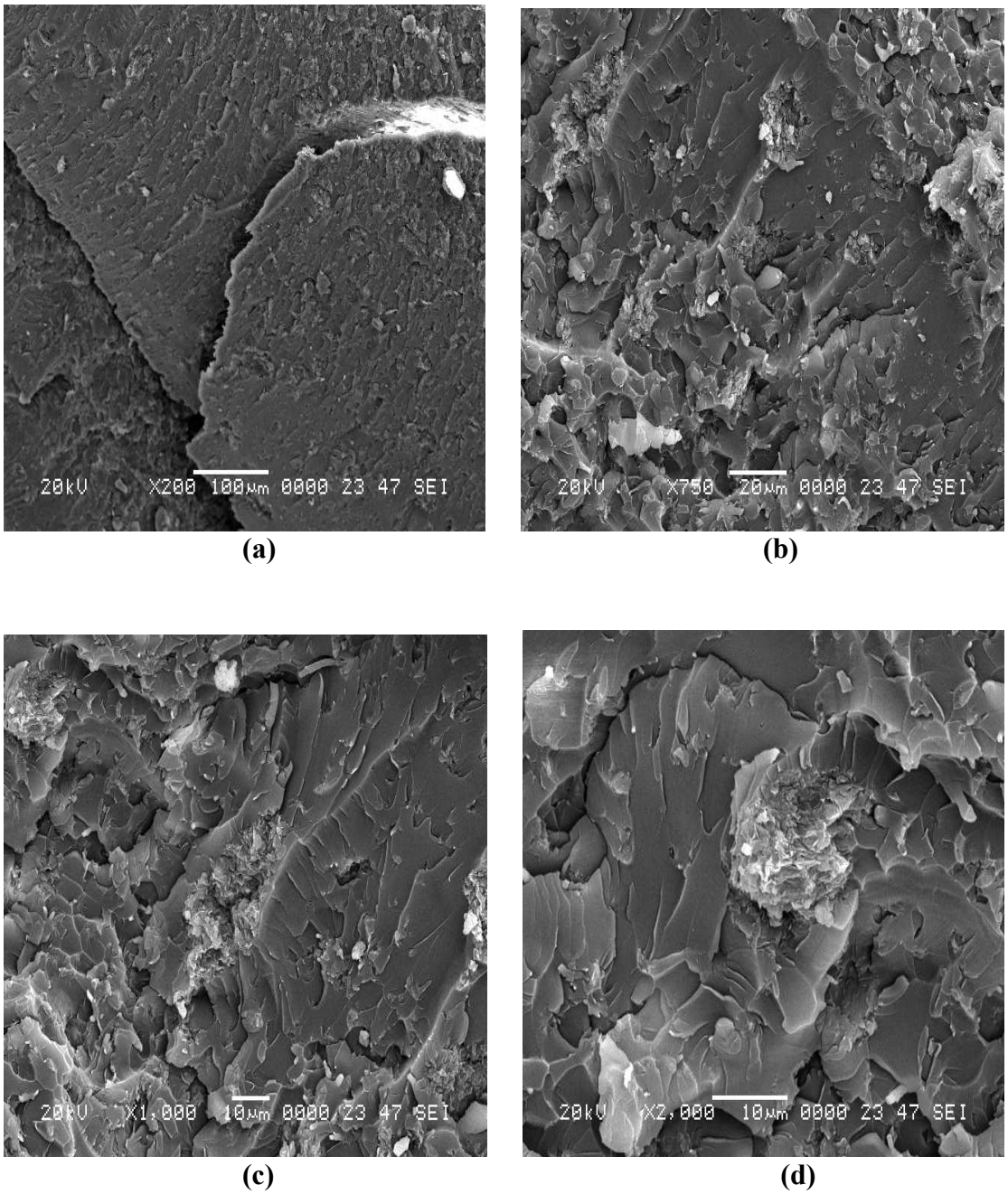

Figure 4.22: SEM images of the fractured surfaces of 5%-5min nanocomposite showing: (a) secondary crack, **A;** (b), (c) & (d) different magnifications [x750, x1000 and x2000, respectively] of its representative microstructure.

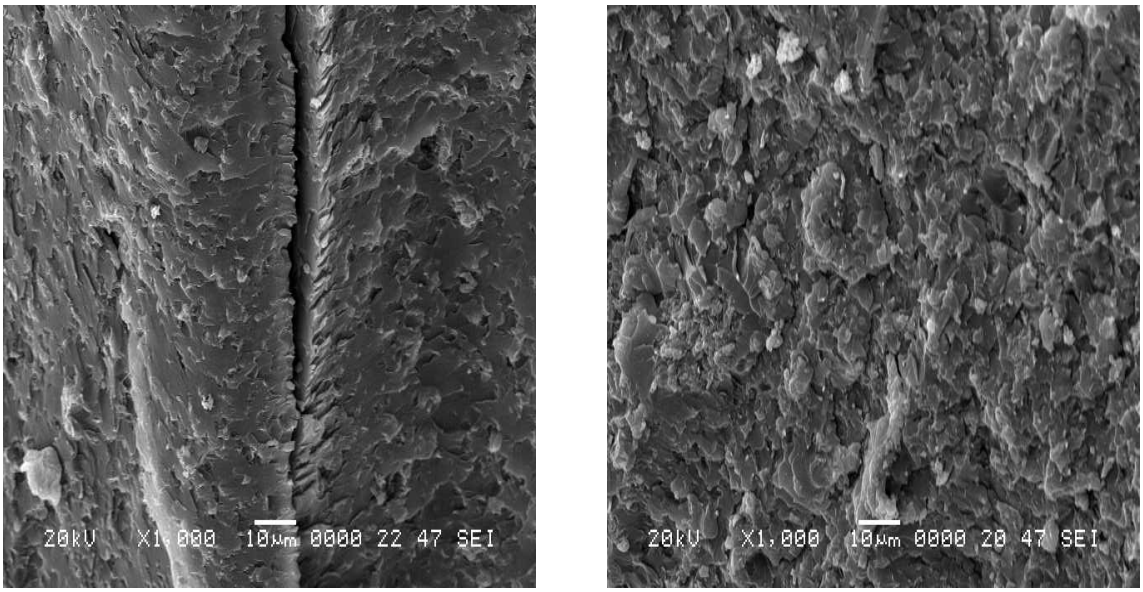

(a) **(b)**

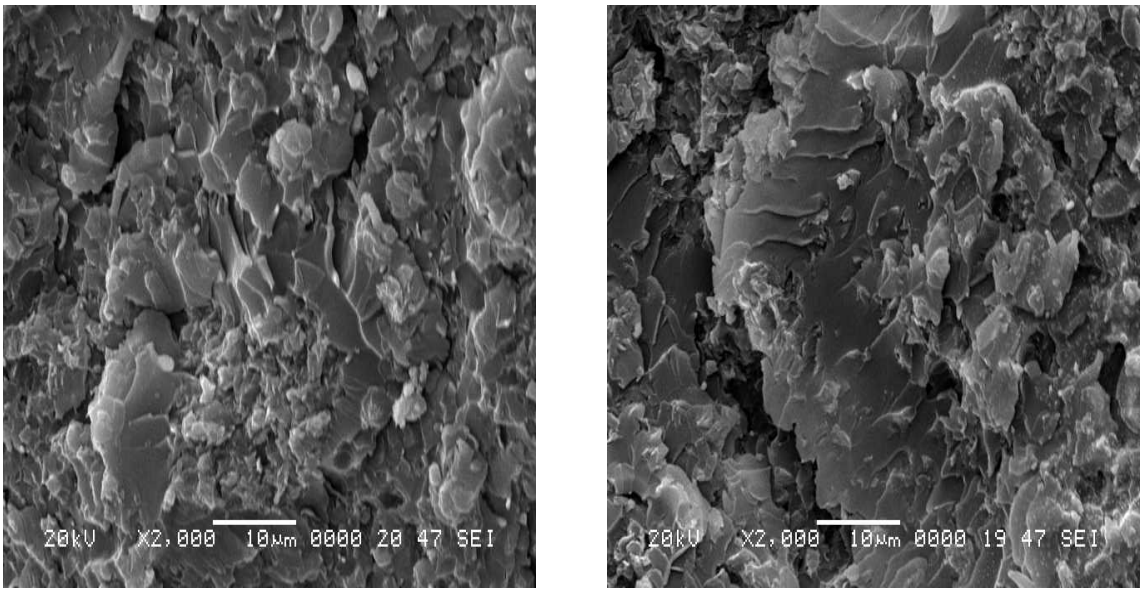

(b) **(d)**

Figure 4.23: SEM images of the fractured surfaces of 5%-10min nanocomposite indicating: (a) secondary crack **A**; (b)&(c) its representative microstructure at x1000 & x2000 magnifications, respectively; (d) secondary crack, **B**.

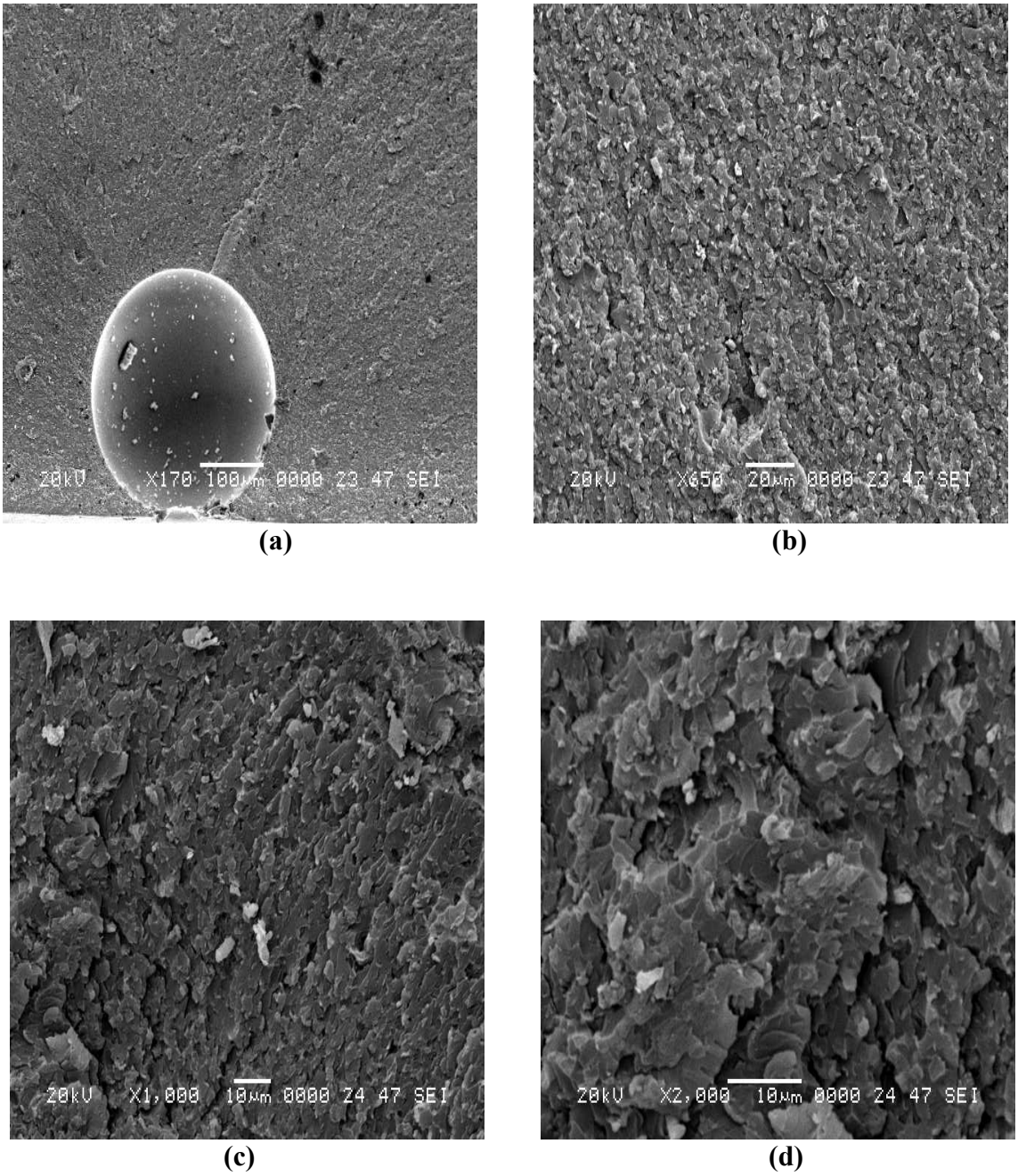

Figure 4.24: SEM images of the fractured surface of 5%-30minute nanocomposite depicting: (a) void, **A;** (b) Slow crack propagation region; (c) & (d) two different magnification [x1000 & x2000, respectively] of its representative structure.

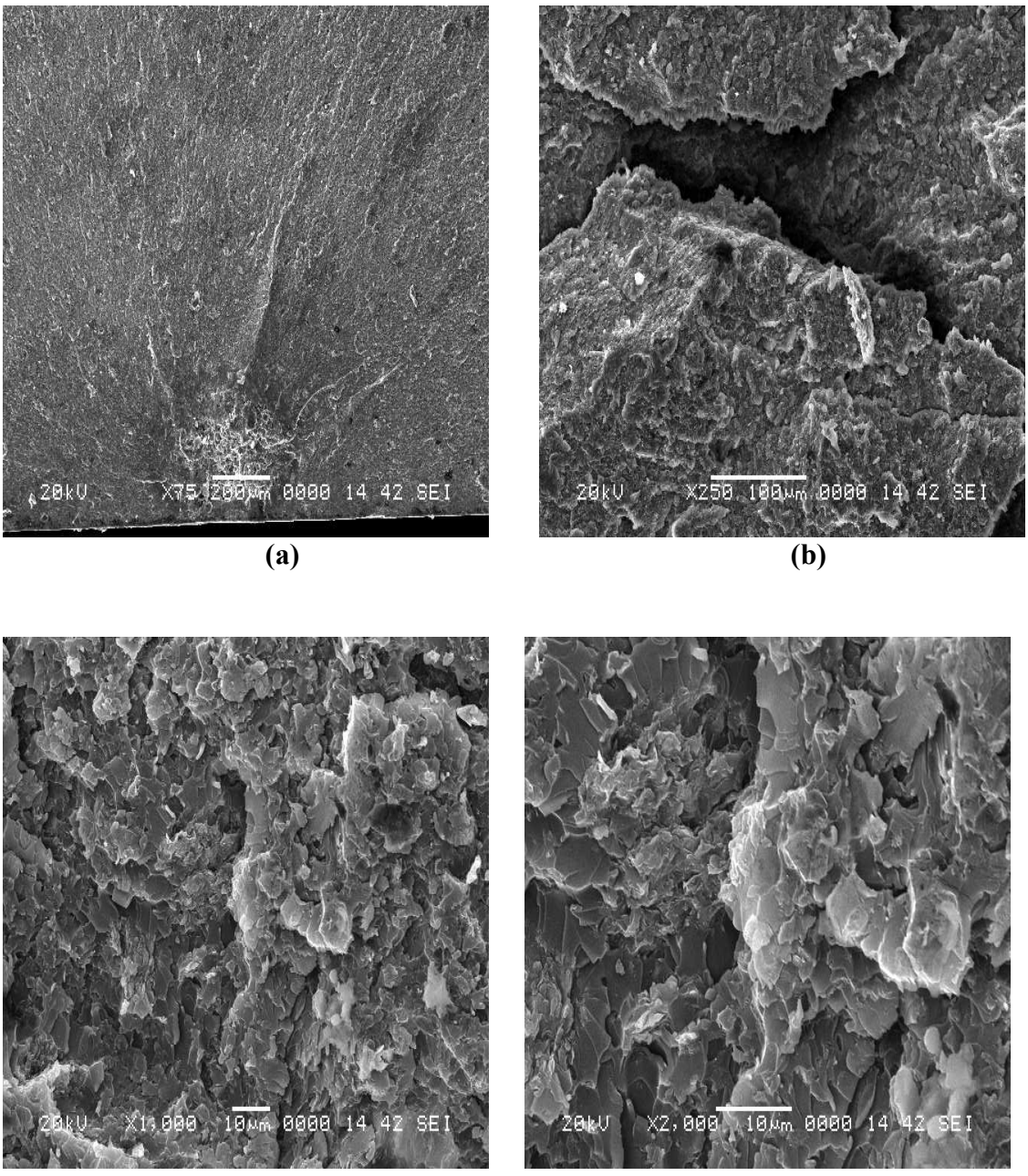

Figure 4.25: SEM images of the fractured surface of 5%-60minute nanocomposite showing (a) crack initiation site, **A**; (b) secondary crack, **B;** (c) & (d) representative microstructure at two different magnifications, x1000 & x2000, respectively.

4.6.2 Energy Dispersive Spectroscopy (EDS)

Energy dispersive spectroscopy (EDS) of clay, neat epoxy and selected sites in the fractured surfaces of some nanocomposite samples were carried out to determine their composition and to identify the different sites present in nanocomposites micro structures. For the neat epoxy, the EDS analysis was carried out on the slow and fast crack propagation region represented by spectra 1 (30 x 30 μm^2) and 2 (30 x 25 μm^2), respectively in figure 4.26a. The results are presented in table 4.7.

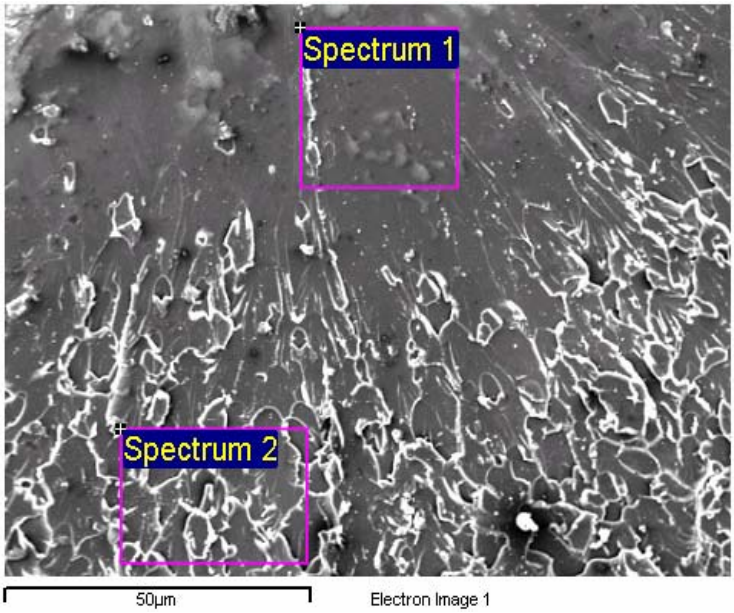

Figure 4.26a: SEM image of fractured surface of the neat epoxy used for EDS analysis.

Table 4.7: Elemental composition of neat epoxy.

Spectrum	C (%)	O (%)	Cl (%)	Total (%)
1	30.78	69.22		100
2	38.04	60.43	1.52	100

It is confirmed here that the epoxy is mainly composed of carbon and oxygen. There is also trace amount of chlorine which may have come from the epoxy or hardener. The composition, nevertheless, agrees with the chemical structure of epoxy in figure 1.2. EDS can not detect elements with atomic number less than four which is why the hydrogen component is not shown.

The SEM images for EDS analysis of the powder nanoclay and nanocomposites are presented in figures 4.26b-e and their corresponding percentage elemental compositions are given in tables 4.8 through 4.12.

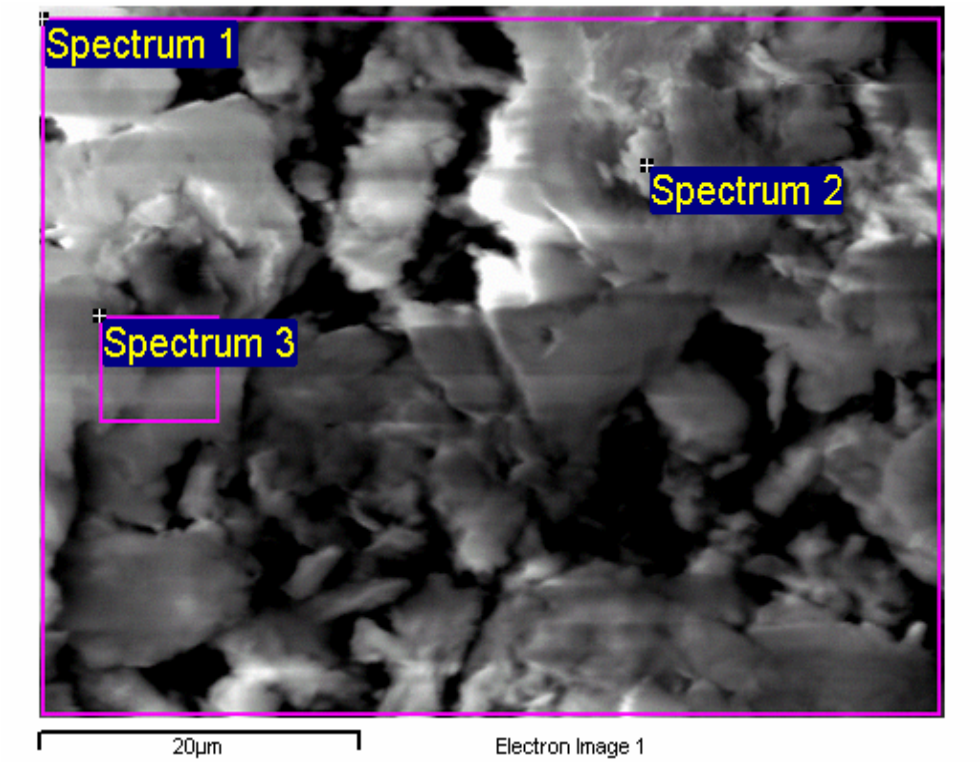

Figure 4.26b: SEM image of the powder clay used for EDS analysis.

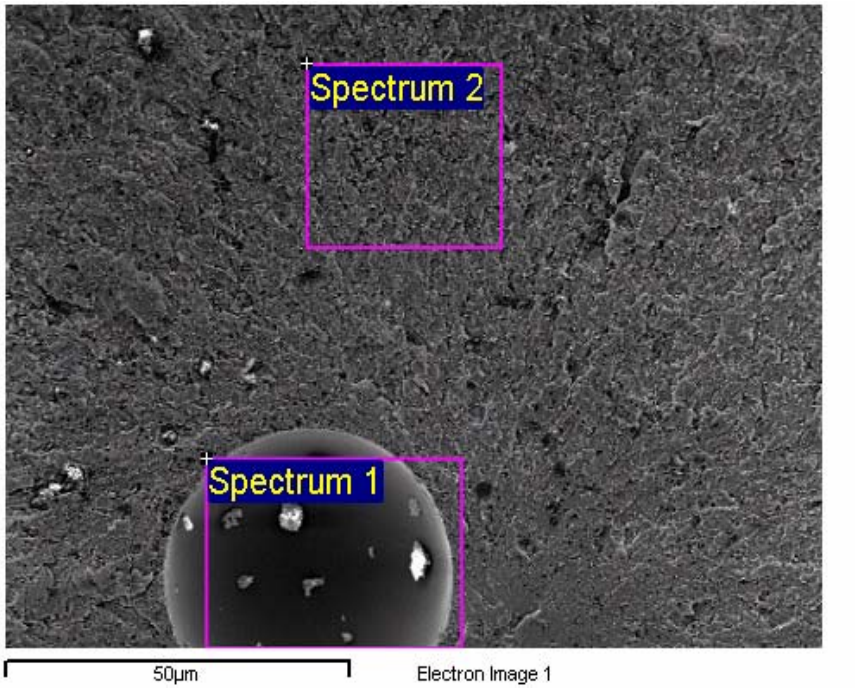

Figure 4.26c: SEM image of 2%-10minutes used for EDS analysis

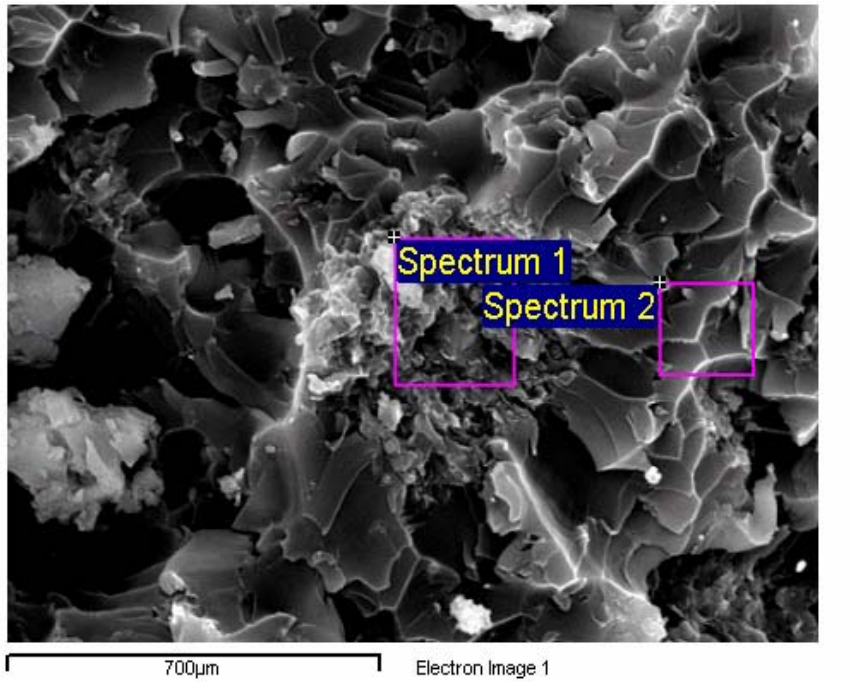

Figure 4.26d: SEM image of 4%-5minutes used for EDS analysis.

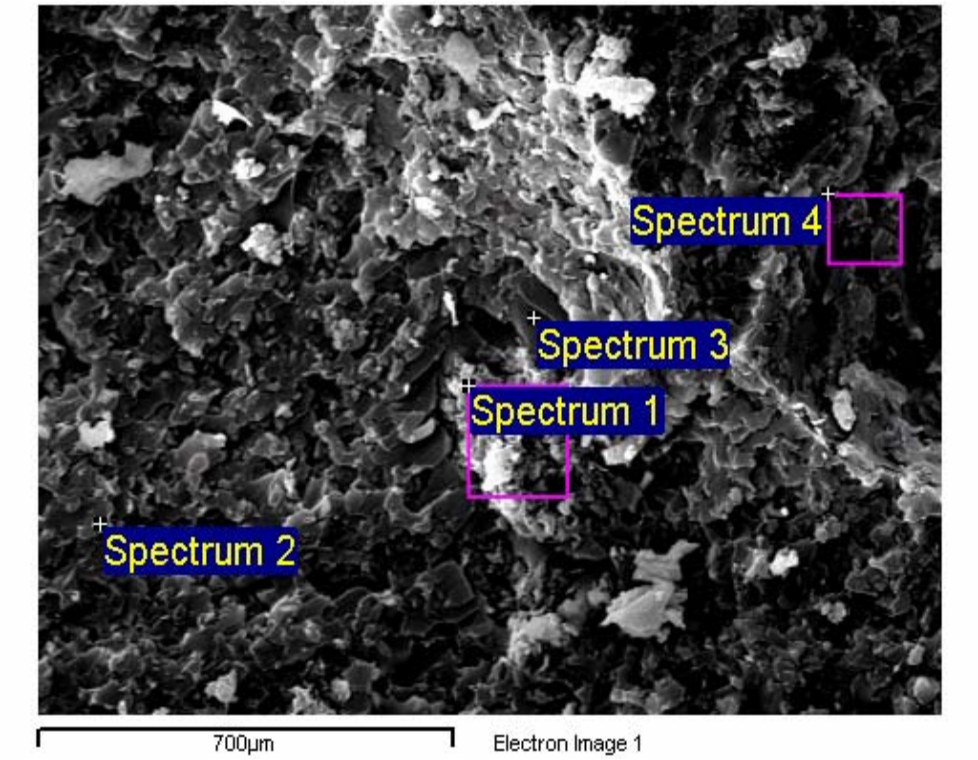

Figure 4.26e: SEM image of 5%-60 minutes used for EDS analysis

Table 4.8: Elemental composition of the powder clay.

Spectrum	**C (%)**	**O (%)**	**Mg (%)**	**Al (%)**	**Si (%)**	**Cl (%)**	**K (%)**	**Ti (%)**	**Fe (%)**	**Total (%)**
1 (entire image)	9.50	50.03	1.74	9.95	26.30	0.51	0.37		1.60	100
2 (a spot)	3.27	60.28	1.98	9.59	23.63			0.17	1.09	100
3 (≈8µm)^2	8.20	46.50	2.29	11.27	29.53	0.58			1.65	100

Table 4.9: Elemental composition for 2%-10min nanocomposite

Spectrum	C (%)	O (%)	Na (%)	Al (%)	Si (%)	Cl (%)	K (%)	Rb (%)	Total (%)
1 (≈1200 μm^2)	32.63	57.92		1.93	4.61	1.78	1.14		100
2 (≈900 μm^2)	25.35	56.68	4.02			4.60	2.73	6.61	100

Table 4.10: Elemental composition of 4%-5min nanocomposite

Spectrum	C (%)	O (%)	Mg (%)	Al (%)	Si (%)	Cl (%)	Fe (%)	Total (%)
1 (≈227 μm)^2	25.88	42.27	1.29	7.52	21.38	0.57	1.09	100
2 (≈182 μm)^2	45.45	51.92			2.63			100

Table 4.11: Elemental composition for 5%-60min nanocomposite.

Spectrum	C (%)	O (%)	Na (%)	Mg (%)	Al (%)	Si (%)	Cl (%)	Fe (%)	Rb (%)	W (%)	Total (%)
1 (≈187 μm)^2	17.31	40.46	0.65	1.79	9.99	27.81	0.72	1.27			100
2 (a spot)	39.10	43.78			1.33				9.87	5.92	100
3 (a spot)	40.52	50.93			2.42	5.29	0.86				100
4 (≈135 μm)^2	29.86	36.56							18.35	15.23	100

The elements present in the clay powder (table 4.8) are similar to those reported in sub-section 1.4.2 and in the idealized clay structure in figure 1.3. This result reveals that oxygen and silicon are the dominant elements in the nanoclay powder. It is noticd that elemental composition is not evenly distributed from point to point in the base materials, that is, the epoxy and the clay powder. This variable distribution is thus expected in the nanocomposite.

Comparing spectrum 1(approximately 227 μm^2) with spectrum 2 (about 182 μm^2) in figure 4.26d along with the result in table 4.10, it is seen that the region of spectrum 1 which is one of the several sites that were reported as clay agglomerate in section 4.5.1. The spectrum 1 is richer in clay elements than the region of spectrum 2, indicating more clay in agglomerates than the region that was uniformly blended. Therefore, it is confirmed here that points that have been reported as clay particles or agglomerates were actually so. This result is also indicative of the distribution of clay from point to point. As seen in figure 4.26e, spectrum 3 which represents a spot is richer in clay elements than spectrum 4 which represents an area of approximately 135^2 μm^2. This is due to the fact that spectrum 3 is in the immediate neighbourhood of spectrum 1 (approximately 187 μm^2) which was richer in clay elements. From these EDS results, it is shown that clay-epoxy composites were formed, while the X-ray spectrum confirms this composite to be nanocomposite on the basis of intergallery spacing.

CHAPTER 5

5.0. CONCLUSIONS AND RECOMMENDATIONS FOR FUTURE WORK

5.1. Conclusions

In the current work, epoxy-clay nanocomposites of 2%, 4% and 5% nanoclay loading were fabricated using sonication times of 5, 10, 30 and 60 minutes to mix the clay with epoxy. Wide angle x-ray diffraction analysis was conducted on the samples to see the level of nanoclay separation. Differential scanning calorimetry was used to determine optimum curing cycle and glass transition temperature (T_g). Tensile and hardness tests were conducted to investigate these properties with respect to sonication time, clay amount and the d-spacing achieved. Both Scanning electron microscope and Energy Dispersive spectroscopy were used to view nanocomposites structure and composition, respectively. The conclusions from the current study are summarized as follows.

Differential Scanning Calorimetry (DSC)

DSC result showed that:

- Only optimum curing could be achieved for the epoxy and nanocomposites.
- The glass transition temperature, T_g, of the 2% nanocomposite were lower than that of the neat epoxy for the same curing cycle.
- Change in the sonication time has no effect on the glass transition temperature, T_g.

X-ray Diffraction

The x-ray diffraction results indicated that:

- Neither full exfoliation nor intercalation was achieved in the present work. The nanocomposites showed both types of structures. Nonetheless, the predominant structures for most of the nanocomposites were intercalation.
- Weak variance and broad peaks are shown by the nanocomposites structure compared to the clay powder which has a very sharp x-diffraction peak. This signifies intergallery spacing distribution for the nanocomposite.
- Generally, increasing sonication time caused the d-spacing to increase, while increase in clay loading lowered nanocomposites d-spacings. However, the change in d-spacing was not proportional to the change in the sonication time and clay loading.
- Optimum sonication time depends on clay loading.

Tensile Properties

From the results of the tensile tests it can be concluded that:

- Nanocomposites tensile strengths were generally lower than that of the neat epoxy at all sonication times and clay loadings, although a modest gain of 3.7% in tensile strength was achieved for the 2% nanocomposites at 10 minutes sonication time.
- The elastic moduli of the nanocomposites were found to be higher than that of the neat epoxy. The increased moduli were due to stiffening effect of the clay, while the low tensile strength was due to void and clay agglomerates effects which result in stress concentration sites.

- Increase in the sonication time generally caused the tensile strength to increase, while nanocomposites moduli of elasticity decreased slightly with increasing sonication time.
- In general, increase in clay loading resulted in the nanocomposite tensile strength to decrease, but the modulus increased with increase in clay loading.
- It can be concluded that higher d-spacing produced improved tensile strength.
- With improved degassing the tensile properties could be enhanced.

Hardness Test

Measured Vickers hardness showed that:

- 4% and 5% clay contents increased the hardness, though marginally, irrespective of sonication time. For the 2% clay loading there was fluctuation in the measured hardness with respect to sonication time.
- The 4% clay loading showed the highest hardness value at all sonication times.
- Nanocomposite hardness varied slightly with change in the sonication time and clay loading.

Fractographic Analysis and Energy Dispersive Spectroscopy (EDS)

Structural characterization from SEM and EDS showed that:

- Nanocomposite structures are characteristically different from that of the neat epoxy.
- Higher sonication time resulted in better clay distribution.
- Clay agglomerates were present in the nanocomposites regardless of sonication time.
- There were presences of voids and clay agglomerates which explain the low tensile strengths of nanocomposites.

- From the EDS, the different sites in the nanocomposites microstructure were identified which correlated with observation made in the fractographic analysis.

In the current study, the effects of sonication times and clay loadings on epoxy-clay nanocomposites have been investigated. The correlations between measured physical, thermal and mechanical properties and test parameters have been performed as set out in the thesis objectives. The results and conclusions drawn from these investigations are useful for further study and application of this material. It can be concluded, therefore, that the objectives outlined for the present work have been achieved.

5.2. Recommendations for Future Work.

Future work should include:

- Further curing study and differential scanning calorimetry (DSC) analysis of samples with the aim of reducing the processing time.
- Transmission electron microscopy (TEM) analysis of the nanocomposites in order to visualize the distribution of clay in the polymer and to confirm the d-spacing achieved.
- Investigation of the fracture toughness of the nanocomposite as it has indicated high stiffness.
- Study on the moisture absorption properties of the materials.

6.0 REFERENCES.

1. Jyi-Jiin Luo and Isaac M. Daniel, "Characterization and Modeling of Mechanical Behavior of Polymer/Clay Nanocomposites", Composites Science and Technology, Vol. 63, 2003, pp. 1607–1616.

2. Isil Isik, Ulku Yilmazer and Goknur Bayram, "Impact Modified Epoxy/Montmorillonite Nanocomposites: Synthesis and Characterization", Polymer, Vol. 44, 2003, pp. 6371–6377.

3. Clois E. Powell and Gary W. Beall, "Physical Properties of Polymer/Clay Nanocomposites", Current Opinion in Solid State and Materials Science, Vol. 10, 2006, pp. 73–80.

4. Chenggang Chen, Mohammad Khobaib and David Curliss, "Epoxy Layered-Silicate Nanocomposites", Progress in Organic Coatings, vol. 47, 2003, pp. 376–383.

5. Jang-Kyo Kim, Chugang Hu, Ricky S.C. Woo and Man-Lung Sham, "Moisture Barrier Characteristics of Organoclay–Epoxy Nanocomposites", Composites Science and Technology, Vol. 65, 2005, pp. 805–813.

6. M.R. Bagherzadeh and F. Mahdavi, "Preparation of Epoxy–Clay Nanocomposite and Investigation on its anti-Corrosive Behavior in Epoxy Coating", Progress in Organic Coatings, Vol. 60, 2007, pp. 117–120.

7. S.R. Ha, S.H. Ryu, S.J. Park and K.Y. Rhee, "Effect of Clay Surface Modification and Concentration on the Tensile Performance of Clay/Epoxy Nanocomposites", Materials Science and Engineering, Part A, Vol. 448, 2007, pp. 264–268.

8. Man-Wai Ho, Chun-Ki Lam, Kin-tak Lau, Dickon H. L and David Hui, "Mechanical Properties of Epoxy-Based Composites Using Nanoclays", Composites Structure, Vol. 75, 2006, pp. 415-421.

9. Saeed Saber-Samandari, Akbar Afaghi Khatibi and Domagoj Basic, "An Experimental Study on Clay/Epoxy Nanocomposites Produced in a Centrifuge", Composites, Part B, Vol. 38, 2007, pp.102-107.

10. Yuanxin Zhou, Farhana Pervin, Mohammad A. Biswas, Vijaya K. Rangari and Shaik Jeelani, "Fabrication and Characterization of Montmorillonite Clay-Filled SC-15 Epoxy", Materials Letters, Vol. 60, 2006, pp. 869–873.

11. Katherine Dean, Julia Krstina, Wendy Tian and Russell J. Varley, "Effect of Ultrasonic Dispersion Methods on Thermal and Mechanical Properties of Organoclay Epoxy Nanocomposites", Macromolecular Material and Engineering, Vol. 292, 2007, pp. 415–427.

12. Zunjarrao S.C., Sriraman R., and Singh R.P., "Effect of Processing Parameters and Clay Volume Fraction on the Mechanical Properties of Epoxy-Clay Nanocomposites", Journal of Material Science, Vol. 41, 2006, pp. 2219–2228.

13. Kornmann X., Rees M., Thomann Y., Necola A., Barbezat M., and Thomann R, "Epoxy-Layered Silicate Nanocomposite as Matrix in Glass Fibre-Reinforced Composites", Composites Science and Technology, Vol. 65, 2005, pp. 2259-2268.

14. Chun-ki Lam, Kin-tak Lau, Hoi-yan Cheung and Hang-yin Ling, "Effect of Ultrasound Sonication in Nanoclay Clusters of Nanoclay/Epoxy Composites", Materials Letters 59, 2005, pp. 1369-1372.

15. Weiping Liu, Suong V. Hoa and Martin Pugh, "Organoclay-Modified High Performance Epoxy Nanocomposites", Composites Science and Technology, Vol. 65, 2005, pp. 307-316.

16. Weiping Liu, Hoa S. V., and Pugh M., "Fracture Toughness and Water Uptake of High-Performance Epoxy/clay Nanocomposites", Composites Science and Technology, Vol. 65, 2005, pp. 2364-2373.

17. Chung-Feng Dai, Pei-Ru Li and Jui-Ming Yeh, "Comparative Studies for the Effect of Intercalating Agent on the Physical Properties of Epoxy-Clay Based Nanocomposite Materials", European Polymer Journal, Vol. 44, 2008, pp. 2439-2447.

18. Velmurugan R. and Mohan. T. P., "Room Temperature Processing of Epoxy-Clay Nanocomposite", Journal of Material Science, Vol. 39, 2004, pp. 7333-7339.

19. Asma Yasmin, Jandro L. Abot, and Isaac M. Daniel, "Processing of Clay/Epoxy Nanocomposites by Shear Mixing", Scripta Materialia, Vol. 49, 2003, pp. 81-86.

20. Farzana Hussain, Jihua Chen and Mehdi Hojjati., 'Epoxy-Silicate Nanocomposites: Cure Monitoring and Characterization", Materials Science and Engineering, Part A, 445–446, 2007, pp. 467–476.

21. B. Akbari and R. Bagheri. "Deformation Mechanism of Epoxy/Clay Nanocomposite" Macromolecular Nanotechnology, European Polymer Journal, Vol.43, 2007, pp.782–788.

22. Jinwei Wang and Shuchao Qin, "Study on the Thermal and Mechanical Properties of Epoxy-Nanoclay Composites: The Effect of Ultrasonic Stirring Time", Materials letters Vol. 61, 2007, pp. 4222-4224.

23. Jinwei Wang, Xianghua Kong, Lei Cheng and Yedong He, "Influence of Clay Concentration on the Morphology and Properties of Clay-Epoxy Nanocomposites Prepared by In-situ Polymerization under Ultrasonication", Journal of University of Science and Technology Beijing, Vol. 15, Number 3, June 2008, pp. 320.

24. Benfarhi S., Decker C., Keller L., and Zahouily K., "Synthesis of Clay Nanocomposite Materials by Light-Induced Crosslinking Polymerization", European Polymer Journal, Vol. 40, 2004, pp. 493-501.

25. Ole Becker, Russell J. Varley and George P. Simon, "Thermal Stability and Water Uptake of High Performance Epoxy Layered Silicate Nanocomposites" European Polymer Journal, Vol. 40, 2004, pp. 187-195.

26. "Handbook of Clay Science: Developments in Clay Science", Edited by FaÙˆiza Bergaya, Benny K.G. Theng and Gerhard Lagaly, 1st Ed., Elsevier, Nertherland, 2006.

27. B. Qi., Q.X. Zhang, M. Bannister and Y.-W Mai, "Investigation of the Mechanical Properties of DGEBA-Based Epoxy Resin with Nanoclay Additives", Composite Structures, Vol. 75, 2006, pp. 514-519.

28. M. Hernandez, B. Sixou, J. Duchet and H. Sautereau. "The Effect of Dispersion State on PMMA-Epoxy-Clay Ternary Blends: In-situ Study and Final Morphologies", Polymer, Vol. 48, 2007, pp. 4075-4086.

29. S. Pavlidou and C.D. Papaspyrides, "A Review on Polymer–Layered Silicate Nanocomposites", Progress in Polymer Science, Vol. 33, 2008, pp.1119–1198.

30. A Usuki, Y. Kojima, Y. Fukushima, T. Kurauchi and O. Kamigiato, "Synthesis of Nylon 6-Clay Hybrid", Journal of Material Resources, Vol. 8, 1993, pp. 1179–1184.

31. Tak-Keun Oh, "Effect of Shear force on Microstructure and Mechanical Property of Epxy/Clay Nanocomposite", Master Thesis, University of Florida, 2004.

32. Muhammed Ali Bashir, "Effect of Nanoclay Dispersion on the Processing of Polyester Nanocomposite", Master Thesis, McGill University, Montreal Canada, 2008.

33. W.G. potter, "Uses of Epoxy Resins", Newnes- Butterworths, London, 1975.

34. "Epoxy Resin Technology" Polymer Engineering and Technology, Edited by Paul F. Bruins, Interscience Publishers, New York, 1968.

35. Araldite GY 6010 CRS, Material Data Sheet, Jubail Chemical Industries Company (JANA), 2004.

36. Aradur 42, Material Data Sheet, Huntsman Advanced Materials Americas, USA, 2007.

37. Organo-Modified Clay, Nanomer I.30E, Material Data Sheet, Nanocor Inc, USA, 2007.

38. Annual Book of ASTM Standards, Plastic, vol.8, 1995

39. http://en.wikipedia.org/wiki/Scanning_electron_microscope

40. Handbook on Polymer Testing: Physical method, Edited by Roger Brown, Marcel Decker Incorporation, New York, 1999.

41. http://en.wikipedia.org/wiki/Vickers_hardness_test

42. Antonio F. Avila and David T.S Morais, "Modeling Nanoclay Effect into Laminates Failure Strength and Porosity", Composite Structures, Vol. 87, 2009, pp.55-62.

43. Sorina-Alexandra Garea, Horia Iovu and Ancuta Bulearca, “New Organophilic Agents of Montmorillonite Used as Reinforcing Agent in Epoxy Nanocomposites”, Journal of Polymer Testing, Vol. 27, 2008, pp. 100–113.

44. Emrah Bozkurt, Elcin Kaya, Metin Tanoglu, “Mechanical and Thermal Behavior of non-Crimp Glass Fiber Reinforced Layered Clay/Epoxy Nanocomposites”, Journal of Composites Science and Technology, Vol. 67, 2007, pp. 3394–3403.

45. Chun-Ki Lam, Hoi-yan Cheung, Kin-tak Lau, Li-min Zhou, Man-wai Ho and David Hui, “Cluster Size Effect in Hardness of Nanoclay/Epoxy Composites”, Composites, Part B, Vol. 36, 2005, pp. 263–269.

VITAE

Name: Adinoyi Muhammed Jamiu

Date of Birth: 13th June, 1980

Place of Birth: Okene, Kogi State, Nigeria.

Address: No 13c Oboroja Quarters, Otutu, P.O. Box 223, Okene, Kogi State, Nigeria.

Nationality: Nigerian

Marital Status: Married with children

email: mjadinoyi@gmail.com, jjasule@yahoo.com

Academic Background:

- Bachelor of Mechanical Engineering (B. Eng) from Bayero University, Kano, Kano State, Nigeria, December, 2005.

- Master of Science in Mechanical Engineering (Material option) from King Fahd University of Petroleum and Minerals, Dhahran, 31261, Kingdom of Saudi Arabia, June 2010.